Politecnico di Torino

Master Degree in Automotive Engineering

A.a. 2025/2026

Aerodynamic Analysis of Different Formula 1 Sidepod Concepts: A CFD Comparison of Ferrari, Mercedes and Red Bull 2022 Designs

Supervisors

Javier Blasco

Baratta Mirko

Candidate

Bollero Umberto

INDEX

ABSTRACT 9
INTRODUCTION 10
1.1 The 2022 Formula 1 Technical Regulations 10
1.2 Aerodynamic Role of Sidepods in the 2022 Regulations 10
1.3 Ferrari F1-75 Concept 13
1.4 Mercedes W13 Concept 14
1.5 Red Bull RB18 Concept 16
1.6 Objectives of the Thesis 17
AERODYNAMIC BACKGROUND AND FORMULA 1 SIDEPOD CONCEPTS 19
2.1 Aerodynamics of Formula 1 Cars 19
2.2 Aerodynamic Forces Acting on the Vehicle 19
2.3 Downforce Generation 21
2.4 Aerodynamic Drag 22
2.5 Aerodynamic Efficiency 23
2.6 Interaction Between Aerodynamic Components 23
2.7 Wake Generation and Sensitivity to Disturbed Air 24
2.8 Aerodynamic Performance and Component Interaction 24
2.9 Aerodynamic Role of the Sidepods 25
METHODOLOGY AND CFD SETUP 28
3.1 Development of the Simplified Formula 1 Model 28
3.2 Main Dimensions of the Model 30
3.3 Modelling of the Three Sidepod Configurations 30
3.4 Ferrari F1-75-Inspired Configuration 31
3.5 Mercedes W13-Inspired Configuration 32
3.6 Red Bull RB18-Inspired Configuration 32
3.7 Isolation of the Sidepods 33
3.8 CFD Simulation Setup 34
3.8.1 Numerical model and solution algorithm 34
3.8.2 Working fluid 34
3.8.3 Turbulence model 34
3.8.4 Computational domain and boundary conditions 34
3.8.5 Discretisation and mesh 35
3.8.6 Operating conditions analysed 36

3.8.7 Aerodynamic coefficients 37
FERRARI CONFIGURATION: RESULTS AND AERODYNAMIC ANALYSIS 38
4.1 Introduction to the Ferrari configuration 38
4.2 Aerodynamic Analysis of the Isolated Ferrari-Inspired Sidepod 39
4.2.1 Pressure distribution 39
4.2.2 Velocity field 41
4.2.3 Streamlines and flow behaviour 42
4.2.4 Wall shear stress 43
4.3 CFD Analysis of the Ferrari Configuration on the Complete Car 44
4.3.1 Global aerodynamic results 45
4.3.2 Pressure distribution on the complete car 46
4.3.3 Velocity field in the sidepod region 48
4.3.4 Streamlines and flow 50
4.3.5 Wall shear stress on the complete car 53
4.4 Comparison between the isolated sidepod and the complete car 53
MERCEDES CONFIGURATION: RESULTS AND AERODYNAMIC ANALYSIS 55
5.1 Introduction to the Mercedes configuration 55
5.2 Aerodynamic Analysis of the Isolated Mercedes-Inspired Sidepod 56
5.2.1 Pressure distribution 57
5.2.2 Velocity field 58
5.2.3 Streamlines and flow behaviour 58
5.2.4 Wall shear stress 60
5.3 CFD Analysis of the Mercedes Configuration on the Complete Car 61
5.3.1 Global aerodynamic results 62
5.3.2 Pressure distribution on the complete car 63
5.3.3 Velocity field in the sidepod region 63
5.3.4 Streamlines and flow 66
5.3.5 Wall shear stress on the complete car 68
5.4 Comparison between the isolated sidepod and the complete car 69
RED BULL CONFIGURATION: RESULTS AND AERODYNAMIC ANALYSIS 71
6.1 Introduction to the Red Bull configuration 71
6.2 Aerodynamic Analysis of the Isolated Red Bull-Inspired Sidepod 72
6.2.1 Pressure distribution 72
6.2.2 Velocity field 74
6.2.3 Streamlines and flow behaviour 75
6.2.4 Wall shear stress 77

6.3 CFD Analysis of the Red Bull Configuration on the Complete Car 78
6.3.1 Global aerodynamic results 79
6.3.2 Pressure distribution on the complete car 80
6.3.3 Velocity field in the sidepod region 81
6.3.4 Streamlines and flow behaviour 83
6.3.5 Wall shear stress on the complete car 86
6.4 Comparison between the isolated sidepod and the complete car 88
COMPARATIVE ANALYSIS OF THE THREE SIDEPOD CONCEPTS 90
7.1 Introduction 90
7.2 Handling the Disturbed Flow from the Front Wing and Front Wheel 90
7.3 Treatment of the Flow Directed Towards the Floor and Diffuser 91
7.4 Design Trade-offs of the Three Philosophies 92
7.5 Comparison of the Global Aerodynamic Coefficients 93
7.6 Comparative Aerodynamic Efficiency 94
7.7 Sensitivity to Operating Conditions and Limitations of the Comparison 94
7.8 Overall Comparison of the Three Sidepod Philosophies 95
CONCLUSIONS AND SUBSEQUENT DEVELOPMENTS 97
8.1 Summary of the Main Results 97
8.2 The Abandonment of the Mercedes Concept 97
8.3 The Abandonment of the Ferrari Concept 99
8.4 Convergence Towards the Red Bull Concept 100
8.5 Concluding Remarks on the Issues Identified 101
8.6 Study Limitations and Future Developments 102
REFERENCES 103

INDEX OF FIGURES

Figure 1 Comparison of the three main Formula 1 sidepod concepts introduced in the 2022 season: Mercedes W13, Ferrari F1-75 and Red Bull RB18. 11
Figure 2 Rear comparison of the Mercedes W13, Ferrari F1-75 and Red Bull RB18. 12
Figure 3 Ferrari F1-75. 13
Figure 4 Ferrari F1-75 sidepod geometry. 13
Figure 5 Mercedes W13. 14
Figure 6 Mercedes W13 sidepod geometry. 15
Figure 7 Red Bull RB18. 16
Figure 8 Red Bull RB18 sidepod geometry. 16
Figure 9 Simplified Formula 1 baseline CAD model. 29
Figure 10 Top view of the simplified Formula 1 baseline CAD model. 29
Figure 11 Top-view comparison of the Ferrari F1-75, Mercedes W13 and Red Bull RB18 sidepod concepts. 31
Figure 12 Comparison between the Ferrari F1-75 and the Ferrari-inspired CAD configuration. 31
Figure 13 Comparison between the Mercedes W13 and the Mercedes-inspired CAD configuration. 32
Figure 14 Comparison between the Red Bull RB18 and the Red Bull-inspired CAD configuration. 32
Figure 15 Isolated Ferrari-, Mercedes- and Red Bull-inspired sidepod geometries used for the CFD analysis. 33
Figure 16 Computational domain and boundary conditions used for the CFD simulations in ANSYS Fluent. 35
Figure 17 Computational mesh around the complete Formula 1 model. 36
Figure 18 Complete Formula 1 CAD model with the Ferrari-inspired sidepod configuration. 38
Figure 19 Isolated Ferrari-inspired sidepod geometry used for the CFD analysis. 39
Figure 20 Pressure distribution around the isolated Ferrari-inspired sidepod at 40, 66.66 and 88.88 m/s. 40
Figure 21 Pressure distribution in the upper basin region of the isolated Ferrari-inspired sidepod at 40, 66.66 and 88.88 m/s. 40
Figure 22 Velocity field around the isolated Ferrari-inspired sidepod at 40, 66.66 and 88.88 m/s. 41
Figure 23 Streamline distribution around the isolated Ferrari-inspired sidepod at 66.66 m/s. 42
Figure 24 Lateral streamline distribution through the lower undercut of the isolated Ferrari-inspired sidepod at 66.66 m/s. 42
Figure 25 Lateral streamline distribution around the isolated Ferrari-inspired sidepod at 66.66 m/s. 43
Figure 26 Wall shear stress distribution around the isolated Ferrari-inspired sidepod at 40, 66.66 and 88.88 m/s. 43
Figure 27 Wall shear stress distribution in the upper basin region of the isolated Ferrari-inspired sidepod at 66.66 m/s. 44
Figure 28 Complete Formula 1 CAD model with the Ferrari-inspired sidepod configuration. 45
Figure 29 Pressure distribution over the complete Ferrari-inspired configuration at 40, 66.66 and 88.88 m/s. 46
Figure 30 Pressure distribution in the Ferrari-inspired sidepod region of the complete car at 66.66 m/s. 47
Figure 31 Velocity field around the Ferrari-inspired sidepod region of the complete car at 66.66 m/s. 48
Figure 32 Lateral velocity field around the Ferrari-inspired sidepod on the complete car at 66.66 m/s. 49
Figure 33 Streamline distribution around the complete Ferrari-inspired configuration at 66.66 m/s. 50

Figure 34 Lateral streamline distribution around the Ferrari-inspired sidepod on the complete car at 66.66 m/s. 51
Figure 35 Streamline distribution around the Ferrari-inspired sidepod region of the complete car at 66.66 m/s. 51
Figure 36 Streamline distribution around the Ferrari-inspired sidepod and rear-wheel region at 66.66 m/s 52
Figure 37 Wall shear stress distribution over the complete Ferrari-inspired configuration at 40, 66.66 and 88.88 m/s. 53
Figure 38 Complete Formula 1 CAD model with the Mercedes-inspired sidepod configuration. 55
Figure 39 Isolated Mercedes-inspired sidepod geometry used for the CFD analysis. 56
Figure 40 Pressure distribution around the isolated Mercedes-inspired sidepod at 40, 66.66 and 88.88 m/s 57
Figure 41 Velocity field around the isolated Mercedes-inspired sidepod at 40, 66.66 and 88.88 m/s 58
Figure 42 Streamline distribution around the isolated Mercedes-inspired sidepod at 66.66 m/s. 59
Figure 43 Lateral streamline distribution around the isolated Mercedes-inspired sidepod at 66.66 m/s. 59
Figure 44 Wall shear stress distribution around the isolated Mercedes-inspired sidepod at 40, 66.66 and 88.88 m/s. 60
Figure 45 Complete Formula 1 CAD model with the Mercedes-inspired sidepod configuration. 62
Figure 46 Pressure distribution over the complete Mercedes-inspired configuration at 40, 66.66 and 88.88 m/s. 63
Figure 47 Lateral velocity field around the complete Mercedes-inspired configuration at 66.66 m/s 64
Figure 48 Velocity field around the Mercedes-inspired sidepod and floor region of the complete car at 66.66 m/s. 64
Figure 49 Streamline distribution around the complete Mercedes-inspired configuration at 66.66 m/s. 66
Figure 50 Lateral streamline distribution around the complete Mercedes-inspired configuration at 66.66 m/s. 67
Figure 51 Lateral streamline distribution around the Mercedes-inspired sidepod and floor region of the complete car at 66.66 m/s. 67
Figure 52 Wall shear stress distribution over the complete Mercedes-inspired configuration at 40, 66.66 and 88.88 m/s 68
Figure 53 Complete Formula 1 CAD model with the Red Bull-inspired sidepod configuration. 71
Figure 54 Isolated Red Bull-inspired sidepod geometry used for the CFD analysis. 72
Figure 55 Pressure distribution around the isolated Red Bull-inspired sidepod at 40, 66.66 and 88.88 m/s 72
Figure 56 Pressure distribution along the lower surface of the isolated Red Bull-inspired sidepod at 66.66 m/s. 73
Figure 57 Velocity field around the isolated Red Bull-inspired sidepod at 40, 66.66 and 88.88 m/s. 74
Figure 58 Streamline distribution around the isolated Red Bull-inspired sidepod at 66.66 m/s. 75
Figure 59 Lateral streamline distribution through the lower region of the isolated Red Bull-inspired sidepod at 66.66 m/s 76
Figure 60 Wall shear stress distribution around the isolated Red Bull-inspired sidepod at 40, 66.66 and 88.88 m/s. 77
Figure 61 Complete Formula 1 CAD model with the Red Bull-inspired sidepod configuration. 78
Figure 62 Pressure distribution over the complete Red Bull-inspired configuration at 40, 66.66 and 88.88 m/s. 80
Figure 63 Pressure distribution around the Red Bull-inspired sidepod region of the complete car at 66.66 m/s. 81

Figure 64 Velocity field around the Red Bull-inspired sidepod and floor region of the complete car at 66.66 m/s. 82
Figure 65 Lateral velocity field around the complete Red Bull-inspired configuration at 66.66 m/s..... 83
Figure 66 Streamline distribution around the complete Red Bull-inspired configuration at 66.66 m/s. 84
Figure 67 Lateral streamline distribution around the Red Bull-inspired sidepod and floor region of the complete car at 66.66 m/s. 84
Figure 68 Lateral streamline distribution around the complete Red Bull-inspired configuration at 66.66 m/s..... 85
Figure 69 Wall shear stress distribution over the complete Red Bull-inspired configuration at 40, 66.66 and 88.88 m/s. 86
Figure 70 Lateral wall shear stress distribution over the complete Red Bull-inspired configuration at 66.66 m/s. 87
Figure 71 Lateral wall shear stress distribution around the complete Red Bull-inspired configuration at 66.66 m/s. 87
Figure 72 Comparison of the Mercedes W14 before and after the 2023 Monaco sidepod update. 98
Figure 73 Comparison of the Ferrari SF-24 sidepod configuration before and after the aerodynamic update. 100
Figure 74 Side-view comparison of the Mercedes W15, Ferrari SF-24 and Red Bull RB20 sidepod concepts for the 2024 Formula 1 season. 101

INDEX OF TABLES

Table 1 Main dimensions of the simplified Formula 1 CAD model. 30
Table 2 Freestream velocities investigated in the CFD simulations and their equivalent vehicle speeds. 36
Table 3 Aerodynamic forces and coefficients of the Ferrari-inspired complete-car configuration at the three investigated velocities. 45
Table 4 Aerodynamic forces and coefficients of the Mercedes-inspired complete-car configuration at the three investigated velocities. 62
Table 5 Aerodynamic forces and coefficients of the Red Bull-inspired complete-car configuration at the three investigated velocities. 79
Table 6 Comparison of drag and lift coefficients for the Ferrari-, Mercedes- and Red Bull-inspired configurations at the three investigated velocities 93
Table 7 Comparison of the aerodynamic efficiency of the Ferrari-, Mercedes- and Red Bull-inspired configurations at the three investigated velocities 94
Table 8 Qualitative and quantitative comparison of the three sidepod design philosophies. 95

ABSTRACT

The technical regulations introduced by the Fédération Internationale de l'Automobile (FIA) in 2022 imposed a radical shift in Formula 1 aerodynamic philosophy, reintroducing ground effect as the primary source of downforce and leaving teams considerable interpretive freedom regarding sidepod design. This design freedom led, from the very first races of the season, to three radically different solutions: the wide, "bulbous" sidepods of the Ferrari F1-75, the minimal-section "zero-pod" concept of the Mercedes W13, and the downwash-oriented solution of the Red Bull RB18. This thesis aims to analyse and compare, through Computational Fluid Dynamics (CFD) simulations, the aerodynamic behaviour of these three concepts.

To this end, a generic Formula 1 car model, not attributable to any specific team, was designed, onto which three sidepod variants conceptually inspired by the Ferrari, Mercedes and Red Bull solutions were modelled. As a first step, each sidepod geometry was isolated and analysed using a dedicated CFD setup, with the aim of characterising its intrinsic aerodynamic behaviour independently of the interactions with the rest of the vehicle. This analysis focused on the pressure distribution, local flow acceleration, recirculation regions and the way in which each geometry influenced the surrounding airflow.

Subsequently, the same sidepod concepts were integrated into the complete Formula 1 model and analysed under identical operating conditions. The complete-car simulations made it possible to evaluate how the aerodynamic behaviour identified in the isolated configurations changed once the sidepods interacted with the front wing, wheels, suspension, and rear aerodynamic structures. Global aerodynamic coefficients, including downforce, drag and aerodynamic efficiency, were evaluated together with the overall flow field around the vehicle.

The comparison between the results obtained at isolated-component and complete-car level made it possible to identify how the intrinsic characteristics of each sidepod concept were modified by its integration into the complete aerodynamic system. The analysis highlights the different approaches adopted by the three geometries in terms of flow management, pressure distribution and interaction with downstream aerodynamic components. The results are finally discussed in relation to what was empirically observed during the 2022 Formula 1 season, providing an interpretive framework for the aerodynamic reasoning behind the different development paths pursued by Ferrari, Mercedes and Red Bull.

Chapter 1

INTRODUCTION

1.1 The 2022 Formula 1 Technical Regulations

The 2022 season represented one of the most significant regulatory changes in the recent history of Formula 1. The new technical regulations introduced a major revision of the aerodynamic philosophy of the cars, with the main objective of reducing the effects of turbulent wake and allowing cars to follow each other more closely [1], [2]. In the previous generation of Formula 1 cars, a significant proportion of downforce depended on highly complex external aerodynamic surfaces designed to precisely control the airflow around the vehicle. This configuration ensured high performance in undisturbed airflow conditions, but also generated a particularly turbulent wake, causing a significant loss of aerodynamic load for following cars.

To reduce this effect, the 2022 regulations increased the importance of the floor in downforce generation, reintroducing the principle of ground effect in a much more prominent way. The new floor features shaped Venturi tunnels designed to accelerate the airflow beneath the car, generating a low-pressure region and therefore a downward aerodynamic force.

This solution allows high levels of aerodynamic load to be generated with relatively limited drag and makes the performance of the car less dependent on the upper aerodynamic surfaces. At the same time, the regulations simplified several components, including the front and rear wings, and removed particularly complex elements such as the bargeboards, with the aim of reducing the generation of vortical structures and improving wake control [1].

Despite the numerous geometric constraints, the 2022 regulations did not impose a single bodywork shape, but instead defined volumes and regions within which designers could develop different solutions. This freedom allowed teams to adopt different approaches to airflow management between the front and rear wheels, the Venturi tunnel inlets, the sidepods and the rear section of the car [1].

In particular, the distribution of airflow between the floor and the upper bodywork became a key aspect of aerodynamic design. Part of the airflow coming from the front of the car has to be directed towards the Venturi tunnel inlets, while the remaining flow is managed along the sides of the car and towards the rear region. The search for the most effective balance between these flow paths directly influenced sidepod design, leading to the development of significantly different aerodynamic solutions among the teams.

1.2 Aerodynamic Role of Sidepods in the 2022 Regulations

The sidepods represent one of the most complex regions of a Formula 1 car. Their design must simultaneously satisfy aerodynamic, thermal, structural and packaging requirements. They must accommodate several components, including radiators, intercoolers, cooling ducts, electronic systems and, depending on the adopted architecture, auxiliary elements of the power unit.

The need to guarantee adequate cooling generally requires sufficiently large inlets and a significant internal volume. From an aerodynamic perspective, however, it may be preferable to reduce the frontal

area, limit drag and leave more free space for the airflow directed towards the rear of the car. The optimal sidepod geometry therefore results from a compromise between requirements that are often conflicting.

The external shape of the sidepod first affects the pressure distribution over the surface of the car. Curvatures, ramps, undercuts and cross-sectional changes produce local accelerations and decelerations of the airflow. These phenomena can directly contribute to downforce generation, but they may also cause flow separation when adverse pressure gradients become too severe.



Figure 1 Comparison of the three main Formula 1 sidepod concepts introduced in the 2022 season: Mercedes W13, Ferrari F1-75 and Red Bull RB18.

Another fundamental function concerns airflow management in the region between the lower edge of the sidepod and the floor. A pronounced undercut allows a greater quantity of air to pass through this region and reach the coke-bottle section and diffuser. However, reducing the external volume may make radiator and duct packaging more difficult. In addition, a larger airflow beneath the sidepod does not automatically guarantee an overall performance improvement, since the direction, energy and quality of the flow are equally important. The upper surface of the sidepod may be used to direct the airflow downwards, according to a philosophy generally referred to as downwash, or to create a broader and more controlled flow region along the bodywork. The lateral surfaces may instead contribute to tyre-wake management and to protecting the floor from turbulent structures generated by the front wheels [1], [3].

The location and shape of the cooling inlet represent another distinguishing feature. The inlet area determines the available cooling airflow, while its orientation and position depend on the total-pressure distribution of the incoming flow. An inlet located in a low-energy region or affected by a particularly intense wake may require a larger area to guarantee the same cooling mass flow rate.

The 2022 regulations substantially changed the flow field in the sidepod region. The presence of Venturi tunnel inlets and the removal of the bargeboards forced designers to identify new methods for controlling the separation between the airflow directed underneath the car and the airflow travelling along the external surfaces. The regulatory simplification of the components located ahead of the sidepods increased the importance of the bodywork shape itself.

The large variety of solutions introduced during the season demonstrated that there was no single obvious interpretation of the new regulations. The ten teams adopted significantly different configurations, including wide sidepods, strongly tapered solutions and geometries characterised by pronounced downwash surfaces.



Figure 2 Rear comparison of the Mercedes W13, Ferrari F1-75 and Red Bull RB18.

Among the most representative solutions, three main philosophies can be identified: the Ferrari F1-75 concept, the Mercedes W13 concept and the Red Bull RB18 concept. These cars are the main focus of the present thesis because they interpret the relationship between cooling, packaging and aerodynamic flow management in radically different ways [3].

1.3 Ferrari F1-75 Concept



Figure 3 Ferrari F1-75

The Ferrari F1-75 featured wide and voluminous sidepods, often described as bulbous sidepods or wide-pods. The upper surface included a distinctive longitudinal depression, while the cooling outlets were distributed through a series of louvres on the top surface. The sidepod maintained a substantial volume in the central region before gradually narrowing towards the coke-bottle section [4], [5].



Figure 4 Ferrari F1-75 sidepod geometry

The upper surface did not follow a simple linear descent towards the rear of the car, but instead formed a concave channel. This configuration may be interpreted as a method for controlling the airflow along the upper part of the car while keeping it separated from the structures travelling along the lateral regions. An undercut was nevertheless present in the forward section to direct part of the airflow underneath the sidepod.

The Ferrari concept therefore did not aim to minimise the sidepod volume. Instead, it used this volume as an actual aerodynamic surface, attempting to guide the airflow towards the rear of the car and control the pressure distribution along the bodywork. A possible disadvantage was the larger surface exposed to the incoming flow and the greater blockage of the lateral region. The main advantage was the availability of a larger cooling volume and the possibility of using the external surfaces to generate additional aerodynamic effects.

1.4 Mercedes W13 Concept



Figure 5 Mercedes W13

The Mercedes W13 represented the most radical interpretation of the regulations. During pre-season testing in Bahrain, the team introduced a configuration with extremely narrow sidepods, which quickly became known as the zero-pod concept. In reality, the car still included the volumes and ducts required for cooling, but their integration into the bodywork was achieved by drastically reducing the visible width and longitudinal extension of the sidepods [5].

The cooling inlets were narrow and vertically oriented, while several lateral components, including the side-impact structure, were integrated into separate aerodynamic supports. The general objective of this philosophy was to free the upper and lateral regions of the floor, allowing a larger quantity of airflow to reach the rear of the car without encountering the obstruction of conventional sidepods.

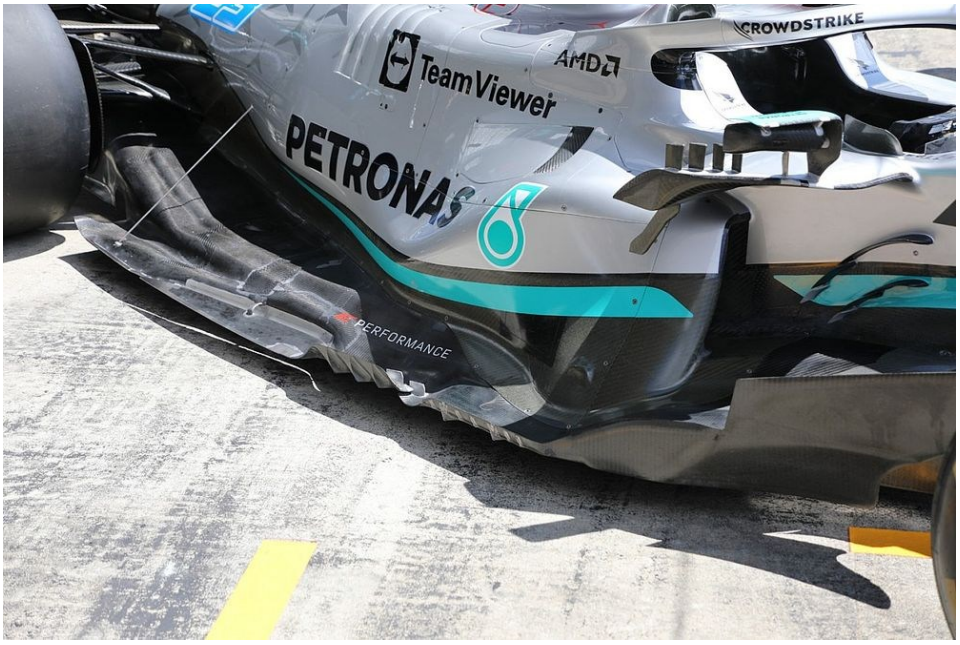


Figure 6 Mercedes W13 sidepod geometry

A reduced frontal section could decrease blockage and increase the quantity of air directed towards the beam wing, diffuser and rear wing. However, this solution required extremely compact packaging and particularly careful thermal management. Furthermore, the absence of an extended lateral volume altered the manner in which the airflow was protected from the wake generated by the front wheels.

During the actual season, the W13 was clearly affected by porpoising, namely vertical oscillations of the car associated with cyclic variations in the downforce generated by the floor. However, it would not be correct to attribute this phenomenon solely to the sidepod geometry. Porpoising depends on the interaction between floor aerodynamics, ride height, suspension stiffness, floor deformation and the dynamic response of the car. The zero-pod concept must therefore be analysed as part of an integrated system rather than as the isolated cause of the issues experienced by the team [6].

1.5 Red Bull RB18 Concept



Figure 7 Red Bull RB18

The Red Bull RB18 adopted a configuration commonly described as a downwash sidepod concept. The upper surface of the sidepods descended markedly towards the rear, contributing to directing the airflow towards the upper region of the floor and the coke-bottle section. A pronounced undercut was present in the lower region, creating a separate airflow path along the lower part of the car [7].

This philosophy may be considered intermediate between the large volume of the Ferrari concept and the extreme reduction adopted by Mercedes. Red Bull retained clearly defined sidepods and sufficient volume for the cooling system, while using strong tapering and surface curvature to energise and guide the airflow towards the rear floor and diffuser.



Figure 8 Red Bull RB18 sidepod geometry

The downward slope of the upper surface can help maintain flow attachment and direct the air towards an aerodynamically useful region. At the same time, the lower undercut allows the flow to feed the path along the floor edge. The separation between these two airflow paths represents one of the most distinctive characteristics of this concept.

The three philosophies therefore demonstrate how the same regulatory framework can result in significantly different geometries. Ferrari adopted a large lateral volume and concave upper surfaces; Mercedes attempted to minimise the sidepod dimensions; and Red Bull developed a configuration strongly oriented towards downwash.

The comparison cannot be limited to the observation of the external shapes. A sidepod must be evaluated in relation to the quality of the airflow reaching the floor, the pressure distribution, the generated drag, the stability of the vortical structures, the behaviour of the diffuser and its ability to provide the required cooling. In addition, the local performance of the component may vary when the sidepod is integrated into the complete vehicle.

A geometry that produces low drag when considered in isolation may not provide the best overall result if it directs the airflow unfavourably towards the diffuser. Similarly, a sidepod that locally generates greater downforce may increase blockage or compromise the operation of the rear aerodynamic surfaces. For this reason, the present thesis includes both an analysis of the complete vehicle and a study of the isolated sidepods.

1.6 Objectives of the Thesis

The main objective of this work is to perform a comparative CFD analysis of three different Formula 1 sidepod concepts inspired by the Ferrari F1-75, Mercedes W13 and Red Bull RB18 from the 2022 season.

The geometries developed in this study are not intended to reproduce the original cars with complete accuracy, but rather to represent the main aerodynamic characteristics of the three different design philosophies. Since the detailed geometry and aerodynamic data of real Formula 1 cars are not publicly available, the models were developed as simplified conceptual interpretations based on publicly available information and visual references.

To ensure a consistent comparison, the three sidepod configurations were applied to the same simplified Formula 1 baseline model, while the other main vehicle components were kept unchanged. This approach makes it possible to reduce the influence of unrelated geometrical differences and to associate the variations observed in the simulations mainly with the sidepod geometry.

The study was carried out at two different levels. First, the sidepods were isolated from the vehicle and analysed individually in order to investigate their local aerodynamic behaviour, with particular attention to pressure distribution, velocity field, flow acceleration and streamline development. In a second stage, the same geometries were integrated into the complete vehicle and analysed again under equivalent operating conditions, allowing the interaction between each sidepod and the rest of the aerodynamic system to be evaluated.

The final objective is therefore to understand both the intrinsic behaviour of the three sidepod concepts and how this behaviour changes once the components are integrated into the complete car. The results

are intended as a relative comparison between different aerodynamic design philosophies rather than as a direct prediction of the actual performance of the original Ferrari, Mercedes and Red Bull cars.

Chapter 2

AERODYNAMIC BACKGROUND AND FORMULA 1 SIDEPOD CONCEPTS

2.1 Aerodynamics of Formula 1 Cars

Aerodynamics plays a fundamental role in the performance of a Formula 1 car, as it involves not only the generation of vertical load but also the management of the entire airflow around the vehicle. Unlike conventional road cars, which are mainly designed to reduce aerodynamic drag and fuel consumption, a Formula 1 car must generate high levels of downforce in order to increase the vertical load on the tyres and improve cornering speed, braking performance and stability.

The aerodynamic design of a Formula 1 car therefore requires an effective compromise between downforce and drag, avoiding excessive resistance that would penalise straight-line performance. At the same time, controlling the airflow around the vehicle is essential to ensure that each aerodynamic component operates under favourable conditions. The front wing, floor, sidepods, diffuser and rear wing do not work independently, but continuously interact with one another.

For this reason, an effective aerodynamic configuration is not simply the one that generates the greatest amount of downforce, but the one that efficiently manages the airflow between the different regions of the car, limits aerodynamic losses and allows the various components to operate as effectively as possible.

2.2 Aerodynamic Forces Acting on the Vehicle

When a vehicle moves through the surrounding air, pressure and viscous stresses act over its external surfaces. The integration of these stresses produces an overall aerodynamic force that can be decomposed into three main components:

- the longitudinal aerodynamic force, generally identified as drag;
- the vertical aerodynamic force, identified as lift or downforce;
- the lateral aerodynamic force, generated when the car is exposed to a non-zero yaw angle or crosswind.

Under ideal straight-line conditions, the lateral component is approximately zero, while drag and downforce represent the dominant aerodynamic forces.

The drag force can be expressed as:

$$D = \frac{1}{2}\rho V_\infty^2 A_{ref} C_D$$

where:

- D is the aerodynamic drag force;
- ρ is the air density;
- $V_\infty$is the freestream velocity;
- A_{ref} is the reference area;
- C_D is the drag coefficient.

Similarly, the aerodynamic lift force is defined as:

$$L = \frac{1}{2}\rho V_\infty^2 A_{ref} C_L$$

where C_L is the lift coefficient. According to the conventional aerodynamic sign convention, a positive value of C_L represents an upward force. Since a racing car is designed to generate a downward force, its lift coefficient is generally negative.

In motorsport applications, it is therefore common to refer directly to the downforce magnitude:

$$F_{\text{downforce}} = -L$$

or to define a positive downforce coefficient:

$$C_{L,\text{downforce}} = -C_L$$

Both drag and downforce increase proportionally to the square of the vehicle velocity. If the speed doubles, the aerodynamic forces theoretically increase by a factor of four, assuming that the aerodynamic coefficients remain constant. This relationship explains why aerodynamic performance becomes increasingly important at high speed, whereas mechanical grip plays a relatively greater role in low-speed corners.

However, the coefficients are not always constant. They may vary with ride height, pitch angle, roll angle, steering angle, yaw angle, wheel rotation and flow separation. Formula 1 cars are particularly sensitive to these parameters because their aerodynamic components operate close to the ground and interact strongly with each other.

2.3 Downforce Generation

Downforce is produced by creating a pressure difference between the upper and lower surfaces of the aerodynamic components. For a Formula 1 car, this effect is mainly obtained through inverted wings, the floor, the diffuser and the interaction between the bodywork and the surrounding airflow.

An inverted wing operates according to the same general aerodynamic principles as an aircraft wing, but the resulting force is directed downwards. The geometry and angle of attack of the wing accelerate the flow along one side of the profile and modify the pressure distribution over its surfaces. The integrated pressure difference generates a net vertical force.

A complete explanation of downforce generation should not be based exclusively on the simplified statement that faster airflow always corresponds to lower pressure. The pressure field around an aerodynamic surface is determined by the combined effects of streamline curvature, flow acceleration, boundary-layer behaviour, viscosity and conservation of momentum. In particular, the wing modifies the momentum of the incoming airflow by deflecting it upwards, while the reaction force acting on the wing is directed downwards.

The front and rear wings produce substantial aerodynamic load, but the underfloor is also one of the major downforce-generating regions of a modern Formula 1 car. Ground-effect race cars may generate aerodynamic loads comparable to several times their own weight under high-speed conditions, although the exact values depend on the vehicle generation, configuration and operating condition [8], [9].

Generating high downforce improves the maximum lateral force that can be transmitted by the tyres. A simplified expression for the available tyre force is:

$$F_{\text{tyre}} = \mu F_z$$

where:

- μ is the tyre-road friction coefficient;
- F_z is the vertical load acting on the tyre.

The total vertical load includes both the static vehicle weight and the aerodynamic downforce:

$$F_z = mg + F_{\text{downforce}}$$

where m is the vehicle mass and g is gravitational acceleration.

Aerodynamic downforce therefore increases the force that the tyres can transmit without requiring an equivalent increase in vehicle mass. This is particularly advantageous because downforce increases with the square of speed, whereas the inertial forces related to vehicle mass remain present under all operating conditions.

Nevertheless, tyre behaviour is load-sensitive. The coefficient of friction does not remain perfectly constant as the vertical load increases. Consequently, doubling the vertical load does not necessarily double the available lateral force. The distribution of aerodynamic load among the four wheels is therefore as important as its total magnitude.

2.4 Aerodynamic Drag

Aerodynamic drag is the component of the aerodynamic force acting opposite to the direction of vehicle motion. It reduces acceleration and limits the maximum speed that can be reached for a given power output.

The drag generated by a Formula 1 car can be divided conceptually into two main contributions:

$$D = D_{\text{pressure}} + D_{\text{friction}}$$

Pressure drag is generated by differences in pressure between the front and rear regions of the vehicle. It is strongly influenced by flow separation, wake formation, exposed wheels, cooling openings and bluff bodywork components.

Skin-friction drag is associated with the tangential shear stresses acting over surfaces due to the viscosity of the fluid. Although the local shear stress may be relatively small, the large total wetted area of the vehicle means that its integrated contribution cannot be neglected.

A further contribution is induced drag, which is associated with the generation of lift or downforce by finite-span aerodynamic surfaces. Pressure differences between the two sides of a wing produce three-dimensional flow around its edges and generate tip vortices. These vortices modify the direction of the local airflow and create an additional drag component.

In Formula 1, drag is generated not only by the wings, but also by the exposed wheels, suspension elements, cooling flow, cockpit, halo and complex interaction between the different aerodynamic components. The open-wheel architecture represents a significant aerodynamic disadvantage compared with closed-wheel vehicles, since each rotating tyre produces a large and highly turbulent wake.

The power required to overcome aerodynamic drag is:

$$P_D = DV_\infty$$

By substituting the expression for drag:

$$P_D = \frac{1}{2}\rho V_\infty^3 A_{\text{ref}} C_D$$

The power required to overcome drag therefore increases with the cube of velocity. At very high speeds, even a small reduction in the drag coefficient can produce a meaningful increase in maximum velocity or reduce the power required to maintain a given speed.

This relationship explains why Formula 1 teams adapt the aerodynamic configuration of the car to each circuit. High-downforce tracks, characterised by numerous medium- and high-speed corners, generally require larger wing angles and higher aerodynamic load. Low-downforce circuits, containing long straights and fewer fast corners, require reduced drag to maximise straight-line performance.

2.5 Aerodynamic Efficiency

The aerodynamic efficiency of a Formula 1 car represents its ability to generate downforce while limiting drag. It is commonly expressed through the ratio between the downforce coefficient and the drag coefficient:

$$\eta_{\text{aero}} = \frac{-C_L}{C_D}$$

Alternatively, when a positive downforce coefficient is used:

$$\eta_{\text{aero}} = \frac{C_{L,\text{downforce}}}{C_D}$$

A higher value indicates that the car produces more downforce for the same amount of drag. However, this ratio should not be interpreted in isolation. A configuration with very low downforce and very low drag could show a high efficiency while still being unsuitable for a racing vehicle. Both the absolute force coefficients and their ratio must therefore be considered.

The required aerodynamic efficiency also depends on the circuit. A car optimised for maximum efficiency may perform particularly well on tracks containing long straights combined with high-speed corners. On slower and more technical circuits, a larger absolute downforce level may be preferred, even when it is associated with a greater drag penalty.

2.6 Interaction Between Aerodynamic Components

The aerodynamic components of a Formula 1 car cannot be optimised independently. The airflow reaching a component is influenced by all the surfaces located upstream, while the wake produced by that component affects the downstream regions.

For example, the front wing determines the quality and direction of the airflow reaching the floor and sidepods. The sidepods subsequently influence the flow entering the coke-bottle section and diffuser. Finally, the diffuser modifies the operating conditions of the beam wing and rear wing.

This phenomenon is commonly referred to as aerodynamic interaction or aerodynamic coupling. It explains why a component that performs well when tested in isolation may produce a smaller improvement, or even a performance reduction, when installed on the complete car.

The same principle is particularly relevant to the present study. The isolated-sidepod simulations will provide information about the local pressure distribution and wake of each geometry. However, only the complete-vehicle simulations will reveal how the sidepods interact with the remaining surfaces.

A meaningful comparison must therefore distinguish between:

- the direct aerodynamic contribution of the sidepod;
- its indirect effect on the performance of downstream components;
- its influence on cooling and internal airflow;
- its effect on aerodynamic stability under different operating conditions.

2.7 Wake Generation and Sensitivity to Disturbed Air

A Formula 1 car leaves behind a complex wake characterised by velocity deficits, turbulence and vortical structures. This wake is generated by flow separation from the bodywork, the rotation of the wheels, the production of downforce and the mixing of airflow streams with different velocities.

When another car follows, its aerodynamic components no longer receive a uniform and undisturbed flow. The reduced local velocity decreases the dynamic pressure:

$$q = \frac{1}{2}\rho V^2$$

where q is the dynamic pressure, ρ is the air density, and V is the flow velocity.

Since aerodynamic forces are proportional to dynamic pressure, a reduction in local velocity directly reduces the available downforce. At the same time, increased turbulence and variations in flow direction may cause premature separation or destabilise the vortices used to control the underfloor.

Studies of racing-car wake effects have shown that a following vehicle may experience substantial aerodynamic losses and changes in aerodynamic balance, with the magnitude depending on both longitudinal and lateral separation [10].

The loss of front downforce is particularly critical because the front wing is the first major component exposed to the disturbed flow. If the front axle loses proportionally more load than the rear axle, the car develops greater high-speed understeer. The driver must reduce speed or increase the distance from the preceding vehicle.

Reducing wake sensitivity was one of the main objectives of the 2022 regulatory changes. The new cars were designed both to generate a less disruptive wake and to be less sensitive to the wake produced by another car. Formula 1 indicated that the revised floor, wings and wheel-control devices were intended to reduce the theoretical downforce loss experienced during close following [2].

From the perspective of the present thesis, the external shape of the sidepods may influence both the wake produced by the car and its sensitivity to upstream disturbances. A wide sidepod may generate a larger blockage and a different lateral wake, whereas a narrow sidepod may expose a greater portion of the floor and rear bodywork to the incoming flow. A downwash configuration may instead guide the airflow towards the rear floor and modify the interaction with the rear-wheel wake.

2.8 Aerodynamic Performance and Component Interaction

The aerodynamic design of a Formula 1 car is ultimately a system-level optimisation problem. The objective is not to maximise the performance of each individual component, but to maximise the performance of the complete vehicle over a lap.

An effective aerodynamic package must provide:

- sufficient total downforce;

- appropriate aerodynamic efficiency;
- stable front-to-rear balance;
- limited sensitivity to ride-height and attitude variations;
- acceptable cooling performance;
- predictable behaviour in yaw and disturbed airflow;
- compatibility with the mechanical and structural requirements of the car.

These objectives are not always compatible. Increasing the cooling inlet area improves thermal management but may increase drag. Increasing front-wing loading may improve low-speed rotation but disturb the airflow reaching the floor. Reducing the sidepod volume may improve the available external flow area but create packaging difficulties.

For this reason, the aerodynamic performance of the three sidepod concepts considered in this work will not be assessed solely through the forces acting on the sidepod surfaces. Their influence on the complete flow field, global force coefficients and aerodynamic balance will also be evaluated.

2.9 Aerodynamic Role of the Sidepods

Sidepods are among the most aerodynamically complex components of a Formula 1 car, since their geometry does not serve a single purpose but must simultaneously reconcile cooling, flow management, downforce generation and drag containment. Unlike the wings, whose objective is directly linked to vertical load, sidepods are multifunctional elements in which aerodynamic, thermal and packaging requirements must coexist within an extremely limited space.

This characteristic became even more critical with the technical regulations introduced in 2022. With the return to a pronounced use of ground effect, the floor became the main contributor to downforce generation, and the role of the sidepods no longer concerns only the flow travelling over their surfaces, but above all the way they condition the air directed towards the Venturi tunnels, the diffuser and the entire rear region of the car. Their external surface must therefore be regarded as an integral part of the aerodynamic system, rather than a mere cover for the internal mechanical components.

From a thermal standpoint, the sidepods house the heat exchangers required to control the temperature of the engine, the forced-induction system and the power unit fluids. External air is channelled from the inlets towards the radiators and expelled through dedicated openings in the bodywork, with the need to guarantee sufficient mass flow through the exchangers. Aerodynamically, however, large inlets and bulky radiators are penalising: they increase frontal area and the disturbance imposed on the flow, while the air passing through the exchangers loses part of its energy due to pressure losses. To this must be added the need to direct the hot exit flow towards regions where it interferes as little as possible with the rear aerodynamic components. Sidepod sizing therefore arises from a balance: excessively small openings improve external flow conditions but compromise thermal reliability, whereas an oversized cooling system entails a significant aerodynamic penalty.

The second main function is the channelling of flow towards the rear of the car. The air impinging on the lateral region is accelerated, deflected and redistributed by the shape of the inlet, the lower profile of the sidepod, the narrowing of the bodywork and the curvature of the upper surface. It is these features that determine how much air is directed along the edge of the floor and how much reaches the diffuser and rear wing directly.

Particularly relevant is the undercut, the recessed region in the lower front part of the sidepod. A pronounced undercut widens the passage between bodywork and floor, allowing a greater amount of high-energy air to reach the rear region, with benefits for diffuser feeding and for maintaining an energetic stream along the floor edges. Its geometry also modifies the local pressure gradient and, consequently, the trajectory followed by the flow. A similar role is played by the upper surface: inclined profiles descending progressively towards the rear generate a downwash effect, deflecting part of the flow downwards, whereas broader, more pronounced surfaces allow the flow expansion and the pressure distribution over the bodywork to be controlled differently. It is precisely in this choice that one of the main differences between the design philosophies observed in 2022 can be recognised.

Sidepods also contribute directly to the aerodynamic forces through the pressure distribution generated over their surfaces. As with any body immersed in a flow, the shape determines local accelerations and decelerations and therefore the pressure acting on the bodywork: suitably shaped surfaces can create low-pressure regions that feed the vertical load, while abrupt changes in geometry or excessive curvature produce adverse gradients, promote boundary layer separation and increase drag.

It follows that a bulky sidepod is not necessarily less efficient than an extremely compact solution. A larger external surface can be exploited to build a favourable pressure distribution and guide the flow along a precise trajectory; conversely, very narrow bodywork reduces the obstruction towards the rear but imposes a more complex internal packaging and appreciably alters the interaction with the floor. Performance therefore does not depend on frontal area in itself, but on the relationship between sidepod geometry and the rest of the car.

A further aspect concerns the flow directed towards the rear wheels. Tyres are strongly disturbing elements: their rotation and geometry generate vortical structures and a wake characterised by marked variations in velocity and pressure. Since turbulent or low-energy flow in the vicinity of the diffuser reduces its efficiency, the terminal shape of the sidepod, the narrowing of the bodywork and the orientation of the surfaces are used to condition the trajectory of the air before it reaches the wheel, limiting the interaction of the rear tyre wake with the rear aerodynamic elements. In this region the bodywork often features a marked inward taper towards the longitudinal axis, commonly referred to as the coke-bottle zone, which frees up space ahead of the wheels and promotes the passage of air towards the central part of the rear end, directly influencing the operating conditions of the diffuser and rear wing.

For the 2022-generation cars, the indirect interaction between sidepod geometry and porpoising must finally be considered — the vertical oscillation linked to the strong dependence of floor-generated load on ride height. As the car approaches the ground, the flow through the Venturi tunnels accelerates and the load increases; if ride height becomes excessively low, the conditions beneath the car can change abruptly, causing a sudden loss of downforce. The car rises, the flow re-establishes itself and the cycle may repeat, generating the oscillations observed particularly in the early races of the season. Although the phenomenon depends mainly on the floor, the suspension and the ride height, it is affected by the lateral geometry: a configuration that conveys large mass flows towards specific areas of the floor, or that generates strong external pressure gradients, can alter the sensitivity of the entire system to ride-height variations. Sidepod design must therefore be compatible with the behaviour of the floor across the full operating range, and not only under nominal conditions [9].

The role of the sidepods must thus be interpreted within a strongly interconnected system, in which the modification of a single geometric feature simultaneously affects cooling, drag, downforce, floor feeding, diffuser performance and the development of the tyre wake. The theoretically optimal solution for a single function does not necessarily coincide with the one that maximises the overall performance of the car: it is precisely this unstable balance that explains why, under identical regulations, such

distant design philosophies emerged in 2022. The broad surfaces of the Ferrari F1-75, the extreme reduction of lateral volumes on the Mercedes W13 and the strongly downwash-oriented approach of the Red Bull RB18 represent three different answers to the same set of aerodynamic and thermal problems, whose effectiveness cannot be assessed by looking at sidepod shape alone. These three philosophies, introduced in Sections 1.3 to 1.5, form the theoretical basis of the CFD comparison developed in the subsequent chapters.

Chapter 3

METHODOLOGY AND CFD SETUP

The methodology adopted in this work was defined with the aim of obtaining a controlled comparison between three different Formula 1 sidepod concepts. The objective of the study is not to reproduce with absolute accuracy the real aerodynamic performance of the Ferrari F1-75, Mercedes W13 and Red Bull RB18, but rather to analyse how different sidepod geometries influence the flow behaviour and aerodynamic performance when subjected to the same operating conditions.

To achieve this objective, a simplified three-dimensional Formula 1 car model was first developed and used as a common reference structure. Based on this model, three different sidepod geometries were then created, conceptually inspired by the solutions adopted by Ferrari, Mercedes and Red Bull during the 2022 season.

The use of the same baseline structure for all configurations represents a fundamental aspect of the methodology. A direct comparison between three completely different cars would not make it possible to clearly determine whether the observed differences were caused by the sidepod geometry or by different wing, floor, suspension and bodywork configurations. By keeping the other main vehicle components unchanged and modifying only the lateral region, the variations observed in the simulations can be associated mainly with the different sidepod geometries.

The analysis was therefore carried out in two consecutive stages. In the first stage, each sidepod was studied in isolation through dedicated CFD simulations. This made it possible to investigate its intrinsic aerodynamic behaviour and to identify the main characteristics in terms of pressure distribution, velocity field, streamline development, wake formation and possible flow-separation phenomena.

In the second stage, the same geometries were integrated into the complete vehicle model and analysed again. This made it possible to evaluate how the behaviour observed in the isolated configuration was modified by the interaction with the other aerodynamic components and by the flow field generated by the complete car.

All simulations were performed at three freestream velocities: 40 m/s, 66.66 m/s and 88.88 m/s, corresponding approximately to 144, 240 and 320 km/h. This allowed the consistency of the aerodynamic behaviour of the different configurations to be evaluated over a range of operating conditions, while keeping the other numerical parameters unchanged as far as possible.

The following sections describe in detail the procedure adopted, from the CAD modelling of the geometries to the definition of the CFD setup used for both the isolated-sidepod and complete-vehicle analyses.

3.1 Development of the Simplified Formula 1 Model

The first stage of the project consisted of developing a simplified three-dimensional model of a Formula 1 single-seater using Siemens NX.

The model was not intended to accurately reproduce a specific car from the 2022 season, since the original geometries developed by the teams are not publicly available with a sufficient level of detail for a faithful reproduction. A common "skeleton" was therefore created, characterised by the proportions and main elements typical of a modern Formula 1 car.

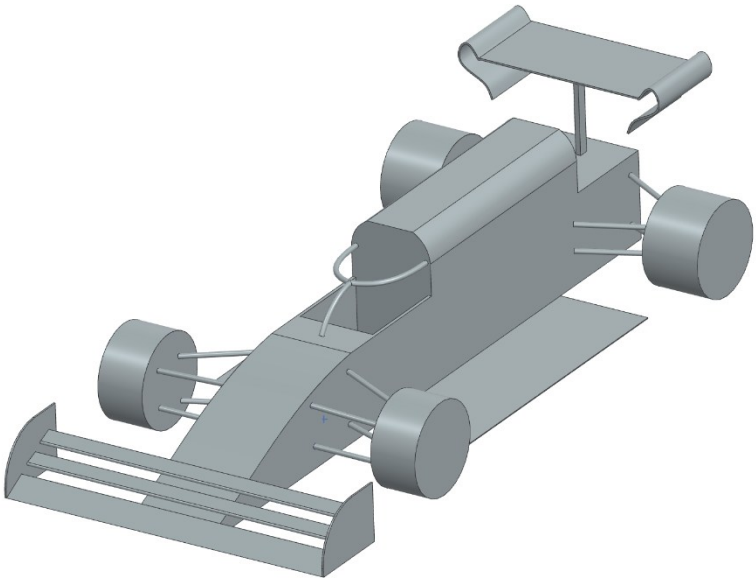


Figure 9 Simplified Formula 1 baseline CAD model.

The geometry includes the main components of a simplified Formula 1 car, including the front wing, nose, front and rear wheels, suspension elements, floor, halo, central bodywork, engine cover and rear wing. The model was intentionally simplified, while preserving the main proportions and aerodynamic elements required for the comparative analysis.

Some minor geometrical details present on an actual Formula 1 car were intentionally simplified or omitted. This choice reduces the complexity of the model and the computational cost of the simulations, while retaining the elements considered most relevant for the comparative analysis of the sidepods.

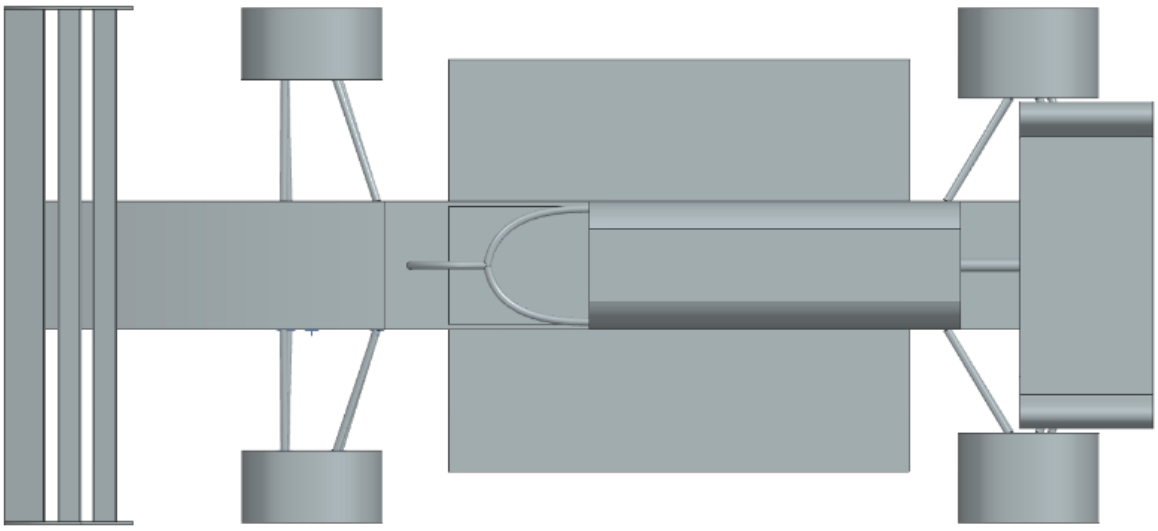


Figure 10 Top view of the simplified Formula 1 baseline CAD model.

It is important to emphasise that exactly the same baseline model was maintained for all configurations. When moving from one configuration to another, the only substantial geometrical variation is therefore represented by the sidepods.

3.2 Main Dimensions of the Model

The simplified Formula 1 model was developed by maintaining the main proportions of a modern single-seater while introducing a number of geometric simplifications required for the CFD analysis. The objective was not to reproduce a specific real Formula 1 car with complete dimensional accuracy, but to create a common baseline geometry suitable for the comparison of different sidepod concepts [1].

Parameter	**Value**
Overall length	**5000 mm**
Overall width	**2000 mm**
Overall height	**1800 mm**
Wheelbase	**3600 mm**
Wheel diameter	**720 mm**
Nominal CAD floor clearance	**50 mm**

Table 1 Main dimensions of the simplified Formula 1 CAD model.

The absolute values obtained from the simulations must therefore be interpreted in light of the geometrical simplifications adopted. The main objective remains the relative comparison between the three configurations rather than the prediction of the absolute performance of a specific real Formula 1 car.

3.3 Modelling of the Three Sidepod Configurations

Once the vehicle skeleton had been completed, three different sidepod geometries were developed on the same baseline structure, based on the main visible characteristics of the solutions introduced by Ferrari, Mercedes and Red Bull during the 2022 season.

The three configurations do not represent exact copies of the original geometries, but rather conceptual interpretations of their respective aerodynamic philosophies.

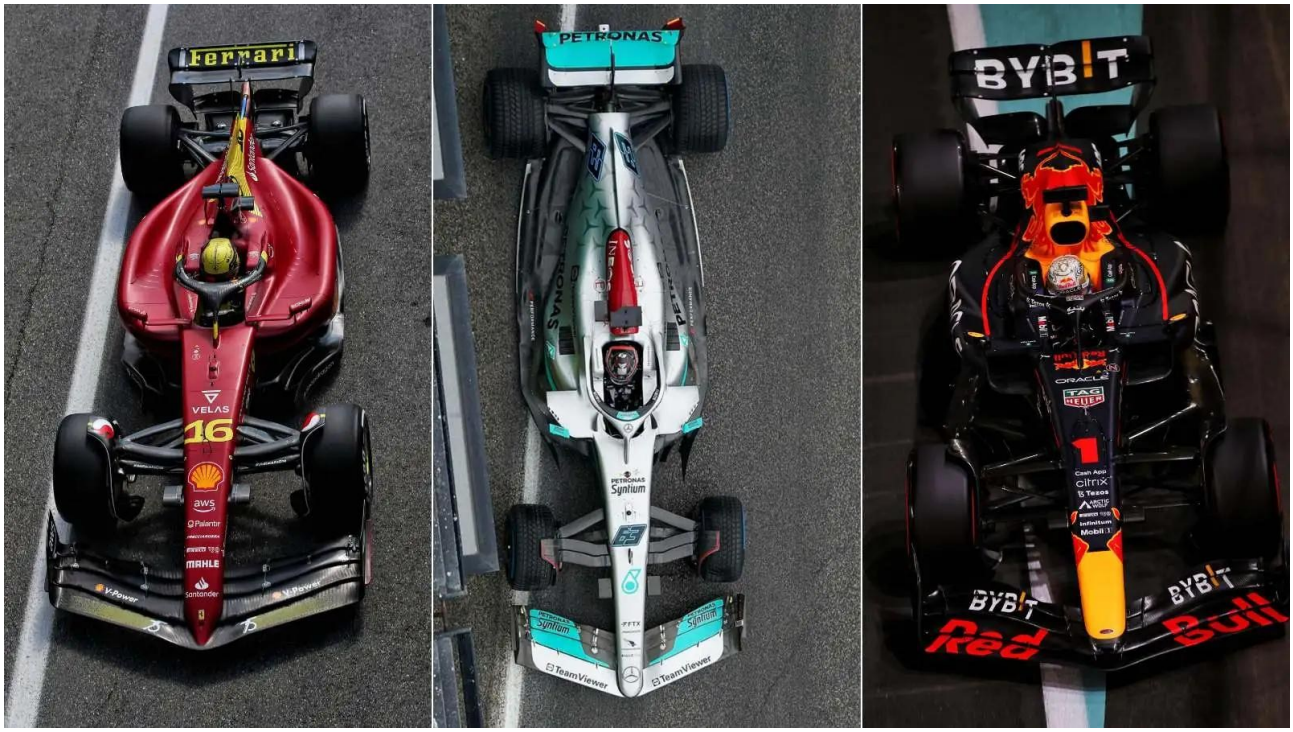


Figure 11 Top-view comparison of the Ferrari F1-75, Mercedes W13 and Red Bull RB18 sidepod concepts.

Maintaining the same vehicle structure makes it possible to investigate the influence of the different lateral geometries under comparable conditions.

3.4 Ferrari F1-75-Inspired Configuration

The first configuration was developed using the aerodynamic philosophy of the Ferrari F1-75 as a reference. It is characterised by a relatively wide and voluminous sidepod, with an extended upper surface and a more developed lateral geometry compared with the other two configurations.

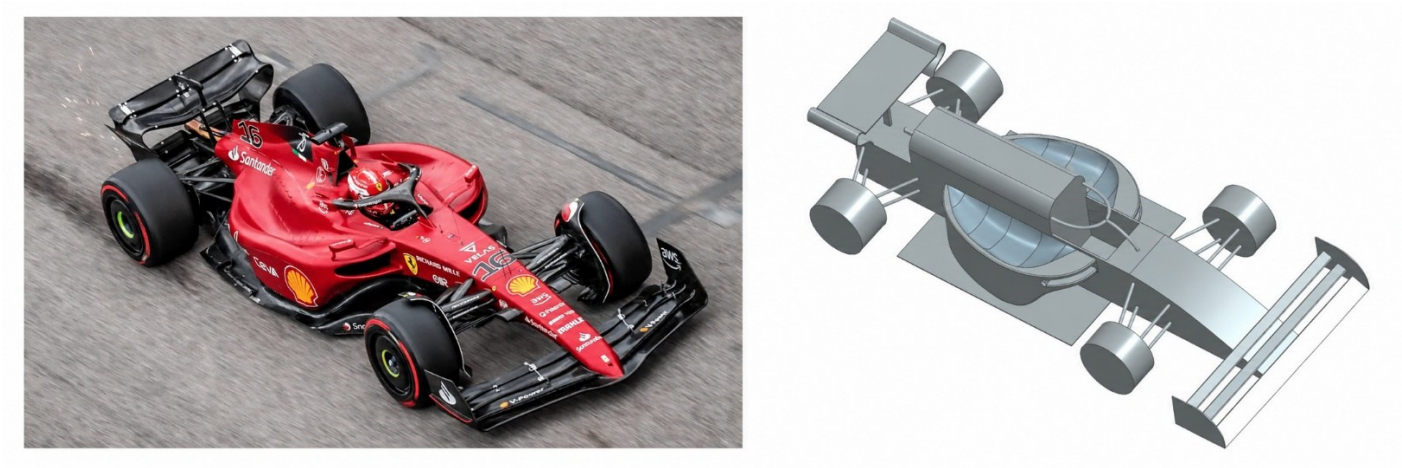


Figure 12 Comparison between the Ferrari F1-75 and the Ferrari-inspired CAD configuration.

The geometry was modelled with the aim of qualitatively reproducing the main distinctive characteristics of the Ferrari configuration.

3.5 Mercedes W13-Inspired Configuration

The second configuration was developed using the Mercedes W13 and the philosophy commonly referred to as the "zero-pod" concept as a reference.

The lateral geometry is significantly reduced compared with the Ferrari solution, resulting in a considerably smaller sidepod volume.

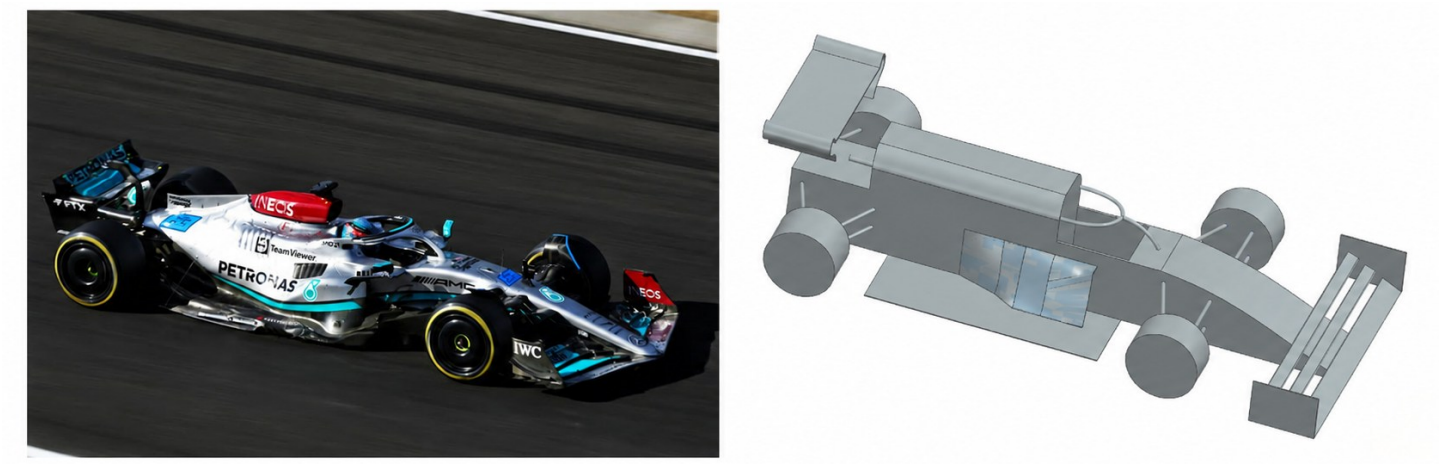


Figure 13 Comparison between the Mercedes W13 and the Mercedes-inspired CAD configuration

The reduction in lateral volume leaves a larger portion of the region adjacent to the floor directly exposed to the external airflow, making it possible to investigate a conceptually very different solution from the Ferrari configuration.

3.6 Red Bull RB18-Inspired Configuration

The third configuration was developed using the aerodynamic philosophy of the Red Bull RB18 as a reference. It is characterised by an upper surface that slopes progressively downward towards the rear of the vehicle, according to the principle commonly referred to as downwash.

An undercut is also present in the lower region, creating a different flow path compared with the upper surface.

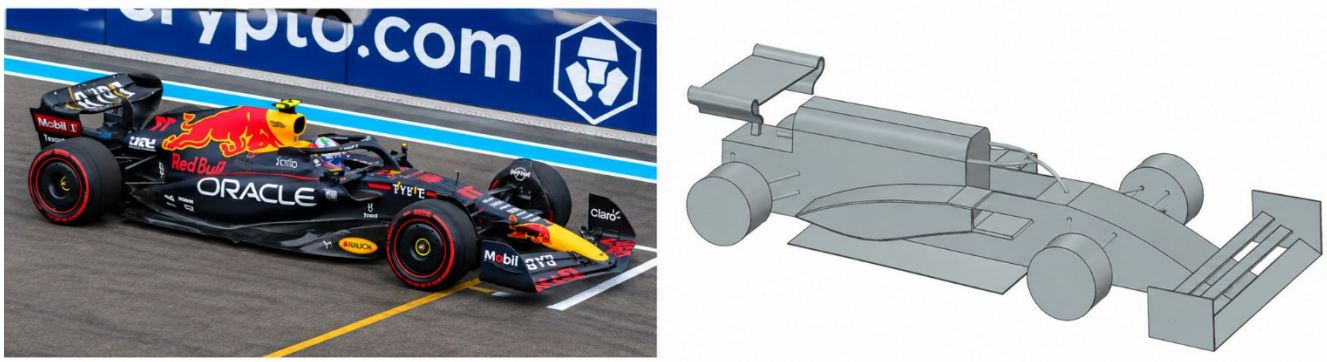


Figure 14 Comparison between the Red Bull RB18 and the Red Bull-inspired CAD configuration.

The Red Bull configuration therefore represents an intermediate and conceptually different solution compared both with the larger lateral volume of the Ferrari configuration and the strong dimensional reduction adopted by the Mercedes configuration.

3.7 Isolation of the Sidepods

Once the three complete vehicle configurations had been developed, the sidepods were isolated from the rest of the model in order to perform an initial CFD analysis dedicated exclusively to the geometries under investigation.

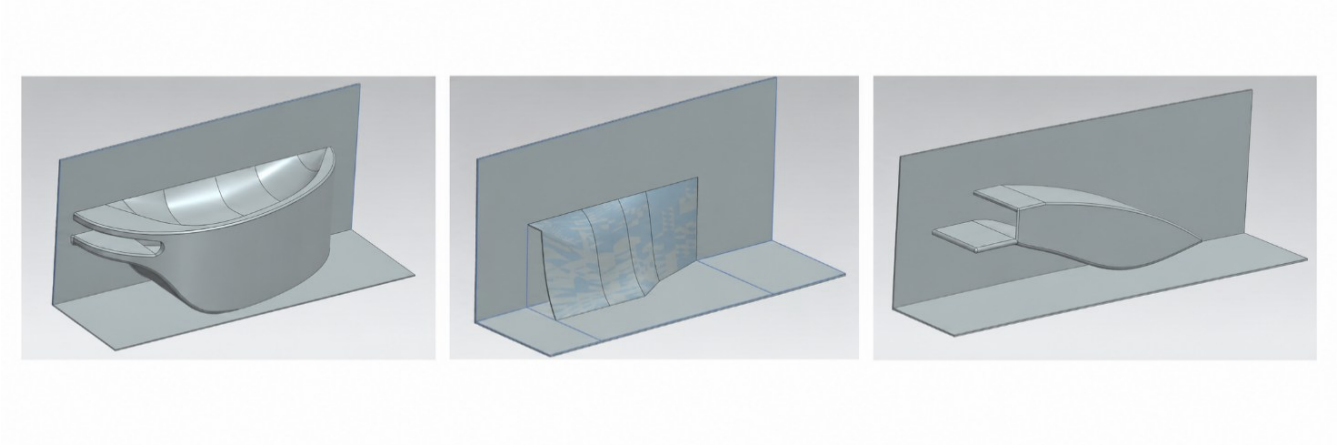


Figure 15 Isolated Ferrari-, Mercedes- and Red Bull-inspired sidepod geometries used for the CFD analysis.

Analysing the sidepod alone makes it possible to observe more clearly the phenomena directly associated with the component geometry, including the pressure distribution over its surface, flow acceleration around the geometry, stagnation regions, wake formation and possible flow separation regions.

This first analysis therefore makes it easier to identify the main aerodynamic advantages and disadvantages of the individual geometries.

However, the behaviour of an isolated sidepod cannot be considered equivalent to that of the same geometry installed on the complete vehicle. In the complete configuration, the airflow approaching the sidepod is influenced by the components located upstream, while the downstream flow interacts with the other components positioned in the rear region of the car.

For this reason, the isolated-sidepod analysis was used as the first stage of the study and was subsequently complemented by simulations of the complete vehicle.

In particular, the isolated analysis makes it possible to answer the following question:

How do the three sidepod geometries behave when subjected to the same flow conditions?

The complete-vehicle analysis instead makes it possible to investigate:

How does the behaviour of the same geometries change once they are integrated into the aerodynamic system of the car?

3.8 CFD Simulation Setup

The aerodynamic analyses were carried out using ANSYS Fluent 2025, adopting the same numerical approach for all three sidepod configurations analysed (Ferrari-inspired, Mercedes-inspired and Red Bull-inspired), in order to ensure a consistent comparison that would not be affected by differences in the solver setup rather than by the geometry itself.

3.8.1 Numerical model and solution algorithm

The simulations were set up using a pressure-based solver, under steady-state flow conditions, keeping the software's default settings with regard to the flow regime. Pressure-velocity coupling was handled using the Coupled algorithm, chosen for its greater robustness in simultaneously solving the continuity and momentum equations, which is particularly suitable in the presence of the strong pressure gradients typical of external automotive flows [11].

3.8.2 Working fluid

Air was used as the working fluid, modelled as an incompressible fluid with constant density, using ANSYS Fluent's default properties: a density of 1.225 kg/m^3 and a dynamic viscosity of 1.7894×10^{-5} kg/(m·s), corresponding to standard conditions (15°C, sea level). These properties were kept unchanged across all simulations, configurations and velocities tested. Given the maximum velocity analysed (88.88 m/s, corresponding to a Mach number of approximately 0.26), the assumption of incompressible flow is fully justified [12].

3.8.3 Turbulence model

Turbulence was modelled using the k-ω SST (Shear Stress Transport) model [13], [11], chosen for its ability to accurately describe both near-wall flow regions and freestream regions away from the body, a characteristic particularly useful when analysing complex geometries with flow separation, such as those found around the sidepods of a Formula 1 car. The same turbulence settings were kept unchanged across all configurations analysed.

3.8.4 Computational domain and boundary conditions

In order to reduce the computational cost of the simulations, only half of the vehicle was analysed, exploiting the car's geometric symmetry about the longitudinal centre plane. A symmetry boundary condition was therefore applied to this plane, which allows the number of mesh elements and computation time to be halved without introducing significant approximations to the flow, given that the motion is symmetric and free of yaw.

Consistent with this setup, the external boundaries of the domain (side and top surfaces) were also defined as symmetry, so as to minimise the interference of the domain boundaries on the flow field around the vehicle and to keep the flow as free as possible from artificial constraints.

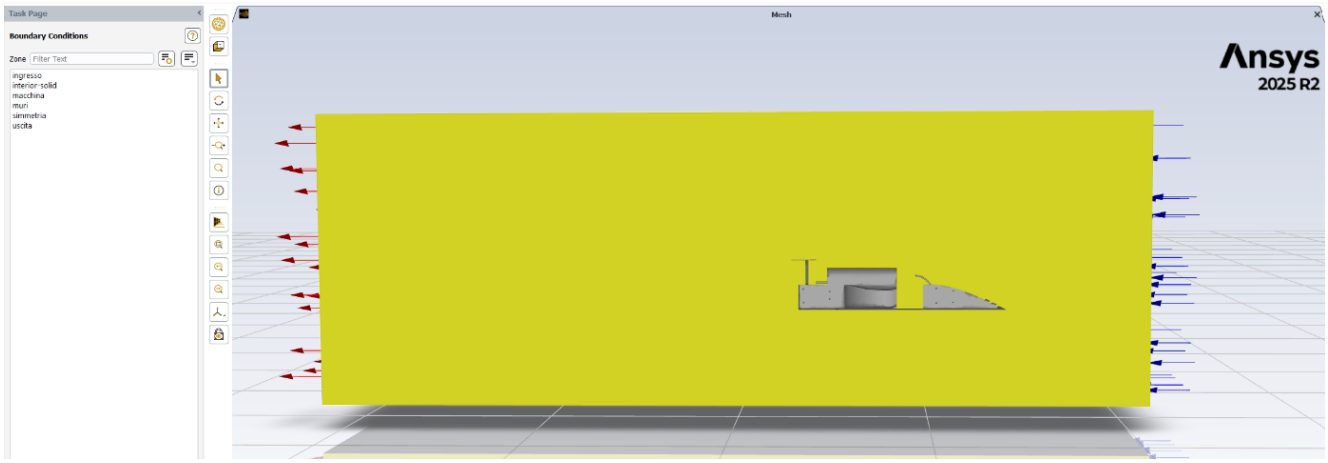


Figure 16 Computational domain and boundary conditions used for the CFD simulations in ANSYS Fluent.

The computational domain was therefore defined with the following boundary conditions:

- a velocity inlet condition upstream of the body, with a uniform velocity profile, corresponding to the three velocities analysed;
- a pressure outlet condition downstream;
- a symmetry condition on the vehicle's longitudinal symmetry plane (half-car model) and on the external side and top surfaces of the domain;
- the vehicle surfaces (bodywork and sidepods) defined as no-slip walls.

Unlike the most common automotive CFD setups, no ground plane was modelled in this study, and no moving-ground condition was applied. Similarly, the wheels were modelled as stationary surfaces, with no rotational condition imposed. This choice was made deliberately in order to minimise the aerodynamic interactions generated by the car's underbody and by wheel rotation (effects that are inherently complex and would require dedicated modelling), so as to focus the analysis exclusively on the effect of the different sidepod geometries on the flow, as well as to further reduce the overall computational cost of the simulations.

3.8.5 Discretisation and mesh

The computational grid was generated using ANSYS's automatic mesh generation tool, keeping the default settings for all configurations, so as not to introduce differences in the results related to spatial discretisation rather than to the geometry. Second-order upwind discretisation schemes were adopted for the momentum and turbulence equations, a choice that ensures greater accuracy compared with first-order schemes, at the cost of a moderately higher computational effort.

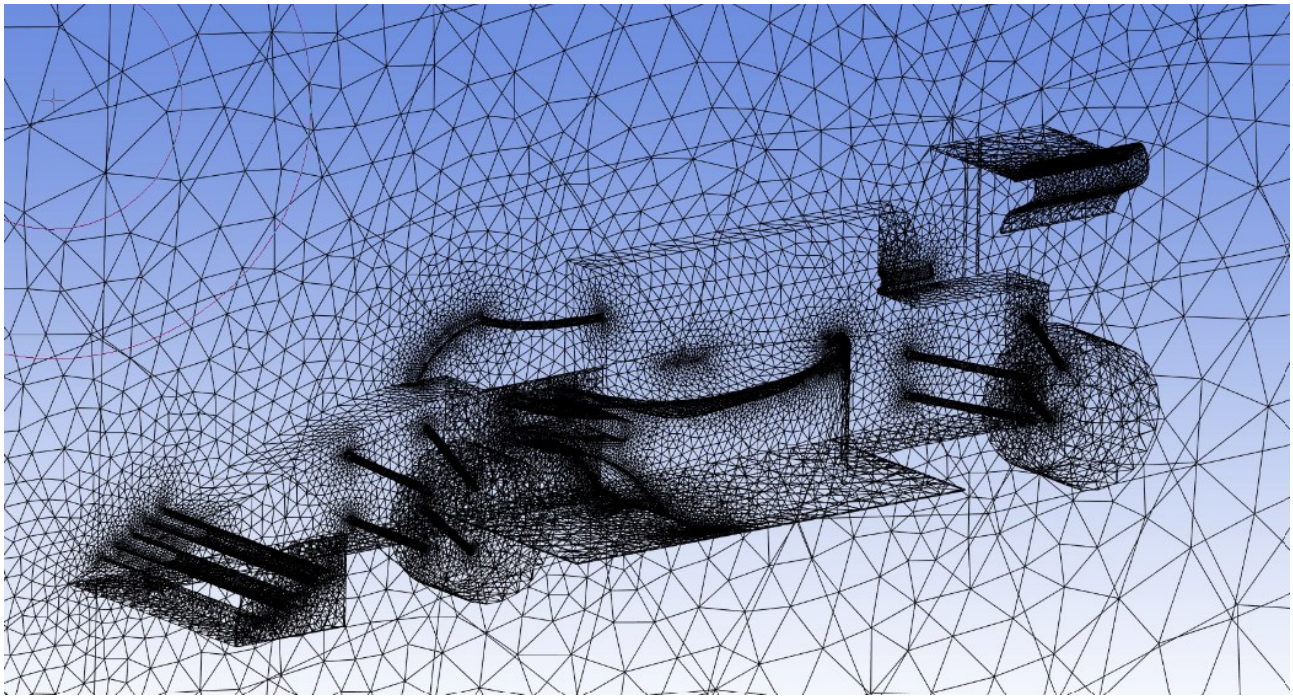


Figure 17 Computational mesh around the complete Formula 1 model.

3.8.6 Operating conditions analysed

For each configuration, three inlet velocities were analysed, representative of different characteristic phases of a lap:

Velocity	Equivalent	Representative condition
40 m/s	144 km/h	low speed
66.66 m/s	240 km/h	medium speed
88.88 m/s	320 km/h	high speed

Table 2 Freestream velocities investigated in the CFD simulations and their equivalent vehicle speeds.

These three conditions were applied both to the isolated-sidepod simulations and to the complete-vehicle simulations, allowing the aerodynamic behaviour of each geometry to be compared under the same operating conditions.

3.8.7 Aerodynamic coefficients

The drag and lift coefficients were calculated using the projected frontal area of the simulated half-vehicle model. The projected area, evaluated in the freestream direction, was approximately 0.74 m^2. Since both the aerodynamic forces and the reference area refer to the same half-vehicle geometry, no additional factor of two was required for the calculation of the aerodynamic coefficients.

All numerical settings (solver, coupling algorithm, turbulence model, boundary conditions, mesh generation strategy) were kept identical across the three configurations. This approach allows the differences observed in the aerodynamic results to be attributed primarily to the different sidepod design philosophies, rather than to variations in the simulation setup.

Chapter 4

FERRARI CONFIGURATION: RESULTS AND AERODYNAMIC ANALYSIS

4.1 Introduction to the Ferrari configuration

The Ferrari-inspired configuration was developed with the aim of reproducing the main aerodynamic features associated with the sidepod concept introduced on the Ferrari F1-75 during the 2022 Formula 1 season. Unlike solutions based on minimising lateral volume, this concept is characterised by a relatively wide bodywork, a pronounced undercut in the lower area, and a distinctive concave upper surface, referred to hereafter as the upper sidepod channel or basin region.

The purpose of this chapter is to analyse how these geometric features influence the surrounding flow field and to identify the main aerodynamic mechanisms generated by the sidepod. The analysis is divided into two phases: first, the Ferrari-inspired sidepod is studied as an isolated component, in order to identify the aerodynamic behaviour directly associated with its geometry; subsequently, the same sidepod is analysed after installation on the complete model of the car, so as to evaluate how the flow structures observed in the isolated case are modified by interaction with the other aerodynamic components.

Three freestream velocities were analysed:

$$V_1 = 40 \text{ m/s} \quad V_2 = 66.66 \text{ m/s} \quad V_3 = 88.88 \text{ m/s}$$

corresponding respectively to approximately 144, 240 and 320 km/h. The analysis focuses on the pressure distribution, the velocity field, the streamlines and the wall shear stress. Particular attention is devoted to the lower undercut and to the concave upper channel, since the simulations show that these two regions perform different but complementary functions in flow management.

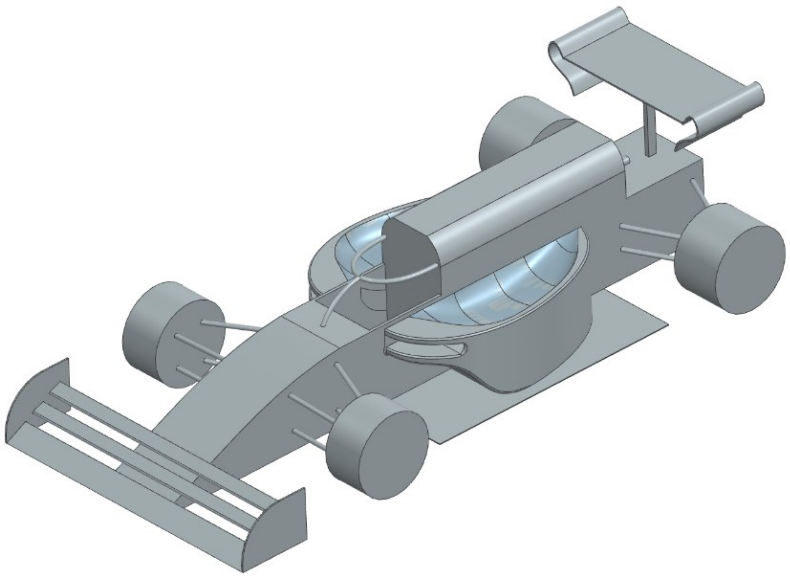


Figure 18 Complete Formula 1 CAD model with the Ferrari-inspired sidepod configuration.

4.2 Aerodynamic Analysis of the Isolated Ferrari-Inspired Sidepod

The simulations of the isolated sidepod were carried out to analyse the aerodynamic behaviour generated directly by the Ferrari geometry, without the influence of the front wing, wheels, suspension or rear aerodynamic components. This configuration therefore provides a useful reference for distinguishing the intrinsic behaviour of the sidepod from the interaction effects that emerge once the same geometry is installed on the complete car.

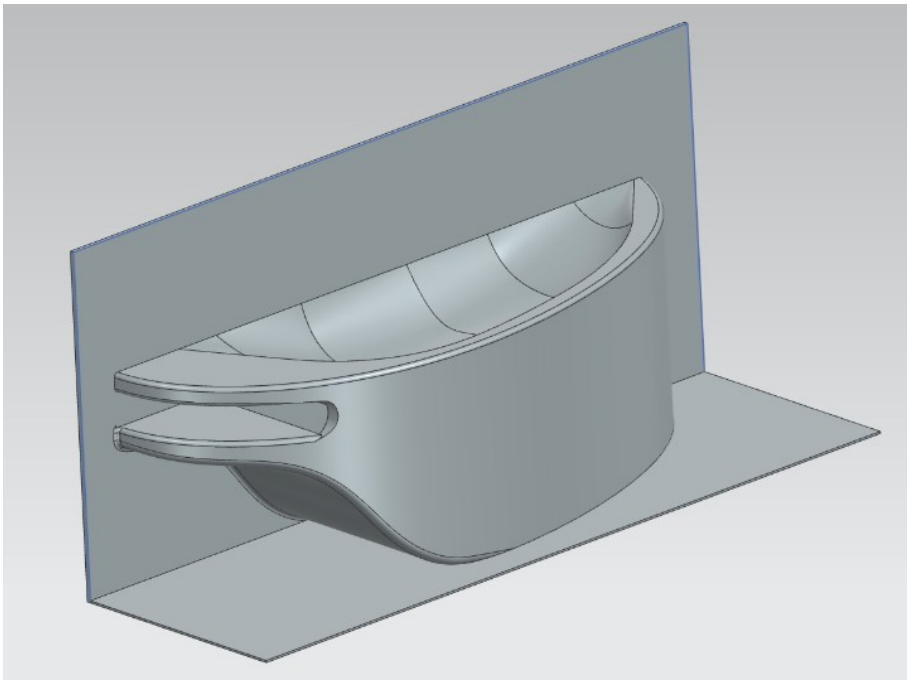


Figure 19 Isolated Ferrari-inspired sidepod geometry used for the CFD analysis

4.2.1 Pressure distribution

Throughout this section, as well as in the corresponding pressure analyses presented for the Mercedes-inspired and Red Bull-inspired configurations in the following chapters, pressure contour plots are displayed using a consistent colour convention: yellow and red tones indicate positive (higher) pressure values, while green and blue tones indicate negative (lower) pressure values. This convention is maintained throughout, unless otherwise stated.

The pressure distribution on the isolated sidepod reveals several characteristic regions, which remain qualitatively similar across the different velocities analysed.

At the front of the sidepod, a region of relatively high pressure is observed, associated with the deceleration of the incoming flow as it meets the bodywork before being redistributed along the upper, lateral and lower surfaces. The front part can therefore be interpreted as a stagnation or partial-stagnation zone, in which part of the flow's kinetic energy is converted into static pressure.

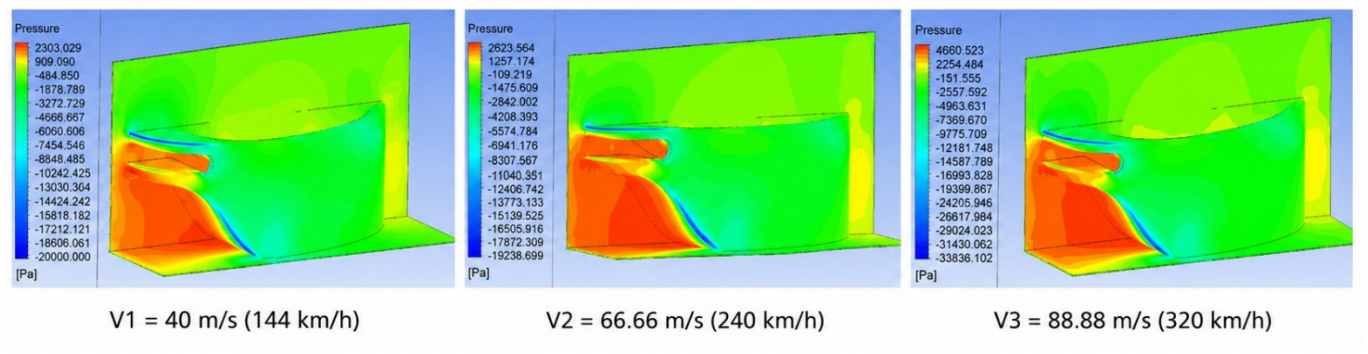


Figure 20 Pressure distribution around the isolated Ferrari-inspired sidepod at 40, 66.66 and 88.88 m/s.

Immediately downstream, the pressure decreases significantly along the front upper curvature: this reduction indicates an acceleration of the flow following the curved surface, and represents one of the first mechanisms through which the geometry modifies the flow field.

A second, particularly pronounced, low-pressure region is visible on the lower part of the sidepod, at the undercut: the flow passing through this region undergoes a marked acceleration. The undercut can therefore be interpreted as a geometric feature designed to create an energised flow path beneath the main volume of the sidepod.

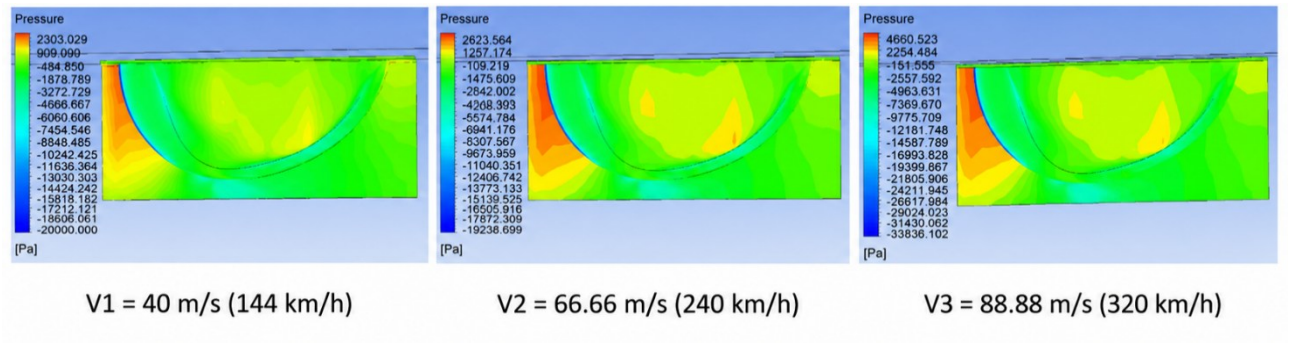


Figure 21 Pressure distribution in the upper basin region of the isolated Ferrari-inspired sidepod at 40, 66.66 and 88.88 m/s.

The concave upper surface shows a different behaviour: the central region of the basin does not coincide with the zone of minimum pressure of the whole geometry, and over most of the surface the pressure values are more moderate. This suggests that the main function of the upper depression is not simply to maximise local suction.

Towards the rear of the upper channel, an increase in pressure is observed, consistent with a pressure recovery phenomenon, in which the flow progressively decelerates after the acceleration phase. This higher pressure could locally contribute to the vertical component of the aerodynamic force, depending on the surface orientation; however, the pressure distribution alone does not allow one to conclude that direct downforce generation is the main function of the upper basin; the streamline pattern instead suggests a flow-direction control function.

4.2.2 Velocity field

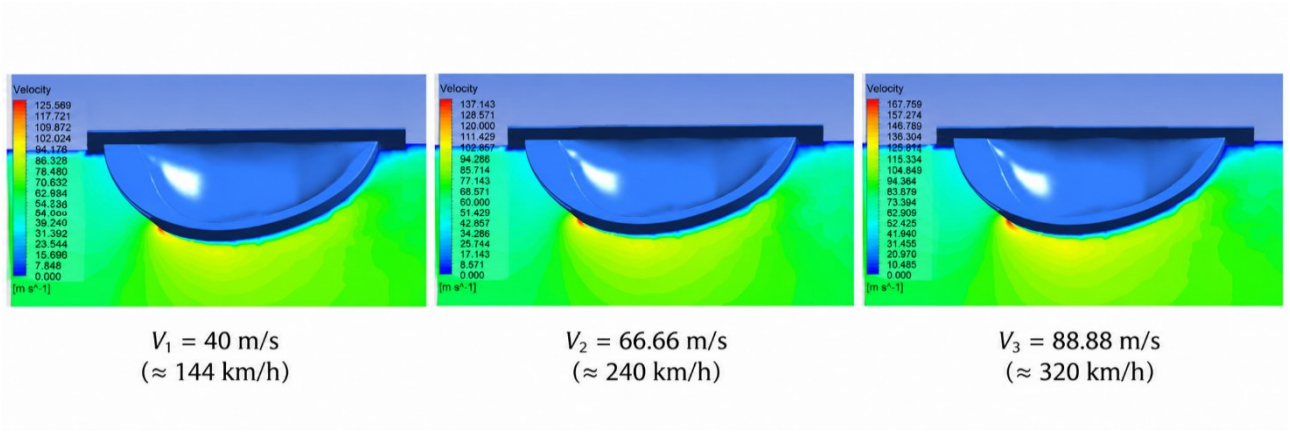


Figure 22 Velocity field around the isolated Ferrari-inspired sidepod at 40, 66.66 and 88.88 m/s.

The comparison of the velocity fields at 40, 66.66 and 88.88 m/s shows that the main flow structures remain qualitatively similar as the freestream velocity increases. In all three cases, the flow decelerates in the front region of the sidepod and is subsequently redistributed around the geometry.

The most evident acceleration occurs in the lower part of the sidepod, particularly through the undercut, where the flow velocity increases as the air follows the curved lower surface. This behaviour is observed at all three investigated velocities, with the same high-velocity region becoming progressively more intense as the freestream velocity increases.

The combined interpretation of the pressure and velocity fields is therefore consistent: regions characterised by lower static pressure correspond to regions of higher local velocity.

The similarity of the velocity-field topology at the three operating conditions suggests that the Ferrari-inspired sidepod maintains the same basic aerodynamic mechanism throughout the analysed velocity range. Increasing the freestream velocity intensifies the acceleration around the geometry, but does not produce an evident change in the main flow paths.

4.2.3 Streamlines and flow behaviour

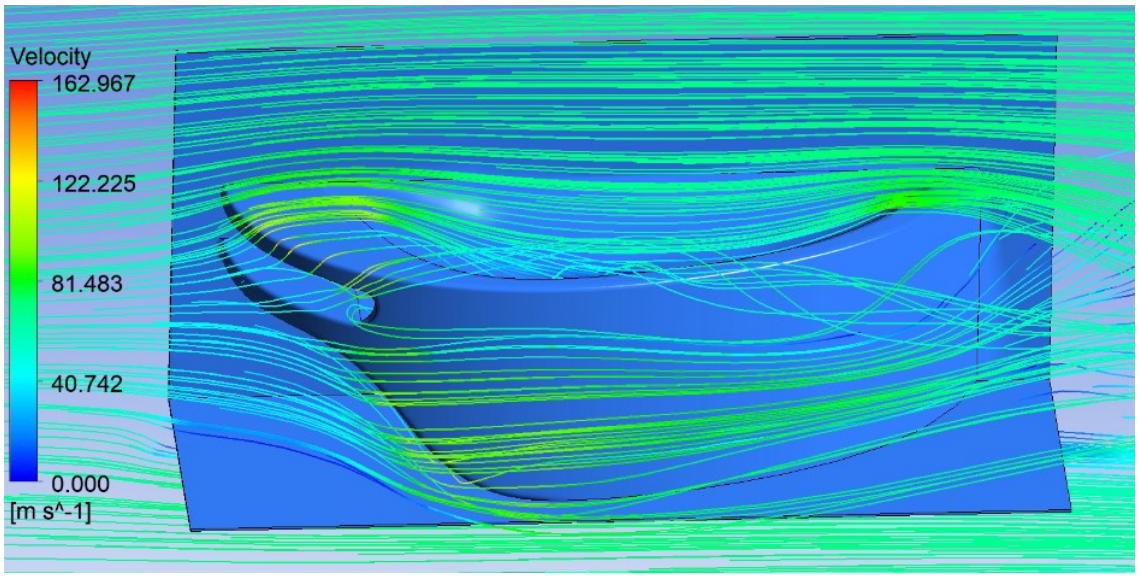


Figure 23 Streamline distribution around the isolated Ferrari-inspired sidepod at 66.66 m/s.

Only the 66.66 m/s condition is shown in the following streamline visualisations, since the overall flow behaviour was found to be analogous at the other investigated velocities. The main streamline paths and the characteristic flow structures remain qualitatively similar, while the primary differences are mainly related to the magnitude of the local velocity.

The incoming flow is split into different paths as it reaches the front region of the sidepod: part follows the upper surface, another follows the lateral part, while a further portion is drawn into the lower undercut region. This flow separation is one of the main features of the Ferrari-inspired concept.

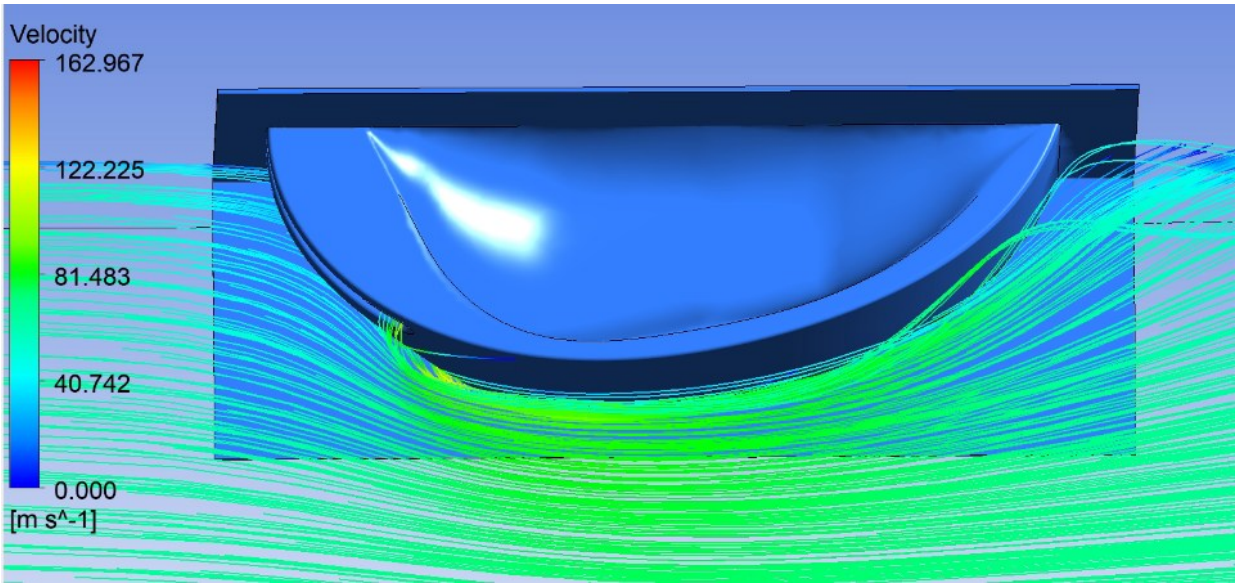


Figure 24 Lateral streamline distribution through the lower undercut of the isolated Ferrari-inspired sidepod at 66.66 m/s.

The streamlines passing through the undercut show a clear acceleration and remain relatively close to the lower surface before being progressively directed downstream after the narrowest section. The lower part of the sidepod therefore acts as a region of active flow acceleration and channelling, rather than as a simple passage.

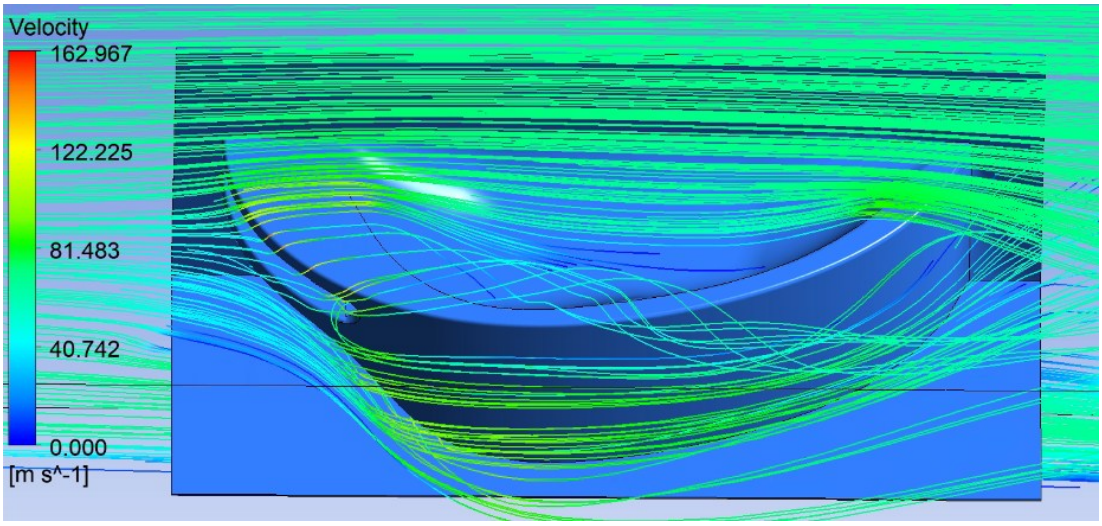


Figure 25 Lateral streamline distribution around the isolated Ferrari-inspired sidepod at 66.66 m/s.

The upper surface shows a different behaviour. The streamlines entering the concave region follow the basin-shaped channel and are progressively deflected towards the rear. The upper depression therefore behaves as an open three-dimensional channel, whose main effect is to gradually modify the direction of the flow rather than to generate the highest local velocity.

Functional summary:

Undercut → acceleration and channelling of the lower flow

Upper channel → organisation and directional control of the flow

The streamline trajectories remain qualitatively similar as velocity increases: local velocities grow, but the main paths generated by the sidepod do not change significantly, confirming the stability of the geometry's aerodynamic function over the analysed range.

4.2.4 Wall shear stress

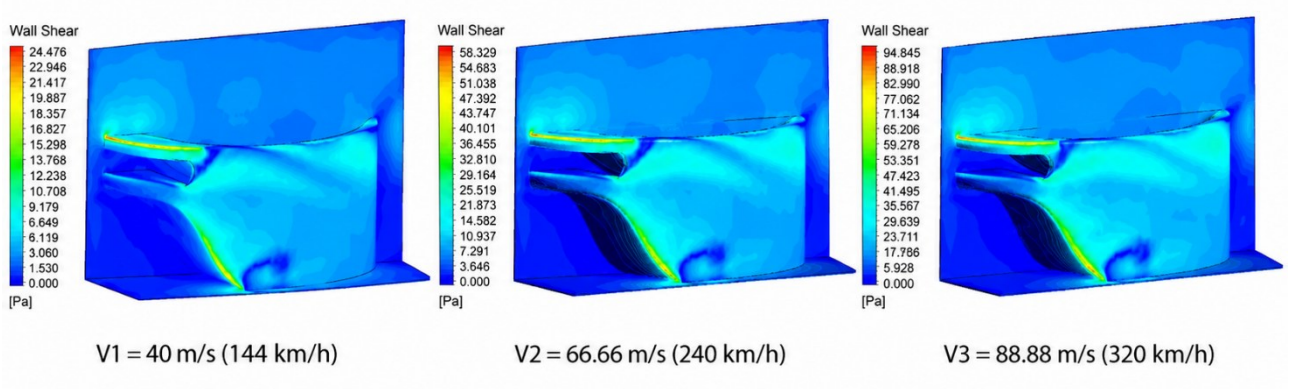


Figure 26 Wall shear stress distribution around the isolated Ferrari-inspired sidepod at 40, 66.66 and 88.88 m/s.

The highest wall shear stress values are concentrated near the front upper curvature and the undercut region, the same zones in which static pressure decreases and the streamlines show strong local acceleration. The combined interpretation of the three quantities is consistent:

$$p \downarrow , V \uparrow , \tau_w \uparrow$$

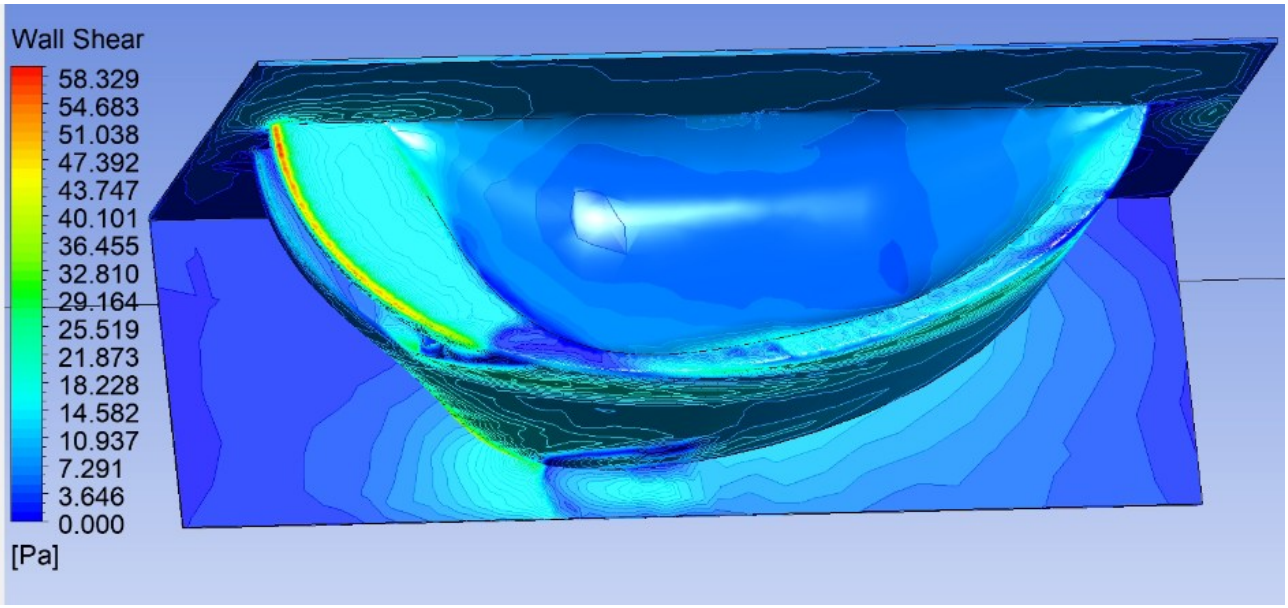


Figure 27 Wall shear stress distribution in the upper basin region of the isolated Ferrari-inspired sidepod at 66.66 m/s.

The central part of the upper channel generally shows lower shear values than the front upper edge and the undercut, further confirming that the basin surface mainly performs a flow-trajectory control function rather than an acceleration function. Despite the increase in intensity, the spatial distribution remains comparable: the same zones remain aerodynamically more active across the different operating conditions.

4.3 CFD Analysis of the Ferrari Configuration on the Complete Car

The second phase of the analysis concerns the Ferrari-inspired sidepod installed on the complete model of the car. This configuration introduces the interaction between the sidepod and the other main aerodynamic elements of the car: the flow reaching the sidepod has already been influenced by the front of the car, the front wheel and the suspension, while the downstream flow interacts with the rear wheel, the floor and the rear aerodynamic components.

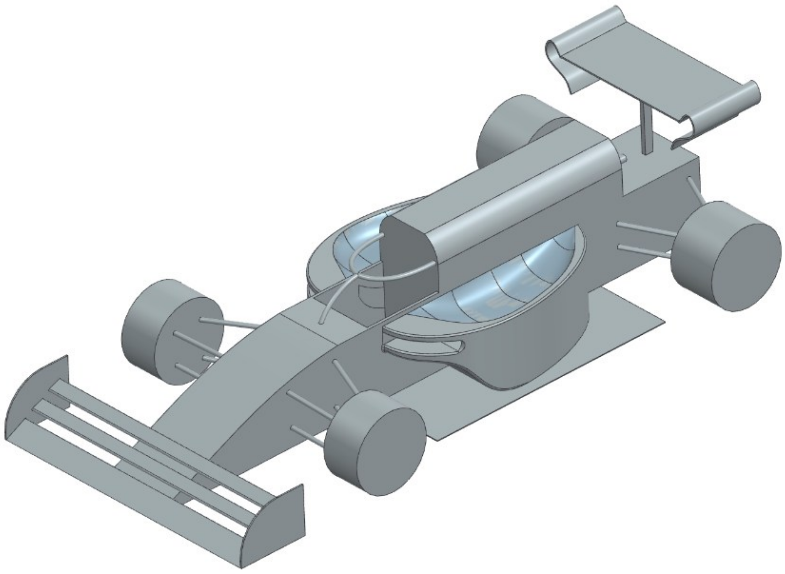


Figure 28 Complete Formula 1 CAD model with the Ferrari-inspired sidepod configuration.

4.3.1 Global aerodynamic results

The global aerodynamic forces obtained for the complete Ferrari-inspired configuration are reported in Table 3.

Velocity	Drag Force	CD	Downforce	CL
40 m/s	470 N	0.65	170 N	-0.23
66.66 m/s	1320 N	0.65	420 N	-0.21
88.88 m/s	2350 N	0.66	720 N	-0.21

Table 3 Aerodynamic forces and coefficients of the Ferrari-inspired complete-car configuration at the three investigated velocities.

In this and in the following tables, downforce is reported as a positive magnitude, consistent with the convention introduced in Section 2.2, while the lift coefficient retains its conventional negative sign.

The aerodynamic coefficients obtained for the complete Ferrari-inspired configuration are lower than the values typically associated with a real Formula 1 car. This difference is mainly due to the simplified aerodynamic model adopted in the present study. In particular, the underfloor geometry does not reproduce the complete Venturi tunnels of a 2022 Formula 1 car, several secondary aerodynamic devices were omitted, the rear wing was simplified, the wheels were stationary, and no moving-ground condition was applied. As a consequence, the model does not generate the same overall aerodynamic load as a complete real vehicle.

Nevertheless, the absolute magnitude of the aerodynamic coefficients is not the primary objective of the present analysis. Since the same baseline geometry, numerical setup, reference quantities, and operating conditions are maintained for all three sidepod configurations, the results remain suitable for a relative comparison between the different concepts. The trends observed for the Ferrari-inspired configuration can therefore be considered meaningful within the scope of this study, particularly when compared with the Mercedes- and Red Bull-inspired cases under the same conditions.

The drag coefficient remains nearly constant over the investigated velocity range, varying only from approximately 0.65 to 0.66. A similar trend is observed for the lift coefficient, whose magnitude also remains within a relatively narrow range as the freestream velocity increases. This indicates that the overall aerodynamic behaviour of the configuration remains fairly stable over the investigated operating conditions, while the aerodynamic forces increase mainly as a consequence of the increase in dynamic pressure.

4.3.2 Pressure distribution on the complete car

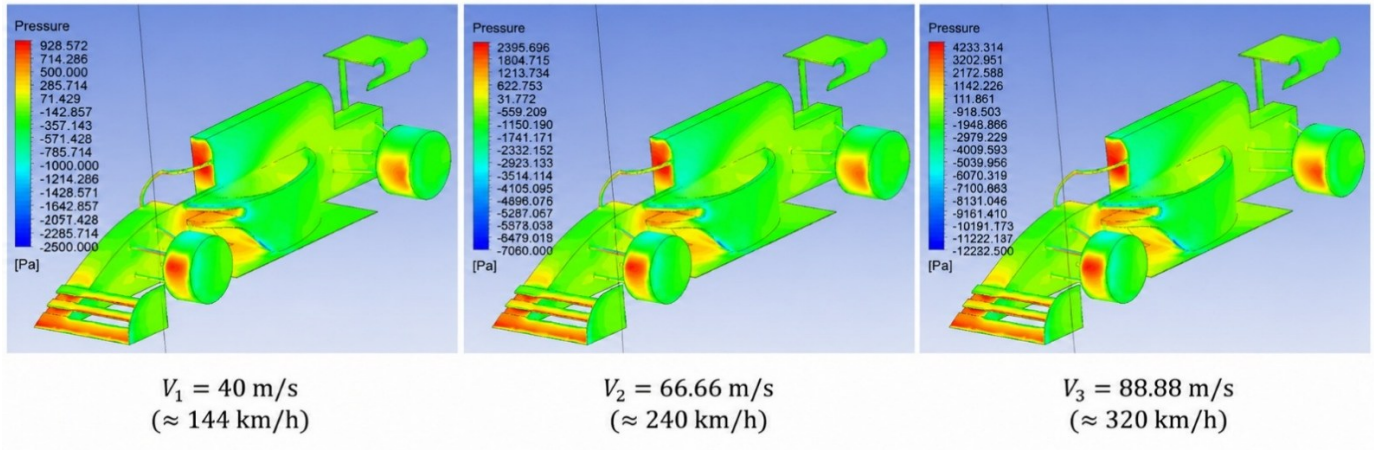


Figure 29 Pressure distribution over the complete Ferrari-inspired configuration at 40, 66.66 and 88.88 m/s.

Unlike the isolated case, the flow reaching the sidepod is no longer uniform: before reaching the lateral region of the car, the air has already interacted with the front section, the wheel and the suspension, and the pressure field around the sidepod is therefore more three-dimensional and less uniform. Nevertheless, the main features identified in the isolated case remain recognisable.

In the front region of the sidepod, a relatively high-pressure zone is still present, but it is less pronounced than in the isolated configuration. This does not demonstrate that the sidepod generates less drag once installed, since a separate force integration is not available, but it does show that the local aerodynamic behaviour of the sidepod changes significantly once the component is placed within the complete car: analysis of the isolated component alone is not sufficient to fully describe its real aerodynamic behaviour.

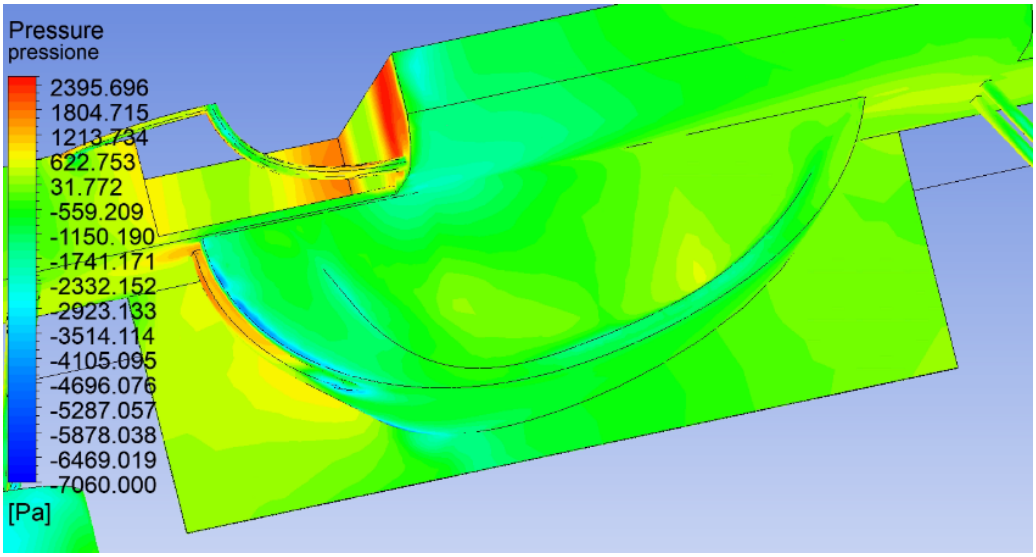


Figure 30 Pressure distribution in the Ferrari-inspired sidepod region of the complete car at 66.66 m/s.

The low-pressure zone associated with the front upper curvature remains visible, as does the undercut depression: the persistence of these regions shows that the main aerodynamic mechanisms of the geometry are preserved even after installation. The upper channel also continues to show more moderate pressures in the central region, followed by a recovery towards the rear, consistent with a geometry designed to progressively control and redirect the upper flow.

The increase in pressure intensity with velocity is not accompanied by a substantial change in spatial distribution: even on the complete car, the main pressure structures remain stable while their intensity increases.

4.3.3 Velocity field in the sidepod region

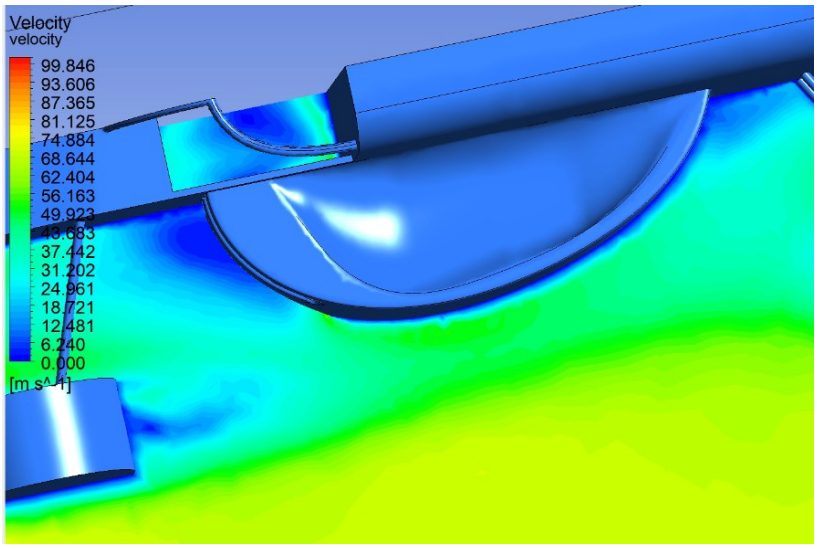


Figure 31 Velocity field around the Ferrari-inspired sidepod region of the complete car at 66.66 m/s.

Only the 66.66 m/s condition, corresponding to approximately 240 km/h, is shown in Figure 31, since the simulations performed at 40 m/s and 88.88 m/s exhibited the same overall flow topology. The main differences between the three operating conditions were associated with the magnitude of the local velocity rather than with significant changes in the flow path.

The velocity field around the complete Ferrari-inspired configuration is clearly influenced by the presence of the upstream vehicle components. As a result, the flow approaching the sidepod is not perfectly uniform, unlike in the isolated-sidepod case.

In the lower region, the undercut continues to create a preferential flow path along the lower surface of the sidepod. The airflow is guided through this region and progressively directed towards the rear, confirming that the lower geometry retains an important flow-management function even when integrated into the complete vehicle.

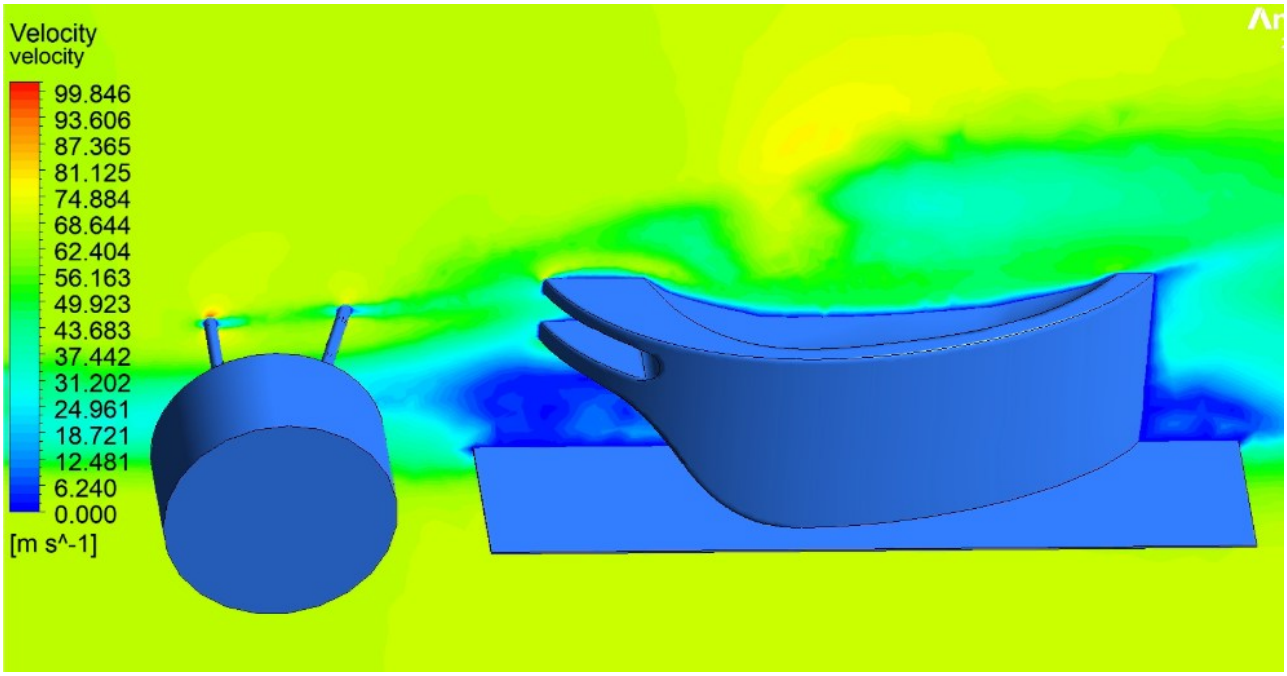


Figure 32 Lateral velocity field around the Ferrari-inspired sidepod on the complete car at 66.66 m/s.

The upper concave region shows a different behaviour. As visible in Figure 32, the flow inside the basin-shaped surface is characterised by a lower velocity than the external flow passing above it. This indicates that the upper depression does not primarily act as a region of strong acceleration. Instead, its main aerodynamic role is to guide and progressively redirect the airflow towards the rear of the vehicle.

The reduced velocity observed within the concave region is therefore consistent with a flow-guiding function, while the faster external flow remains above the upper surface. This behaviour confirms the complementary roles of the two main regions of the Ferrari-inspired sidepod: the lower undercut mainly controls and channels the airflow along the lower part of the bodywork, whereas the upper concave surface primarily influences its direction.

Overall, the complete-vehicle simulation shows that the characteristic flow-management behaviour already identified in the isolated-sidepod analysis is preserved, although the velocity field becomes more complex because of the interaction with the rest of the car.

4.3.4 Streamlines and flow

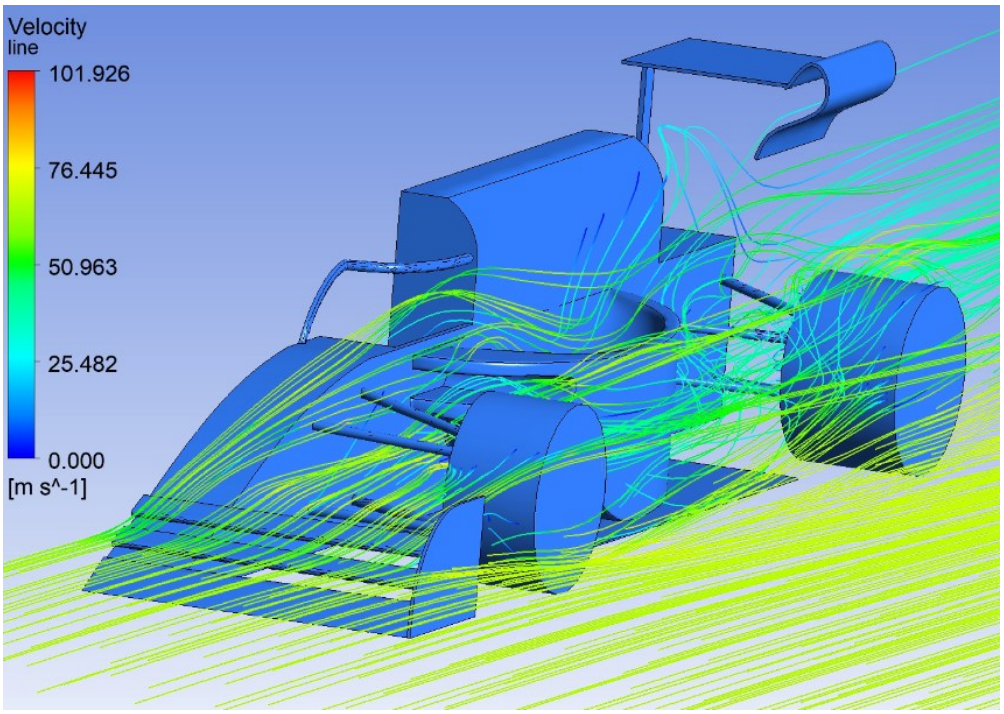


Figure 33 Streamline distribution around the complete Ferrari-inspired configuration at 66.66 m/s.

Although the flow reaching the sidepod is already disturbed, the lower path maintains behaviour similar to the isolated case: the air is drawn into the undercut, accelerates, and is then directed towards the rear of the car. The complete configuration shows more clearly the fate of this flow: whereas in the isolated case it was simply released downstream of the domain, on the complete car it is directed towards the lower region of the rear end, where it can interact with the floor edge, the diffuser area and the flow structures associated with the rear wheel.

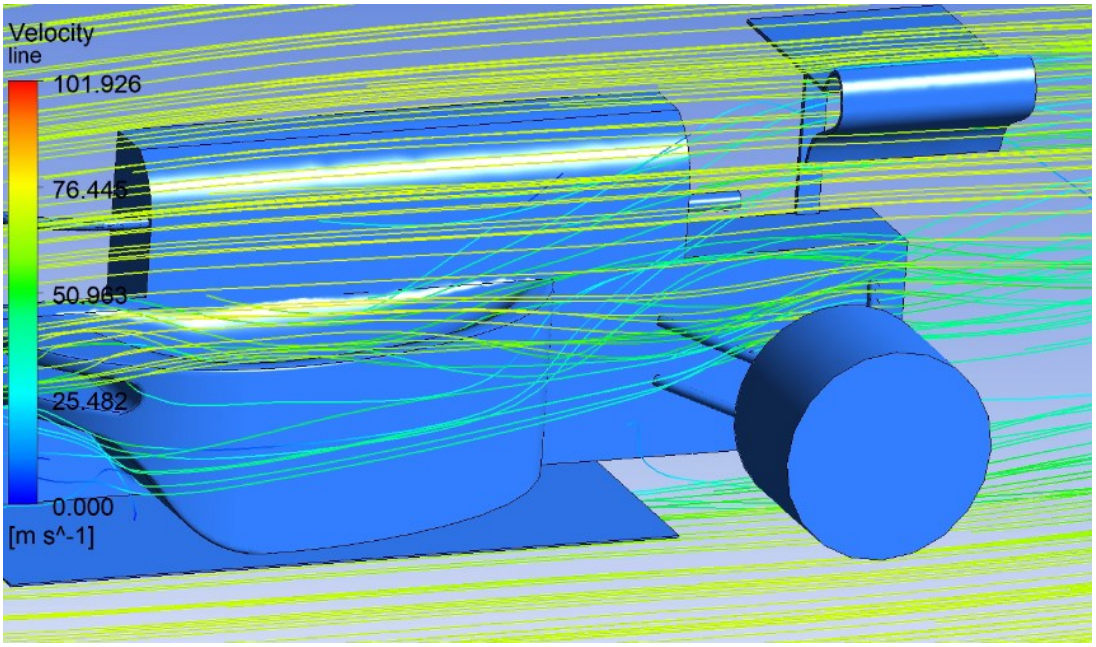


Figure 34 Lateral streamline distribution around the Ferrari-inspired sidepod on the complete car at 66.66 m/s.

The upper channel instead generates a different path: the streamlines following the concave surface are progressively redirected towards the upper part of the rear end. This is one of the most significant observations obtained from the complete-car simulation. The basin surface behaves as a three-dimensional channel that gradually changes the direction of a substantial portion of the upper flow, directing it towards the region occupied by the rear aerodynamic system (rear wing).

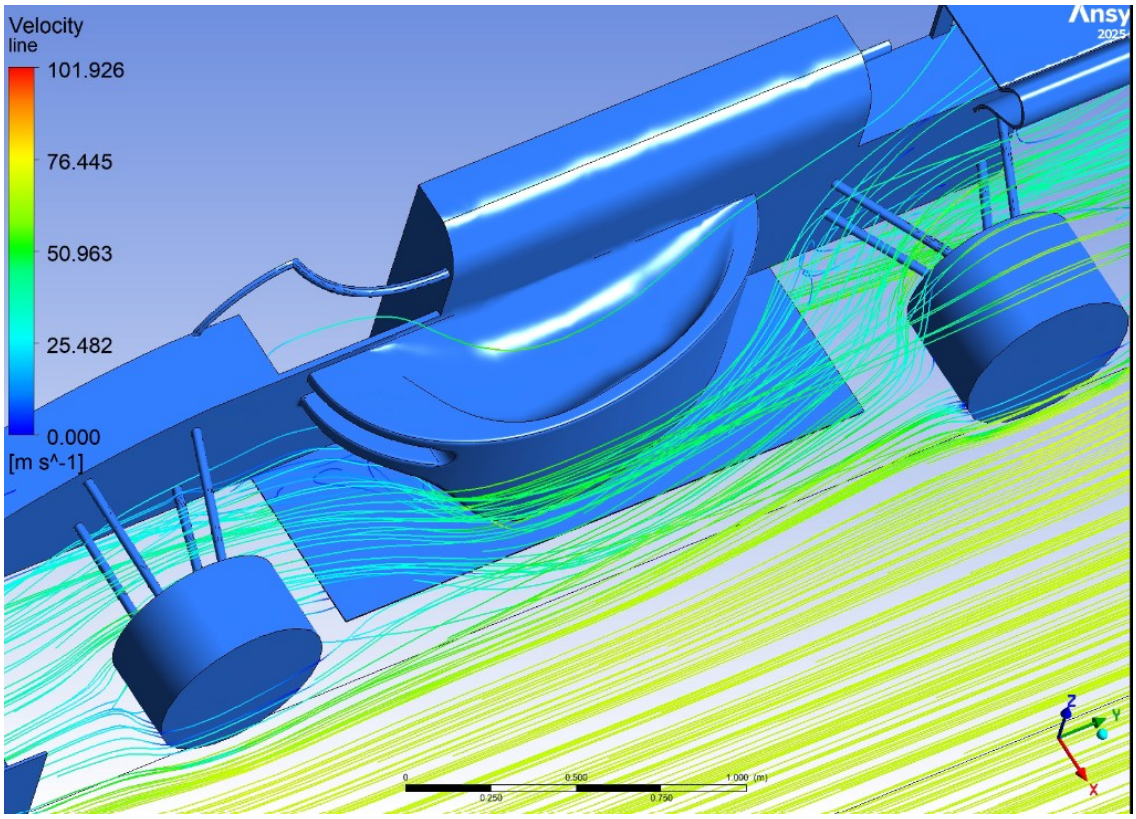


Figure 35 Streamline distribution around the Ferrari-inspired sidepod region of the complete car at 66.66 m/s.

A more energetic, better-oriented flow reaching these components could potentially improve their operating conditions; however, the CFD results obtained in this study do not directly quantify the load generated by the rear wing as a consequence of this flow. The possible improvement in the efficiency of the rear system should therefore be regarded as a qualitative aerodynamic interpretation, not as a quantitatively demonstrated effect.

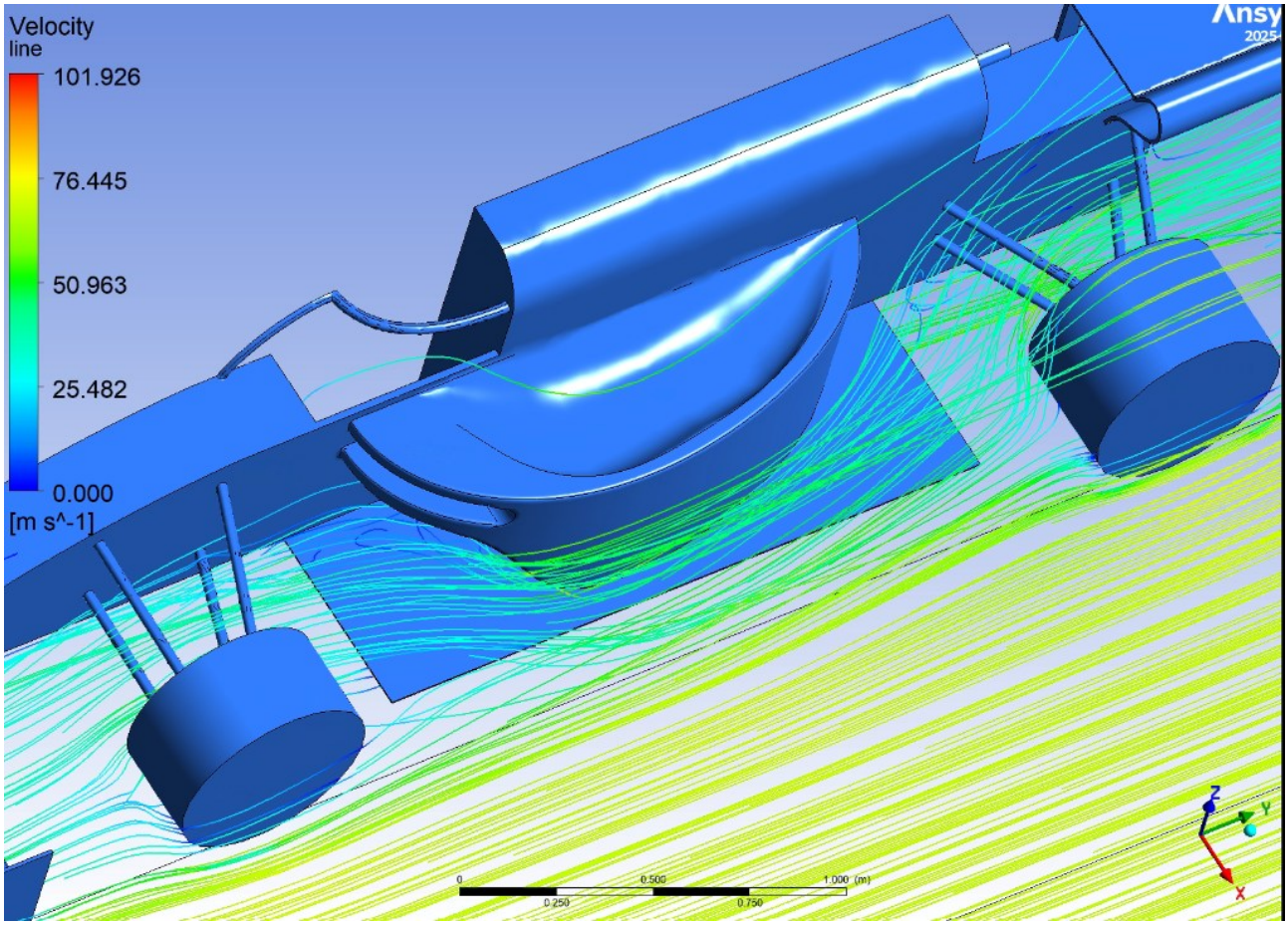


Figure 36 Streamline distribution around the Ferrari-inspired sidepod and rear-wheel region at 66.66 m/s.

The higher pressure observed towards the rear end of the basin should mainly be interpreted as part of the pressure-recovery process associated with the deflection and subsequent deceleration of the flow. Although this pressure distribution may locally contribute to the vertical force component, depending on the surface inclination, the streamline analysis suggests that the main function of the geometry is not to generate local aerodynamic load directly. Instead, the basin-shaped surface primarily manages and redirects the airflow towards the rear of the car, with the objective of providing more favourable flow conditions for downstream aerodynamic components, particularly the floor and diffuser, whose performance strongly depends on the quality, direction and energy of the incoming flow.

4.3.5 Wall shear stress on the complete car

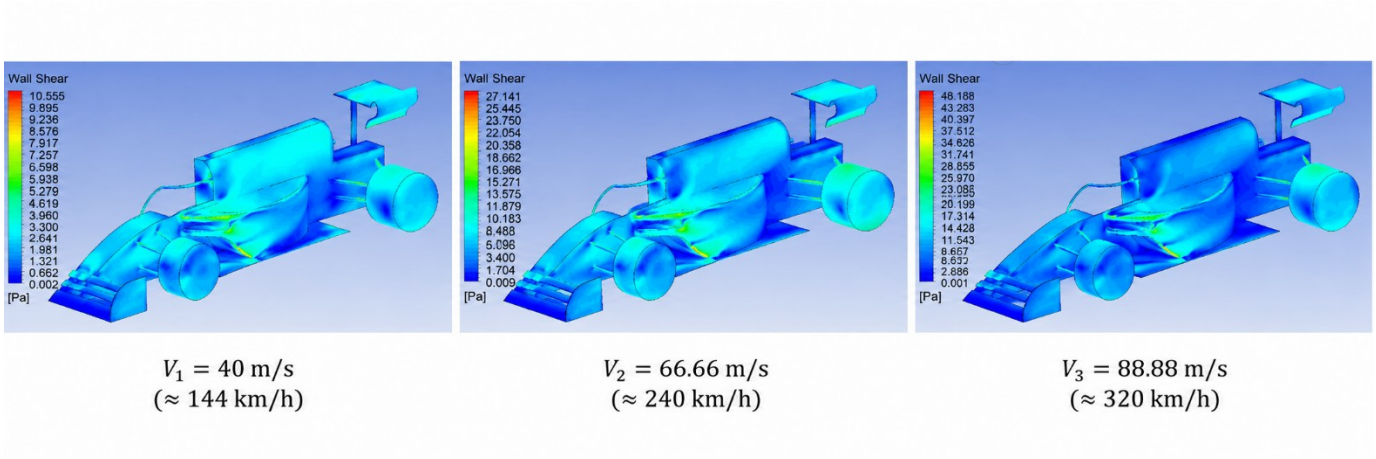


Figure 37 Wall shear stress distribution over the complete Ferrari-inspired configuration at 40, 66.66 and 88.88 m/s.

Despite the increase in intensity, the regions with the highest shear values remain substantially similar: the front upper edge and the undercut entry continue to represent some of the aerodynamically most active surfaces. The central part of the basin generally shows lower values, reinforcing the distinction between the strongly accelerated lower flow and the mainly guided upper flow. Regions of reduced wall shear stress are also visible in the rear areas and in the zones affected by the car's wake, indicating a weaker near-wall flow interaction, though these cannot be identified with certainty as separation zones on the basis of shear intensity alone.

4.4 Comparison between the isolated sidepod and the complete car

The analysis of the Ferrari-inspired configuration reveals a sidepod concept in which the relatively large bodywork volume is actively exploited to control the external flow, rather than simply being minimised to reduce frontal area.

Simulations of the isolated sidepod show a geometry that generates clearly distinct aerodynamic regions. At the front, a high-pressure zone forms where the flow decelerates and splits into different paths; immediately downstream, the upper curvature and the undercut produce a marked acceleration of the air. The undercut in particular emerges as one of the most aerodynamically active areas of the sidepod: pressure, velocity, streamlines and wall shear stress all converge in indicating an energised flow path close to the lower surface and directed downstream.

The upper concave surface serves a different purpose. It coincides neither with the region of maximum acceleration nor with that of minimum pressure, but instead progressively alters the direction of the upper flow, guiding it towards the rear of the car. It therefore behaves more as a flow-management channel than as a direct generator of local aerodynamic load.

The underlying design choice is significant: achieving flow deflection through a concave surface integrated into the bodywork rather than through a separate aerodynamic element. A small wing profile could produce a similar effect and generate a local aerodynamic force, but it would also introduce its own drag and additional wake, risking degradation of the flow delivered to the rear of the car. The Ferrari-inspired solution instead uses a surface already required by the bodywork to steer a considerable amount of flow in a continuous, gradual manner — the upper low-pressure region can thus be interpreted as an integrated flow-management solution.

When the sidepod is installed on the complete car, the fundamental mechanisms remain recognisable, despite an inlet flow made far more complex by the upstream elements: the undercut continues to accelerate the lower flow, while the upper channel continues to redirect the upper flow. Integration with the rest of the monocoque does, however, attenuate some features observed in the isolated case — in particular, the front high-pressure region appears less pronounced — confirming that the aerodynamic behaviour of the sidepod cannot be fully assessed by considering the component in isolation.

One of the most significant results concerns the upper streamline trajectories: the concave surface deflects part of the flow towards the rear aerodynamic region, suggesting that the aim of the geometry is not only to generate local load on the sidepod, but also to improve the quality and direction of the flow supplied to the downstream components. The two regions can therefore be read as complementary systems:

- **Undercut** → acceleration and channelling of the lower flow
- **Upper channel** → organisation and redirection of the upper flow

Increasing the velocity intensifies these effects without substantially altering their spatial distribution or overall topology: within the range analysed, the Ferrari-inspired configuration exhibits a coherent and stable aerodynamic mechanism.

Overall, the results suggest that the primary aerodynamic objective of this sidepod philosophy is neither purely local drag reduction nor the direct generation of downforce by the surface itself. The large, strongly sculpted volume acts instead as a three-dimensional flow-management device, capable of creating and controlling distinct air paths and subsequently influencing the aerodynamic behaviour of the entire car. This consideration will be particularly important in the forthcoming comparison with the Mercedes and Red Bull sidepod concepts: the Ferrari-inspired configuration should be assessed not so much through the local behaviour of the component, but above all through the effect that the flow field it generates produces on the car's overall aerodynamic system.

Chapter 5

MERCEDES CONFIGURATION: RESULTS AND AERODYNAMIC ANALYSIS

5.1 Introduction to the Mercedes configuration

The Mercedes configuration was developed with the aim of reproducing the main aerodynamic features associated with the sidepod concept introduced on the Mercedes W13 during the 2022 Formula 1 season. This concept is characterised by an extremely reduced lateral bodywork volume, a very narrow radiator inlet region, and a large open area between the central bodywork and the outer portion of the floor.

The purpose of this chapter is to analyse how these geometric features influence the surrounding flow field and to identify the main aerodynamic mechanisms generated by the sidepod. The analysis is divided into two phases: first, the Mercedes-inspired sidepod is studied as an isolated component, in order to identify the aerodynamic behaviour directly associated with its geometry; subsequently, the same sidepod is analysed after installation on the complete model of the car, so as to evaluate how the flow structures observed in the isolated case are modified by interaction with the other aerodynamic components. Three freestream velocities were analysed:

V_1 = 40 m/s V_2 = 66.66 m/s V_3 = 88.88 m/s

corresponding respectively to approximately 144, 240 and 320 km/h. The analysis focuses on the pressure distribution, the velocity field, the streamlines and the wall shear stress. Particular attention is devoted to the narrow central bodywork, to the lower and lateral flow paths, and to the large open region between the sidepod and the floor, since the simulations show that these areas play a central role in reducing flow obstruction and managing the airflow towards the floor and the rear of the car.

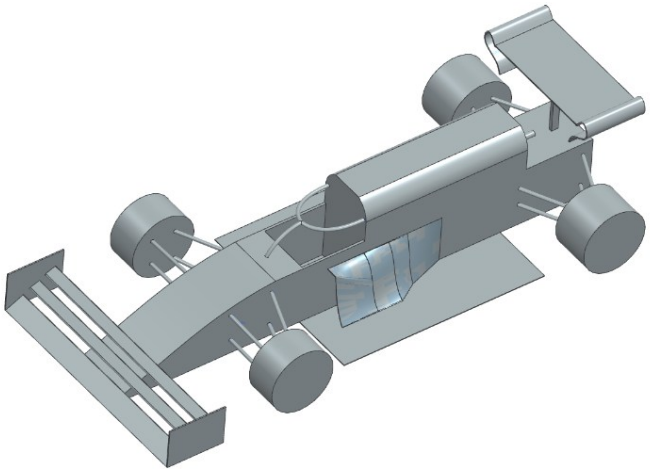


Figure 38 Complete Formula 1 CAD model with the Mercedes-inspired sidepod configuration.

5.2 Aerodynamic Analysis of the Isolated Mercedes-Inspired Sidepod

The isolated-sidepod simulations were performed to identify the aerodynamic behaviour generated directly by the Mercedes-inspired geometry, without the influence of the other vehicle components.

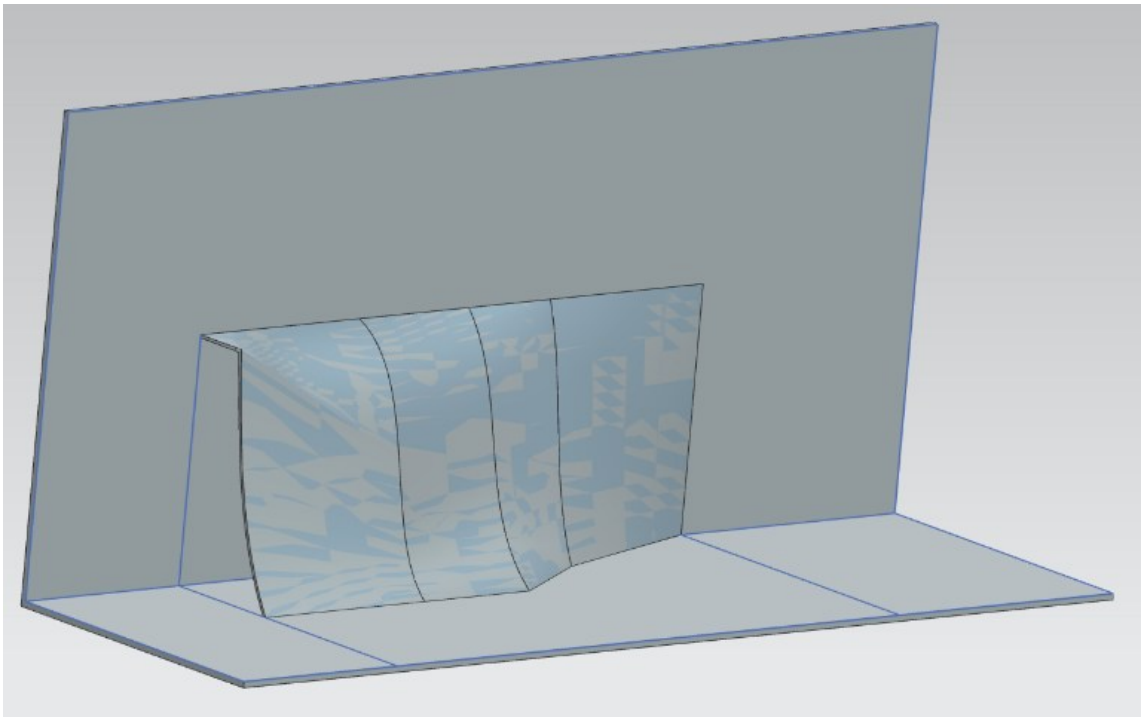


Figure 39 Isolated Mercedes-inspired sidepod geometry used for the CFD analysis.

This configuration provides a useful reference because the incoming flow is approximately uniform. Consequently, pressure variations, acceleration regions and possible local flow separation can be directly associated with the sidepod geometry itself.

The isolated analysis allows the aerodynamic behaviour of the Mercedes concept to be examined independently of the rest of the vehicle. Unlike configurations based on a large external bodywork volume, the Mercedes-inspired concept relies on a strong reduction of the lateral volume. The analysis therefore aims to determine whether the compact geometry promotes a relatively unobstructed and energetic lateral flow path, while also identifying any local aerodynamic effects associated with rapid changes in surface curvature.

5.2.1 Pressure distribution

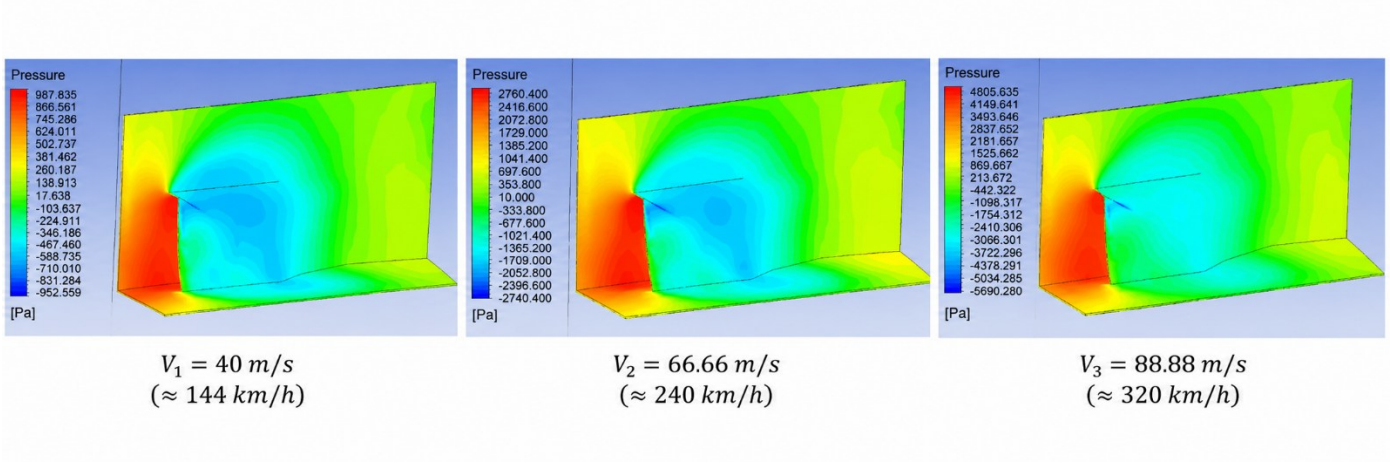


Figure 40 Pressure distribution around the isolated Mercedes-inspired sidepod at 40, 66.66 and 88.88 m/s.

The pressure distributions obtained for the three investigated freestream velocities are shown in Figure 40. A qualitatively similar pressure pattern can be observed across the entire velocity range, while the magnitude of the pressure variations increases progressively with freestream velocity.

In all three cases, a high-pressure region develops at the front of the Mercedes-inspired sidepod, where the incoming flow decelerates before being redirected around the geometry. Immediately downstream of this region, the pressure decreases significantly, producing a pronounced low-pressure area that extends along the lateral surface of the sidepod. This behaviour is consistent with a local acceleration of the flow around the compact bodywork.

Further downstream, the pressure gradually recovers as the influence of the initial acceleration decreases. The overall pressure distribution can therefore be described by a sequence of frontal overpressure, rapid pressure reduction around the leading portion of the sidepod, and progressive pressure recovery towards the rear.

As the freestream velocity increases from 40 m/s to 66.66 m/s and finally to 88.88 m/s, the same characteristic regions remain approximately in the same positions, while both the positive and negative pressure values increase in magnitude. This indicates that increasing velocity mainly strengthens the aerodynamic effects generated by the geometry rather than significantly modifying the overall topology of the pressure field.

The results therefore suggest that the reduced lateral volume of the Mercedes-inspired concept allows the external flow to accelerate rapidly around the front and lateral regions of the sidepod, generating a clearly defined low-pressure region downstream of the leading edge.

5.2.2 Velocity field

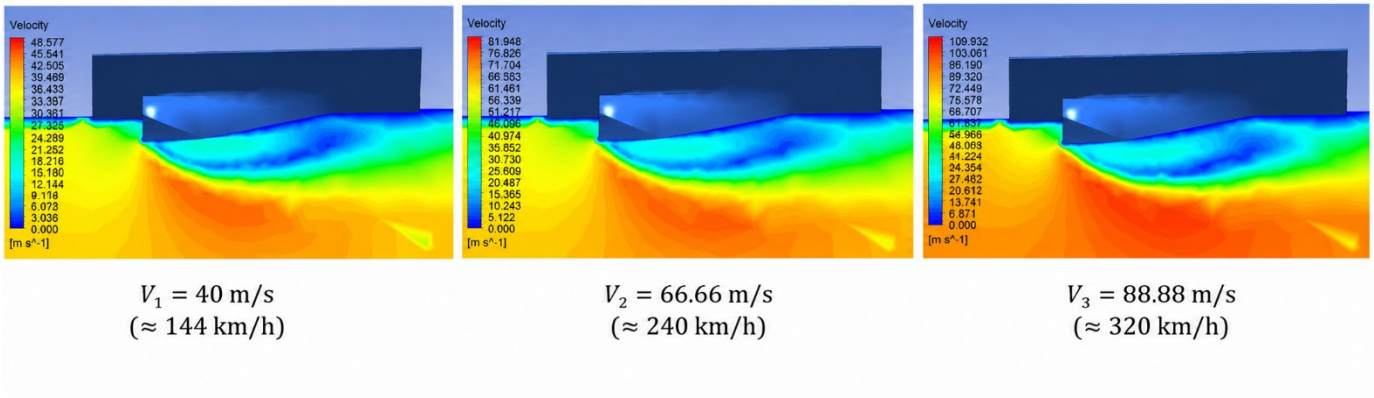


Figure 41 Velocity field around the isolated Mercedes-inspired sidepod at 40, 66.66 and 88.88 m/s.

The velocity fields obtained for the three investigated freestream conditions are shown in Figure 41. In all cases, the same general flow pattern can be observed, while the magnitude of the local velocity increases with the freestream velocity.

A clear acceleration region develops around the lower part of the Mercedes-inspired sidepod and immediately downstream of its leading portion. This behaviour is consistent with the pressure distribution discussed previously, since the regions characterised by lower static pressure correspond to areas in which the local flow velocity increases.

At 40 m/s, the flow already accelerates beyond the freestream value in the lower and lateral regions of the geometry. At 66.66 m/s, the same acceleration pattern becomes more intense, with local velocities reaching approximately 80 m/s. At 88.88 m/s, the maximum values visible in the contour approach approximately 110 m/s.

These values represent local velocity peaks and should not be interpreted as characteristic velocities of the entire flow field. The location of the main acceleration region remains approximately unchanged across the three operating conditions, indicating that the increase in freestream velocity mainly amplifies the aerodynamic effect generated by the geometry without substantially altering the overall flow-field topology.

5.2.3 Streamlines and flow behaviour

Only the 66.66 m/s condition is shown in the following streamline visualisations, since the overall flow behaviour was found to be qualitatively similar at 40 m/s and 88.88 m/s. The main streamline trajectories remain substantially unchanged as the freestream velocity increases, while the main differences are related to the magnitude of the local velocity.

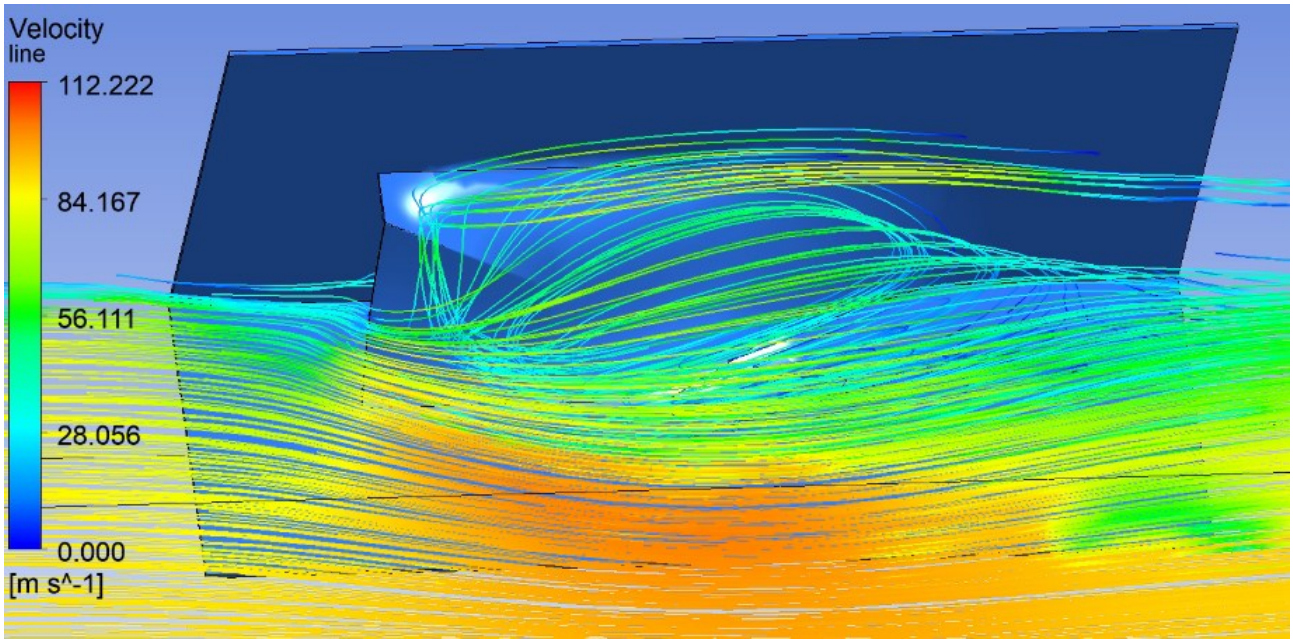


Figure 42 Streamline distribution around the isolated Mercedes-inspired sidepod at 66.66 m/s.

The lateral streamline view shows that the incoming flow is rapidly redistributed around the compact sidepod geometry. A significant portion of the air is accelerated along the lower and lateral regions, where the reduced bodywork volume leaves a relatively open path around the sidepod. This behaviour is consistent with the low-pressure region previously identified in the pressure maps and with the increase in local velocity observed in the velocity field.

At the same time, the lateral view reveals a local recirculation region downstream of the leading portion of the sidepod. Several streamlines undergo strong curvature and form a low-energy region close to the surface, suggesting that the flow is not able to remain fully attached throughout the geometric transition.

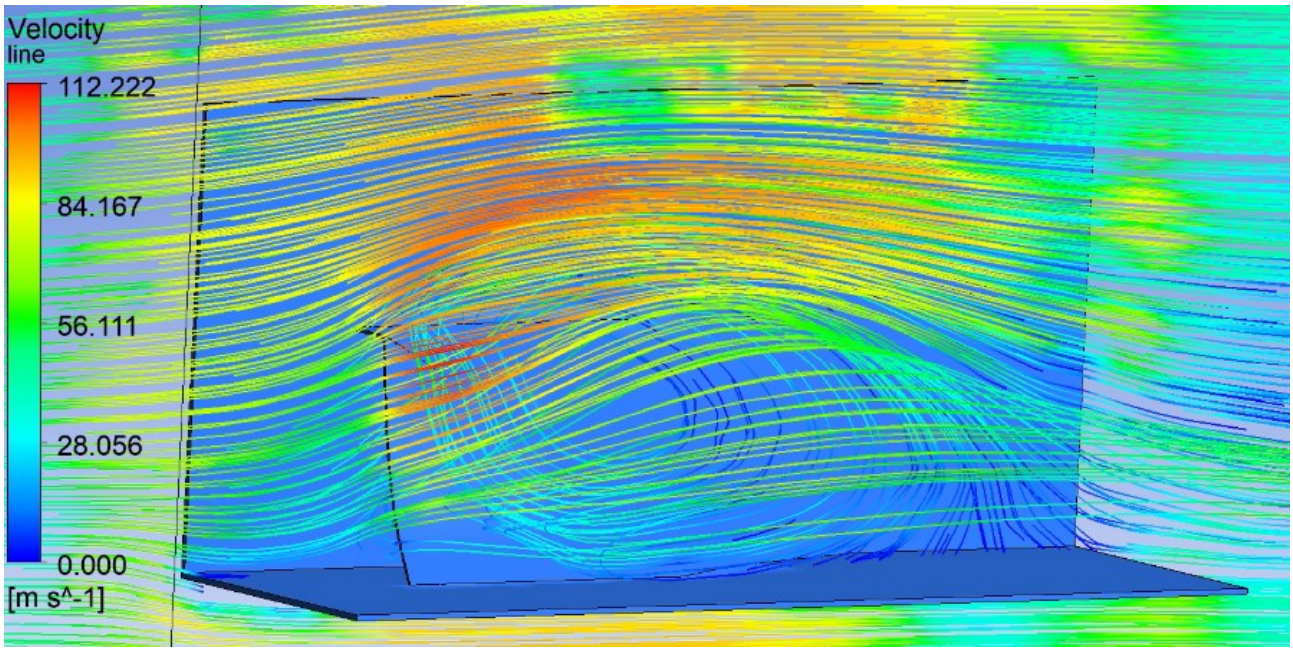


Figure 43 Lateral streamline distribution around the isolated Mercedes-inspired sidepod at 66.66 m/s.

This recirculation may be influenced by the simplified and non-optimised nature of the present Mercedes-inspired geometry. The model reproduces the general concept of the W13 sidepod but does not include the detailed surface optimisation of the real Formula 1 component. Therefore, the observed local separation should be interpreted as a characteristic of the present numerical model rather than as direct evidence of the behaviour of the real W13.

The vertical streamline view provides complementary information on the three-dimensional behaviour of the flow. It shows how part of the incoming air is diverted around the upper and lower portions of the sidepod, while the compact bodywork leaves a large proportion of the flow free to continue downstream. The streamlines therefore confirm that the geometry produces not only local acceleration, but also a significant redistribution of the flow around the sidepod volume.

The combined interpretation of the lateral and vertical views suggests that the main aerodynamic characteristic of the Mercedes-inspired sidepod is the reduction of global blockage rather than the generation of a strongly controlled flow path through a large bodywork volume. The geometry allows a substantial amount of air to pass around the sidepod, although the local recirculation region indicates that this low-blockage strategy may be accompanied by local flow-separation effects.

Overall, the streamline analysis supports the following interpretation:

Reduced sidepod volume → large available flow passage and limited global blockage

Rapid local geometric transition → local recirculation and reduced flow attachment

5.2.4 Wall shear stress

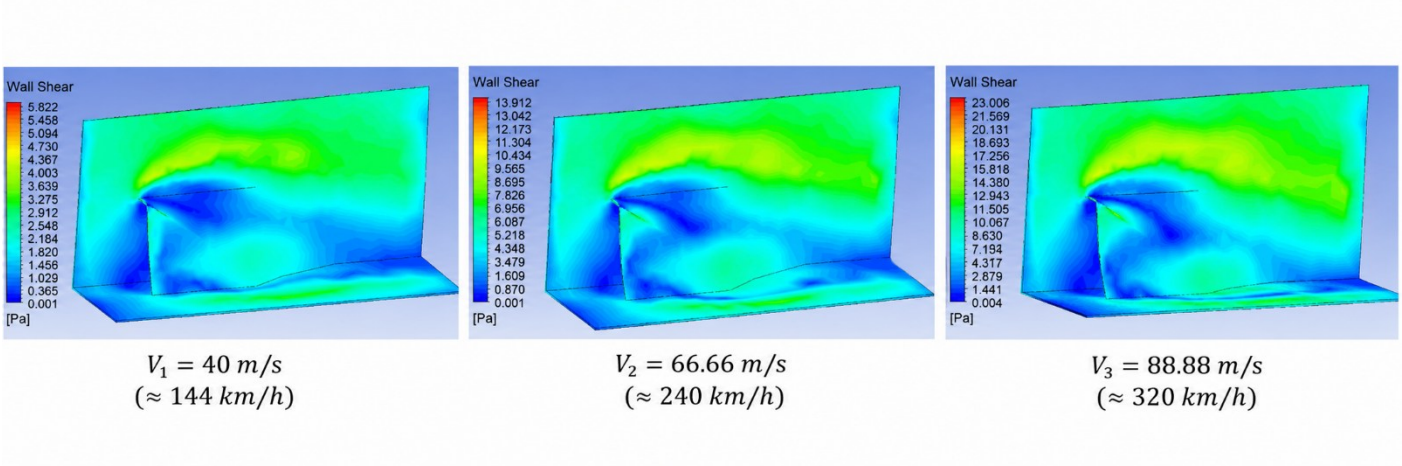


Figure 44 Wall shear stress distribution around the isolated Mercedes-inspired sidepod at 40, 66.66 and 88.88 m/s.

The wall shear stress distribution shows a qualitatively similar pattern across the three investigated freestream velocities. As the velocity increases, the intensity of the wall shear stress rises, while the location of the main regions remains substantially unchanged.

Higher wall shear stress is observed in the areas where the flow remains energetic and attached to the surface, particularly around the leading region and along the zones affected by stronger local acceleration. Conversely, lower wall shear stress values appear in the region downstream of the leading portion, where the near-wall flow loses momentum.

This distribution is consistent with the streamline analysis, which indicates the presence of a local recirculation region in the same area. Although low wall shear stress alone cannot be considered definitive evidence of flow separation, the agreement between the two quantities supports the same qualitative interpretation.

Overall, the wall shear stress results confirm that the Mercedes-inspired geometry maintains a similar aerodynamic behaviour throughout the investigated velocity range, with strongly accelerated attached-flow regions coexisting with a local low-energy region downstream of the leading portion.

5.3 CFD Analysis of the Mercedes Configuration on the Complete Car

The second phase of the analysis concerns the Mercedes-inspired sidepod installed on the complete vehicle model.

The interaction with the rest of the car represents a fundamental aspect of the aerodynamic analysis, since the flow reaching the sidepod is no longer uniform. Before entering the lateral region of the vehicle, the air has already interacted with the front wing, nose, front wheel and suspension. As a result, the flow approaching the sidepod is strongly three-dimensional and characterised by non-uniform velocity and pressure distributions.

Once integrated into the complete car, the sidepod therefore operates in a considerably more complex aerodynamic environment than in the isolated configuration. The local flow structures generated by the geometry are modified by the upstream disturbances, while the downstream flow interacts with the floor, rear wheel, diffuser region and rear aerodynamic components.

The complete-car analysis is particularly important for the Mercedes-inspired concept because the main aerodynamic benefit of the reduced sidepod volume is expected to emerge from its interaction with the overall vehicle rather than from the local behaviour of the sidepod alone. The narrow bodywork leaves a large lateral region available to the airflow, potentially reducing aerodynamic blockage and preserving a more energetic flow path towards the floor and the rear of the car.

The objective of this section is therefore to determine whether the main aerodynamic characteristics identified in the isolated-sidepod analysis remain recognisable after installation and to evaluate how the reduced bodywork volume influences the pressure distribution, velocity field, streamline trajectories and wall shear stress of the complete configuration.

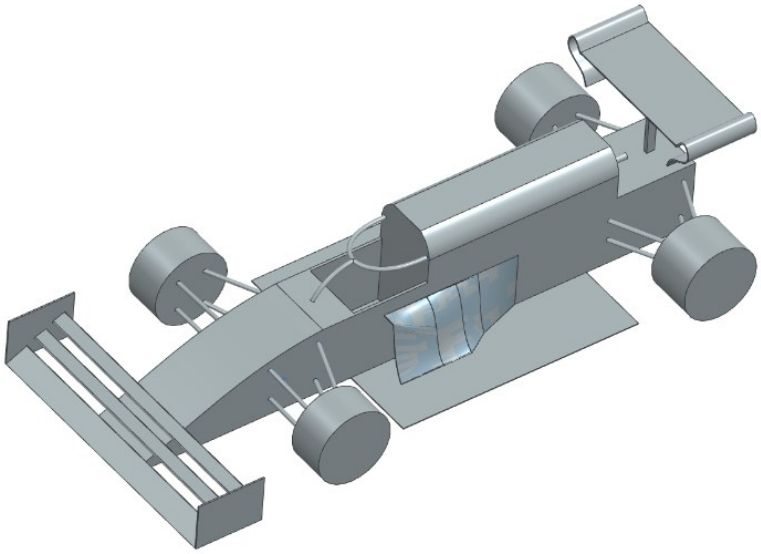


Figure 45 Complete Formula 1 CAD model with the Mercedes-inspired sidepod configuration.

5.3.1 Global aerodynamic results

The global aerodynamic forces obtained for the complete Mercedes-inspired configuration are reported in Table 4.

Velocity	**Drag Force**	C_D	**Downforce**	C_L
40 m/s	455 N	0.63	190 N	-0.26
66.66 m/s	1270 N	0.63	521 N	-0.26
88.88 m/s	2230 N	0.62	950 N	-0.27

Table 4 Aerodynamic forces and coefficients of the Mercedes-inspired complete-car configuration at the three investigated velocities.

The interpretation of these values should be based primarily on their comparative significance rather than on their absolute magnitude. The simplified vehicle model represents only half of the car, exploiting the symmetry of the geometry and flow field to reduce computational cost. In addition, the model does not reproduce the complete aerodynamic performance of a real Formula 1 car, since several important features, including the full Venturi-floor geometry and a number of secondary aerodynamic devices, were simplified or omitted. For this reason, the aerodynamic coefficients obtained in the present study should be considered mainly as indicators for comparing the different sidepod configurations under the same numerical and operating conditions, rather than as direct predictions of the performance of an actual Formula 1 car.

5.3.2 Pressure distribution on the complete car

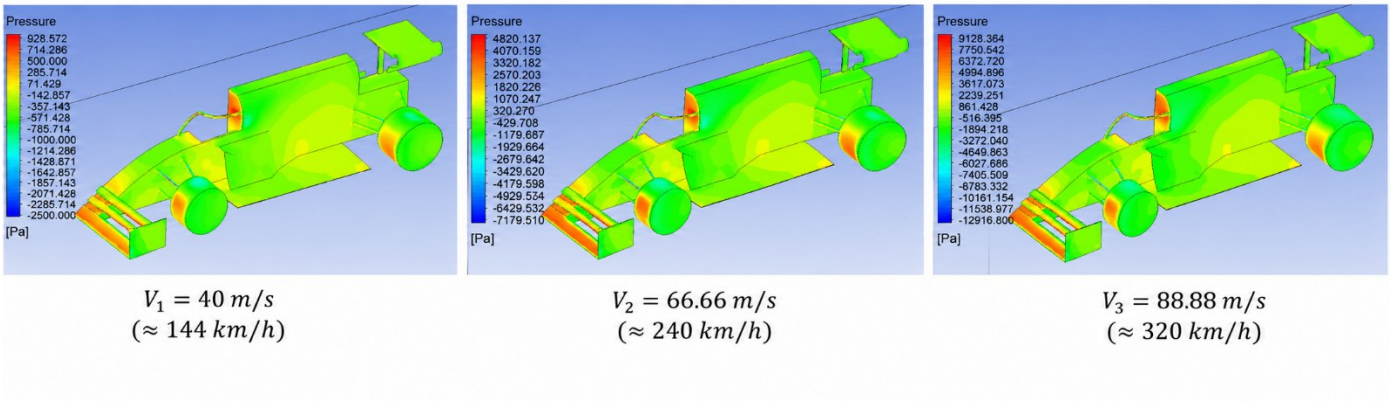


Figure 46 Pressure distribution over the complete Mercedes-inspired configuration at 40, 66.66 and 88.88 m/s.

Once the Mercedes-inspired sidepod is installed on the complete car, the pressure field becomes more complex than in the isolated configuration. The incoming flow is no longer approximately uniform, since it has already interacted with the front wing, nose, front suspension and front wheel before reaching the sidepod region.

Despite this increased complexity, the same general pressure behaviour remains recognisable across the three investigated freestream velocities. High-pressure regions develop on the surfaces directly exposed to the incoming flow, particularly around the frontal components and the sidepod inlet area, while lower-pressure regions form immediately downstream as the flow accelerates around the lateral bodywork.

As the freestream velocity increases, the pressure gradients become stronger, but the overall spatial distribution remains qualitatively similar. This indicates that the main aerodynamic mechanism is preserved over the investigated range and that increasing velocity mainly amplifies the pressure differences already generated by the geometry.

Most of the sidepod body itself does not exhibit pressure variations as pronounced as those observed on the more directly loaded frontal components. This supports the interpretation that the Mercedes-inspired concept is not primarily intended to generate large aerodynamic forces through the sidepod surface alone. Instead, its reduced lateral volume appears to play a broader role in limiting blockage and allowing the airflow to reach the downstream aerodynamic regions with relatively little obstruction.

5.3.3 Velocity field in the sidepod region

Only the 66.66 m/s condition is shown in the following velocity-field visualisations, since the simulations performed at 40 m/s and 88.88 m/s exhibited the same overall flow topology. The main differences between the three operating conditions were associated with the magnitude of the local velocity rather than with significant changes in the spatial distribution of the flow.

The velocity field of the complete vehicle shows that the flow reaching the sidepod region has already been strongly influenced by the upstream components. The front wing, front wheel, suspension and central bodywork generate a non-uniform and three-dimensional incoming flow, which is clearly visible in the lateral and vertical views.

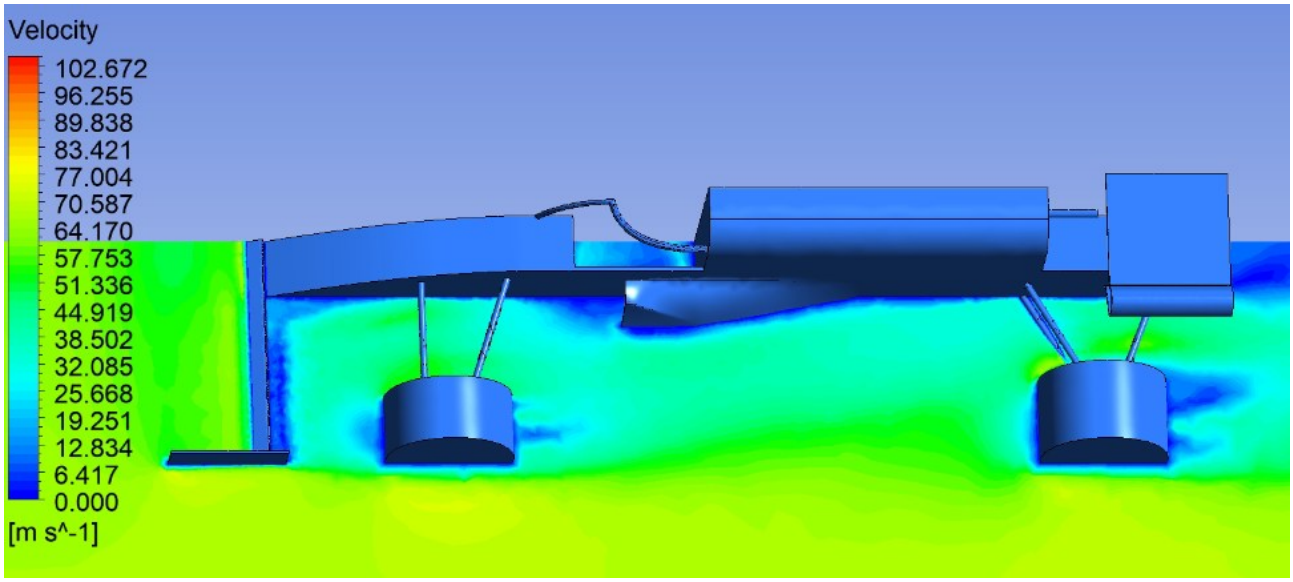


Figure 47 Lateral velocity field around the complete Mercedes-inspired configuration at 66.66 m/s.

The lateral view shows that the compact Mercedes-inspired sidepod leaves a large amount of space available around the central bodywork. A substantial portion of the airflow is able to continue along the lower and lateral regions of the car without being forced to negotiate a large sidepod volume. The flow remains relatively energetic in the open region between the sidepod and the outer portion of the floor, while lower-velocity zones are visible close to the bodywork and in regions affected by the wake of the front wheel.

The same figure also shows that the flow is progressively redistributed towards the rear of the car. The reduced sidepod volume therefore limits the obstruction created by the central bodywork and preserves a relatively wide passage through which the airflow can travel downstream.

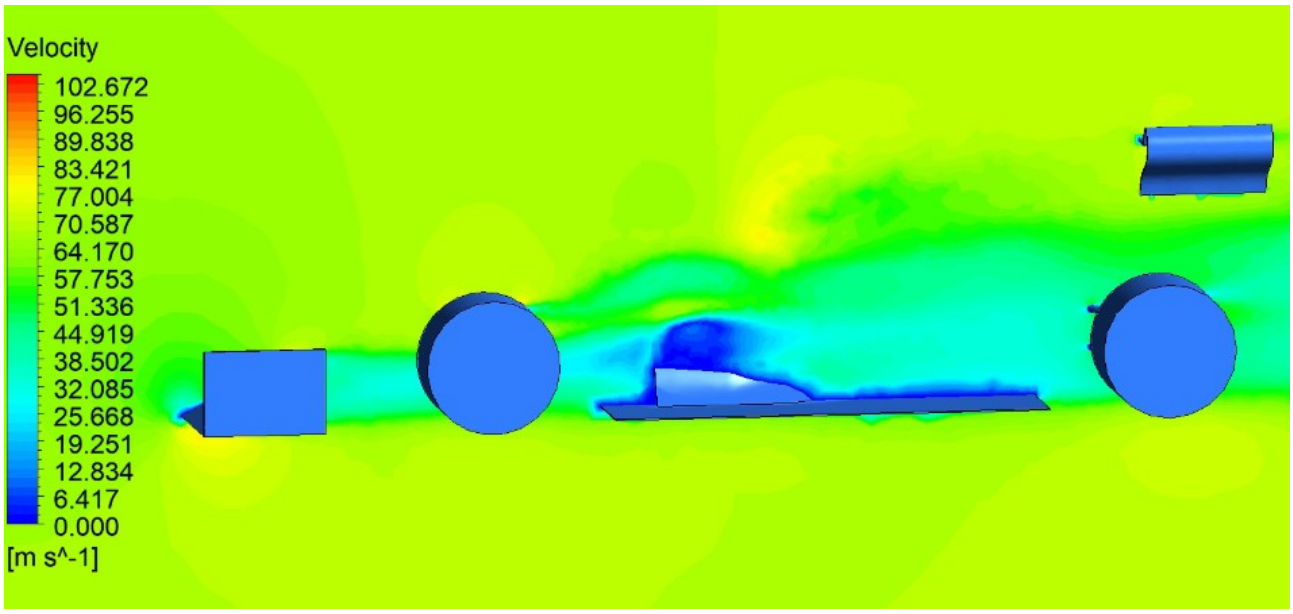


Figure 48 Velocity field around the Mercedes-inspired sidepod and floor region of the complete car at 66.66 m/s.

The vertical view provides complementary information on the development of the flow close to the floor. A pronounced low-velocity region forms immediately downstream of the front-wheel and sidepod area, while the external flow remains more energetic. Further downstream, the flow gradually recovers and continues towards the rear-wheel and diffuser regions.

This distribution highlights the strongly three-dimensional nature of the flow around the complete car. The sidepod is not exposed to a uniform freestream, but to a flow field already affected by velocity deficits and wake structures generated by the upstream components. Despite these disturbances, the compact geometry of the Mercedes-inspired sidepod leaves a relatively wide external flow path available along the lateral and lower regions of the car.

Across the investigated operating conditions, the overall structure of the velocity field remains qualitatively similar. Increasing the freestream velocity mainly strengthens the local acceleration and velocity gradients without substantially changing the location of the main high- and low-energy regions.

The complete-car analysis therefore supports the interpretation of the Mercedes-inspired sidepod as part of a low-blockage aerodynamic architecture. Its reduced lateral volume does not eliminate the flow disturbances generated upstream, but limits the additional obstruction introduced by the sidepod itself and preserves a relatively open flow path towards the floor and rear region of the vehicle.

5.3.4 Streamlines and flow

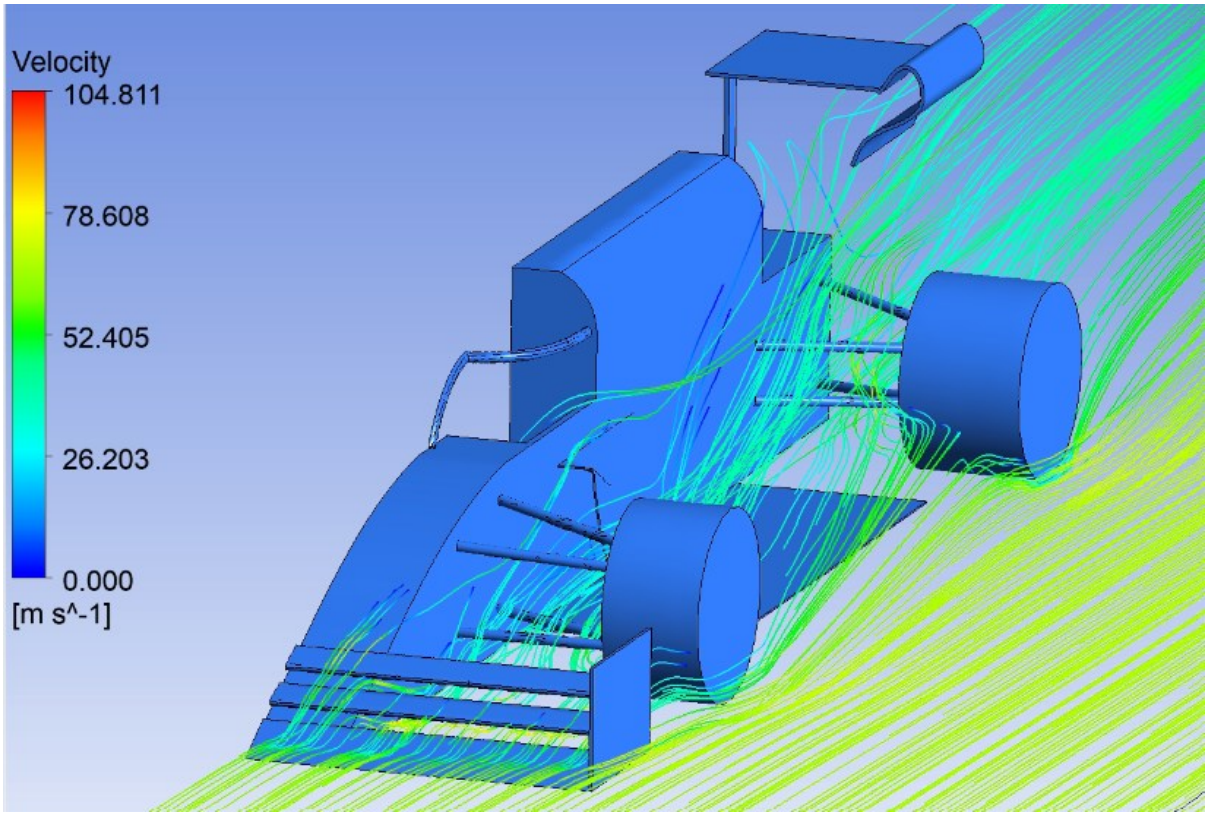


Figure 49 Streamline distribution around the complete Mercedes-inspired configuration at 66.66 m/s.

Only the 66.66 m/s condition is shown in the following streamline visualisations, since the simulations performed at 40 m/s and 88.88 m/s exhibited the same overall flow topology. Increasing the freestream velocity mainly changes the magnitude of the local velocities, while the principal streamline trajectories and the main flow structures remain qualitatively similar.

The streamline analysis is particularly useful for understanding how the reduced sidepod volume affects the overall flow around the complete vehicle.

The first view shows that the compact Mercedes-inspired bodywork leaves a large lateral passage available around the central section of the car. A significant portion of the airflow is able to pass alongside and beneath the sidepod without being forced to negotiate a large bodywork volume. The flow is progressively redirected towards the rear of the vehicle, while local lower-velocity regions remain visible close to the bodywork and in areas influenced by the wake of the front wheel.

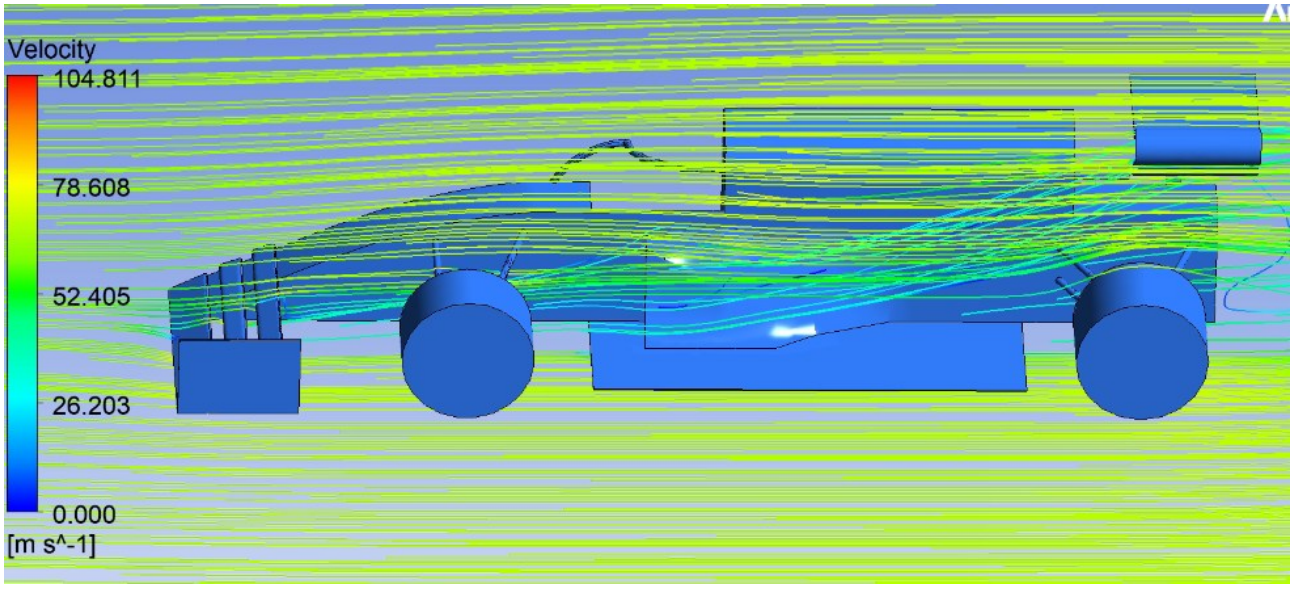


Figure 50 Lateral streamline distribution around the complete Mercedes-inspired configuration at 66.66 m/s.

The second, lateral view provides a clearer representation of the global flow redistribution around the vehicle. The streamlines show that a substantial portion of the airflow continues along the lower and lateral region of the car, while the upper flow is progressively deflected over the bodywork. This confirms that the reduced sidepod volume leaves a relatively wide external flow corridor towards the rear section of the vehicle.

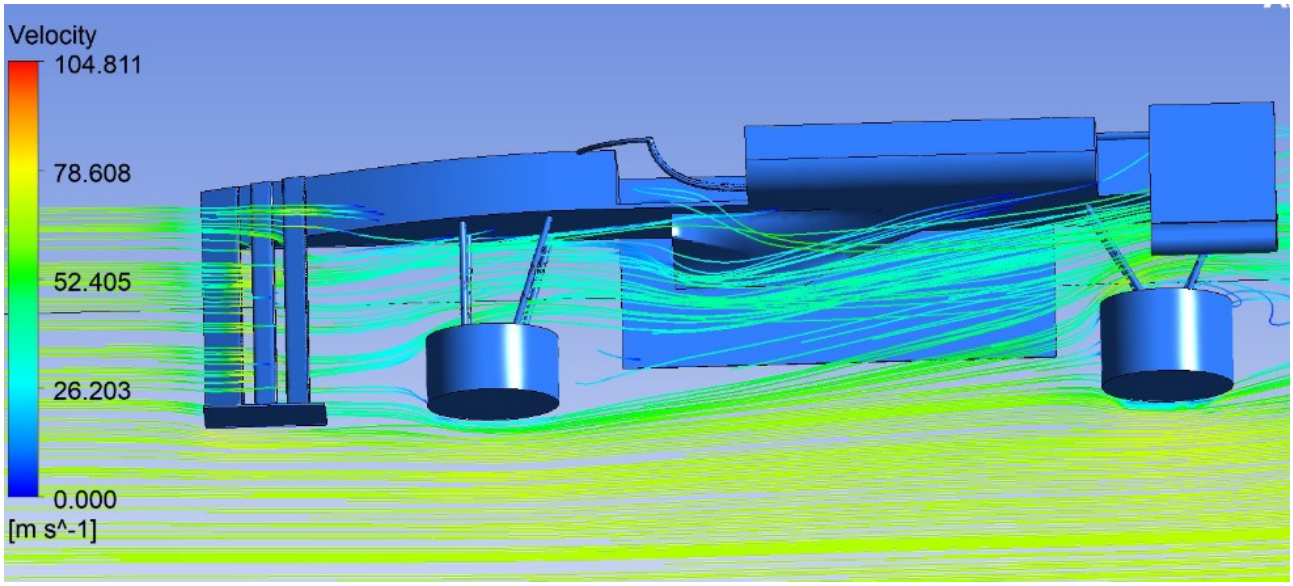


Figure 51 Lateral streamline distribution around the Mercedes-inspired sidepod and floor region of the complete car at 66.66 m/s.

The lateral view also highlights that the flow reaching the sidepod is already highly non-uniform. The front wing, front wheel and suspension generate wake structures and velocity deficits before the air reaches the central bodywork. Consequently, the low-blockage geometry does not eliminate these upstream disturbances, but reduces the additional obstruction that would otherwise be introduced by a larger sidepod volume.

Compared with the isolated-sidepod configuration, the complete-car flow field is therefore considerably more complex. The local acceleration and recirculation observed around the isolated geometry are now embedded in a strongly three-dimensional flow field generated by the complete

vehicle. Nevertheless, the main aerodynamic characteristic of the Mercedes-inspired concept remains visible: the compact sidepod allows a substantial amount of air to continue downstream through the lateral region with relatively limited additional blockage.

The same qualitative behaviour was observed at 40 m/s and 88.88 m/s. The increase in freestream velocity intensifies the local velocities, but does not substantially modify the principal rearward flow paths.

Overall, the streamline analysis supports the interpretation of the Mercedes-inspired sidepod as part of a low-blockage flow-management strategy, in which the reduction of bodywork volume is used to preserve a large lateral flow passage towards the floor and rear of the vehicle.

The present CFD results do not directly demonstrate an improvement in diffuser or rear-wing performance. However, the observed streamline trajectories are consistent with a geometry designed to reduce interference with the downstream flow and to leave a greater portion of the airflow available to the rear aerodynamic system.

5.3.5 Wall shear stress on the complete car

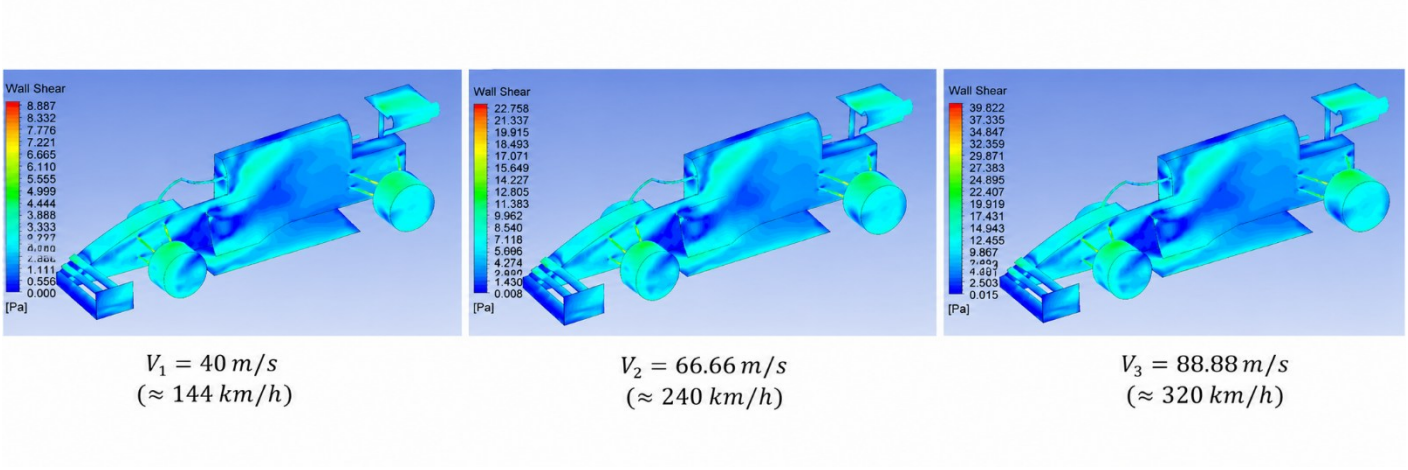


Figure 52 Wall shear stress distribution over the complete Mercedes-inspired configuration at 40, 66.66 and 88.88 m/s.

The wall shear stress distribution shows a qualitatively similar pattern across the three investigated operating conditions. As the freestream velocity increases, the wall shear stress becomes more intense, while the location of the main regions remains substantially unchanged.

Higher wall shear stress is concentrated on surfaces directly exposed to stronger local acceleration and near-wall momentum transfer, particularly around the front region of the car, the suspension elements, the sidepod leading area and some portions of the rear aerodynamic surfaces. These regions indicate the presence of a more energetic flow remaining closely attached to the bodywork.

Conversely, lower wall shear stress values are visible over extended areas of the sidepod body and in regions where the near-wall flow is less energetic. This behaviour is consistent with the more complex flow field generated by the interaction between the sidepod and the upstream components of the complete car.

The persistence of the same general distribution at the three velocities indicates that the aerodynamic behaviour of the configuration remains qualitatively stable throughout the investigated range.

Increasing the freestream velocity mainly amplifies the wall shear stress levels without producing a substantial change in the location of the main high- and low-shear regions.

Overall, the wall shear stress field supports the interpretation already obtained from the pressure and velocity analyses: the Mercedes-inspired configuration maintains a relatively open lateral flow path, while the local flow interaction with the bodywork is mainly concentrated in specific regions rather than uniformly distributed over the entire sidepod surface.

5.4 Comparison between the isolated sidepod and the complete car

Comparing the isolated Mercedes-inspired sidepod with the complete-car configuration highlights the difference between local component behaviour and system-level integration. In isolation, exposed to a nearly uniform incoming flow, the sidepod displays a clear frontal overpressure region, generated as the flow decelerates against the bodywork, followed by a marked low-pressure acceleration zone around the lower and lateral surfaces; the streamline field also reveals a local recirculation region immediately downstream of the sidepod's leading portion. Once installed on the complete car, the incoming flow is no longer uniform, having already been shaped by the front wing, front wheel and suspension before reaching the sidepod: as a result, the recirculation structure seen in isolation becomes less dominant and the near-wall flow pattern appears considerably more fragmented. Despite this, the geometry's essential low-blockage behaviour remains recognisable in both cases: the reduced sidepod volume allows a substantial share of the airflow to accelerate around the lower and lateral region, and the complete-car simulation further shows that this flow can continue towards aerodynamically relevant areas downstream rather than being disrupted by the bodywork itself.

The extremely narrow bodywork appears designed to achieve two aerodynamic objectives beyond a simple reduction in pressure drag: increasing the distance between the central bodywork and the disturbed airflow generated by the front wing and front wheel, thereby reducing the likelihood of turbulent air being drawn laterally into the underfloor inlets where it could compromise the Venturi tunnels' effectiveness; and, thanks to the reduced sidepod volume, opening exceptionally wide external floor channels that let a large amount of air travel along the sides of the car and reach the rear diffuser region with limited obstruction. The CFD results support this interpretation: the isolated geometry shows that reducing the bodywork volume enables rapid flow acceleration around the sidepod, at the cost of a local separation region, while the complete-car simulation shows that a substantial share of the lateral flow can continue rearward with relatively little resistance from the sidepod itself. The underlying design logic can be summarised as follows: reduced central blockage creates a wide lateral flow channel, which in turn preserves the flow towards the floor and rear region. Direct drag reduction should therefore be regarded as a possible benefit of this architecture rather than its primary aerodynamic objective. This same design choice, however, exposes a considerably larger portion of the floor to the external flow — particularly significant given that the 2022 technical regulations placed strong emphasis on underfloor downforce generation through Venturi tunnels, making the floor's aerodynamic behaviour especially sensitive to surrounding flow conditions. It should be noted that the present CFD analysis is steady-state and relies on a simplified floor geometry, and therefore cannot capture the dynamic coupling between ride height, floor deformation, aerodynamic stall and vertical vehicle motion that governs phenomena such as porpoising: the results obtained should not be read as demonstrating that this architecture directly causes such dynamic instabilities, but only that the

geometry produces a large exposed lateral flow region and strongly prioritises the interaction between sidepod, floor and rear aerodynamic system.

Overall, the Mercedes-inspired sidepod can be described as a low-blockage flow-management concept, built around three closely related objectives: reducing the physical obstruction introduced by the sidepod bodywork, limiting the interaction between the central bodywork and the disturbed flow generated by the front wheel, and preserving an energetic lateral flow path towards the floor, diffuser and rear aerodynamic system. The isolated simulations reveal both the advantage and the compromise inherent to this approach: the reduced volume produces strong lateral flow acceleration, but the abrupt geometric transition also generates a local low-energy recirculation region; once integrated into the complete car, this local effect becomes less significant within the overall flow field, while the geometry's system-level role becomes clearer, with a substantial share of the lateral airflow able to reach the floor and rear regions of the car without being obstructed by a large sidepod volume. A reduced sidepod volume should therefore not be read as the absence of a flow-management function: on the contrary, removing bodywork material is itself a deliberate strategy, since by defining where solid surfaces are absent, the geometry establishes a wide aerodynamic corridor available to the external flow. Quantifying the resulting effect on downforce or drag at the level of the floor, diffuser or rear wing would, however, require dedicated force and pressure analyses beyond the visualisations presented in this section.

Chapter 6

RED BULL CONFIGURATION: RESULTS AND AERODYNAMIC ANALYSIS

6.1 Introduction to the Red Bull configuration

The Red Bull-inspired configuration was developed with the aim of reproducing the main aerodynamic features associated with the sidepod concept introduced on the Red Bull RB18 during the 2022 Formula 1 season. Compared with the Ferrari- and Mercedes-inspired solutions, this concept is characterised by a pronounced lower undercut, a relatively compact sidepod volume and upper surfaces that progressively descend towards the rear of the vehicle.

The purpose of this chapter is to analyse how these geometric characteristics influence the surrounding flow field and to identify the main aerodynamic mechanisms associated with the Red Bull-inspired sidepod. Particular attention is devoted to the lower undercut and to the descending upper surface, since these represent the most distinctive features of the geometry.

The analysis is divided into two phases. First, the Red Bull-inspired sidepod is studied as an isolated component in order to identify the aerodynamic behaviour directly associated with its geometry, independently of the influence of the other vehicle components. The analysis focuses on the pressure distribution, velocity field, streamlines and wall shear stress.

Subsequently, the same sidepod is analysed after installation on the complete vehicle. This second stage makes it possible to evaluate how the aerodynamic behaviour observed in the isolated configuration changes once the sidepod interacts with the front wing, suspension, wheels, floor and rear aerodynamic components. Three freestream velocities were analysed:

$$V_1 = 40 \text{ m/s}, \; V_2 = 66.66 \text{ m/s}, \; V_3 = 88.88 \text{ m/s}$$

corresponding respectively to approximately 144, 240 and 320 km/h.

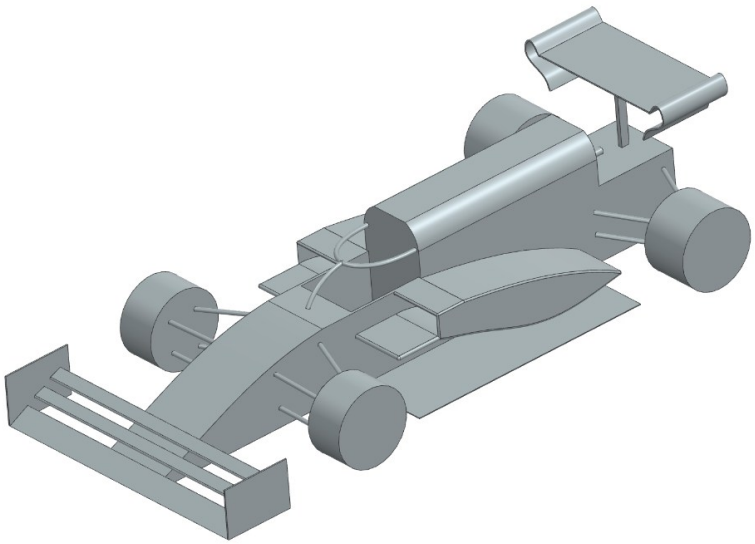


Figure 53 Complete Formula 1 CAD model with the Red Bull-inspired sidepod configuration.

6.2 Aerodynamic Analysis of the Isolated Red Bull-Inspired Sidepod

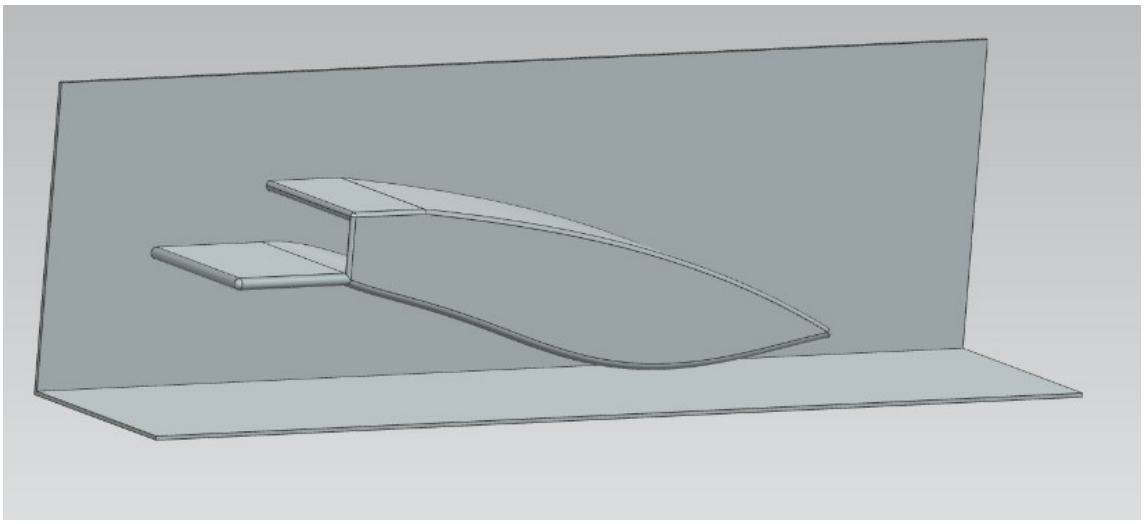


Figure 54 Isolated Red Bull-inspired sidepod geometry used for the CFD analysis.

The simulations of the isolated sidepod were performed in order to identify the aerodynamic behaviour directly generated by the Red Bull-inspired geometry without the influence of the front wing, wheels, suspension or rear bodywork.

This simplified configuration provides a useful reference because the incoming flow is approximately uniform. Consequently, the changes in pressure, velocity and streamline direction can be associated primarily with the sidepod geometry itself.

The isolated analysis highlights two principal mechanisms. The first is the acceleration of the lower flow through the pronounced undercut. The second is the progressive downward and rearward redirection of the upper flow produced by the external sidepod surface.

These mechanisms can be interpreted respectively as a Venturi-like acceleration of the lower branch and a downwash-driven redirection of the upper branch.

6.2.1 Pressure distribution

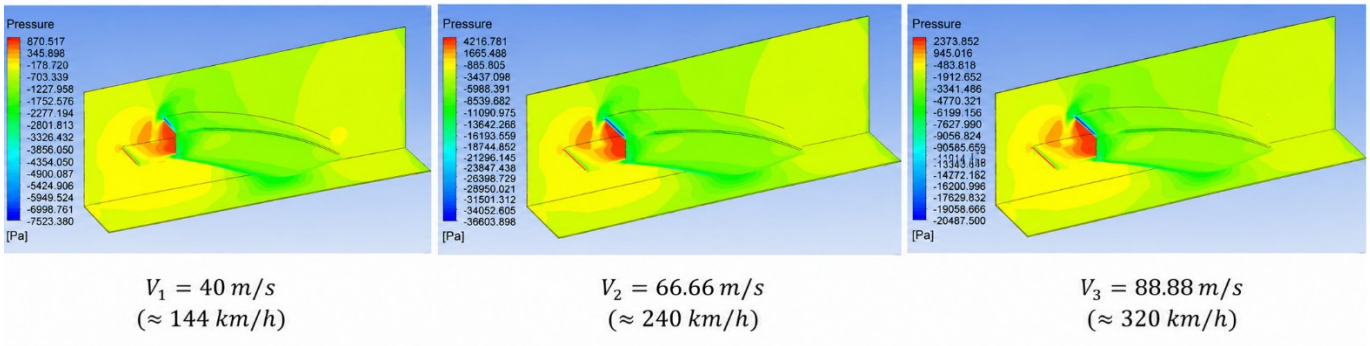


Figure 55 Pressure distribution around the isolated Red Bull-inspired sidepod at 40, 66.66 and 88.88 m/s.

The pressure distribution around the isolated Red Bull-inspired sidepod exhibits a characteristic pattern that remains qualitatively similar over the three investigated velocities.

A relatively high-pressure region develops at the front of the sidepod, where the incoming airflow decelerates as it encounters the bodywork. This region can be interpreted as a partial stagnation area, in which part of the kinetic energy of the incoming flow is converted into static pressure before the airflow is redistributed around the geometry.

Immediately downstream of the frontal region, the static pressure decreases significantly. One of the most relevant low-pressure areas develops along the lower portion of the sidepod, particularly in correspondence with the pronounced undercut. The pressure reduction is not confined to a small region near the leading edge but extends over a significant part of the lower surface.

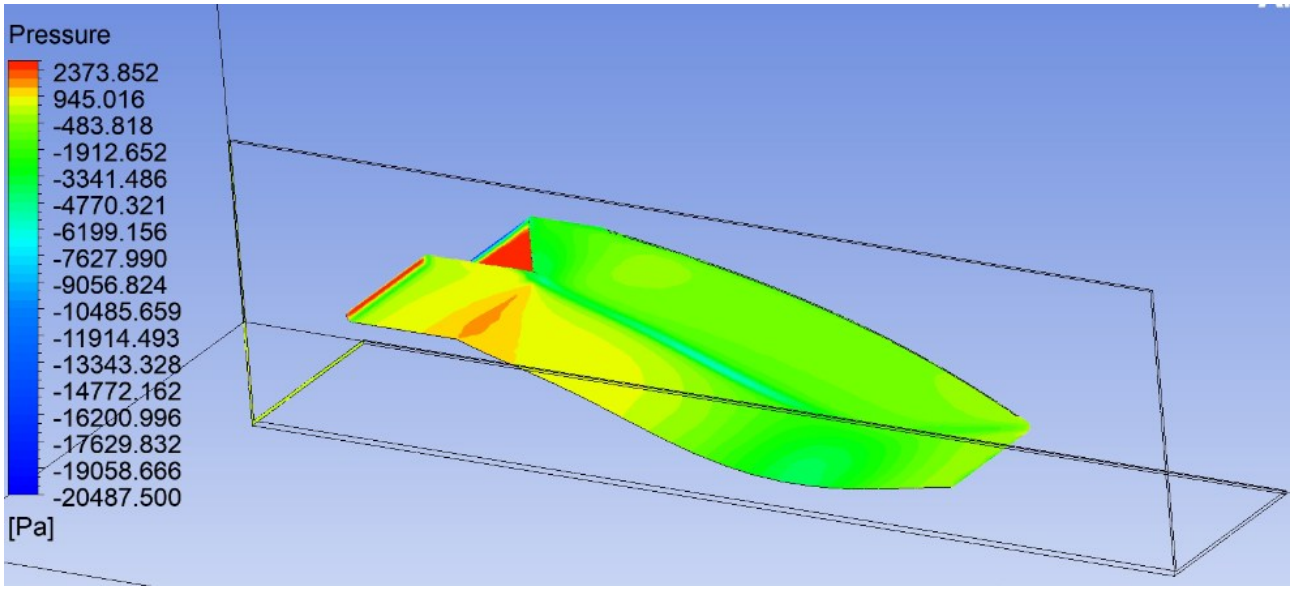


Figure 56 Pressure distribution along the lower surface of the isolated Red Bull-inspired sidepod at 66.66 m/s.

The underside view highlights the presence of a continuous low-pressure region along the lower side of the geometry. This region becomes particularly evident along the curved undercut surface and remains visible as the sidepod progressively narrows towards the rear.

The pressure distribution therefore suggests that the undercut plays an important role in managing the airflow along the lower part of the sidepod. The local reduction in static pressure is consistent with an acceleration of the flow through this region, although the present pressure contour alone does not provide a direct measurement of the local velocity.

Towards the rear of the geometry, a gradual pressure recovery can be observed as the sidepod shape opens and the flow is progressively redirected downstream.

The comparison between the three operating conditions shows that the position and spatial distribution of the main high- and low-pressure regions remain substantially unchanged. Increasing the freestream velocity mainly changes the magnitude of the pressure differences rather than the overall aerodynamic mechanism.

Overall, the pressure-field topology generated by the Red Bull-inspired sidepod remains stable over the investigated velocity range. In particular, the persistent low-pressure region along the undercut confirms the aerodynamic importance of the lower sidepod geometry in controlling the flow directed towards the rear.

6.2.2 Velocity field

The velocity field confirms the interpretation obtained from the pressure distribution.

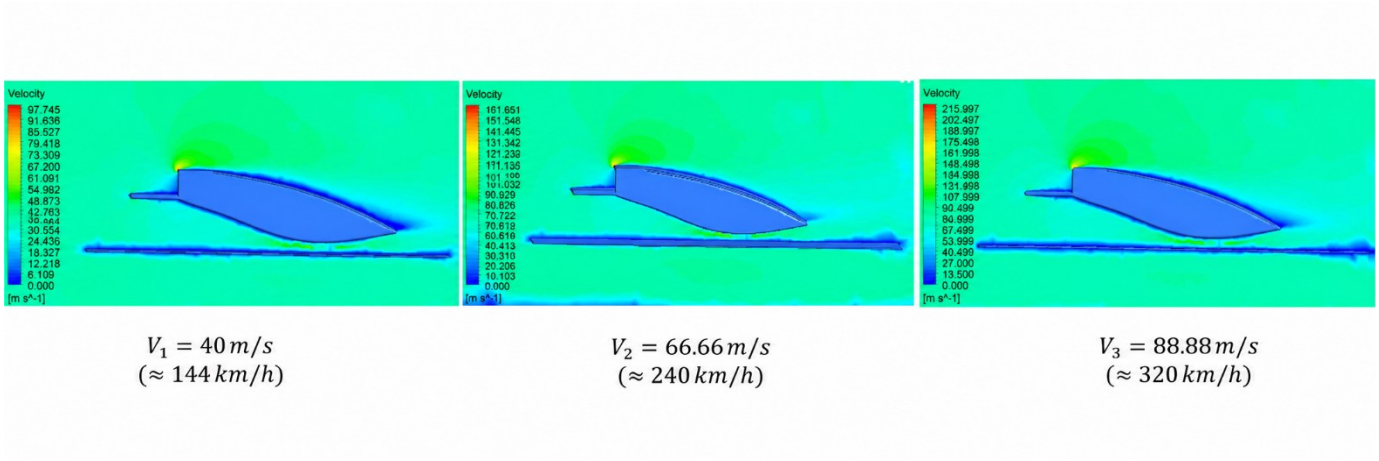


Figure 57 Velocity field around the isolated Red Bull-inspired sidepod at 40, 66.66 and 88.88 m/s.

At the front of the sidepod, the incoming airflow is initially decelerated and redistributed around the geometry. A portion of the flow travels above the sidepod, while another significant portion is directed towards the lower region.

The most evident acceleration occurs through the undercut.

As the available passage beneath the main volume of the sidepod becomes more restricted, the airflow accelerates and forms a relatively high-velocity region extending downstream. The position of this region corresponds closely to the low-pressure area identified in the pressure contours.

The combined analysis is therefore consistent:

$$p \downarrow \; V \uparrow$$

This correspondence supports the interpretation of the lower region as a Venturi-like flow passage.

The simulations also show that the accelerated flow does not immediately disperse after passing through the narrowest region. Instead, a relatively energetic flow path continues towards the rear of the sidepod.

This behaviour is aerodynamically significant because the role of the undercut appears not to be limited to producing a local pressure reduction. Its geometry also creates a preferential high-energy flow path directed towards the rear of the vehicle.

The comparison between the three investigated velocities shows essentially the same flow-field topology. As the freestream velocity increases, the magnitude of the local acceleration becomes greater, but the position and direction of the principal high-velocity regions remain substantially unchanged.

The Red Bull-inspired geometry therefore appears to maintain the same basic aerodynamic mechanism throughout the investigated speed range.

6.2.3 Streamlines and flow behaviour

The streamline analysis provides a clearer understanding of how the Red Bull-inspired geometry separates and manages the incoming flow.

As the flow approaches the front region of the sidepod, it is divided into different paths. One portion passes above and around the external surface of the sidepod, while another significant portion is directed towards the lower undercut region.

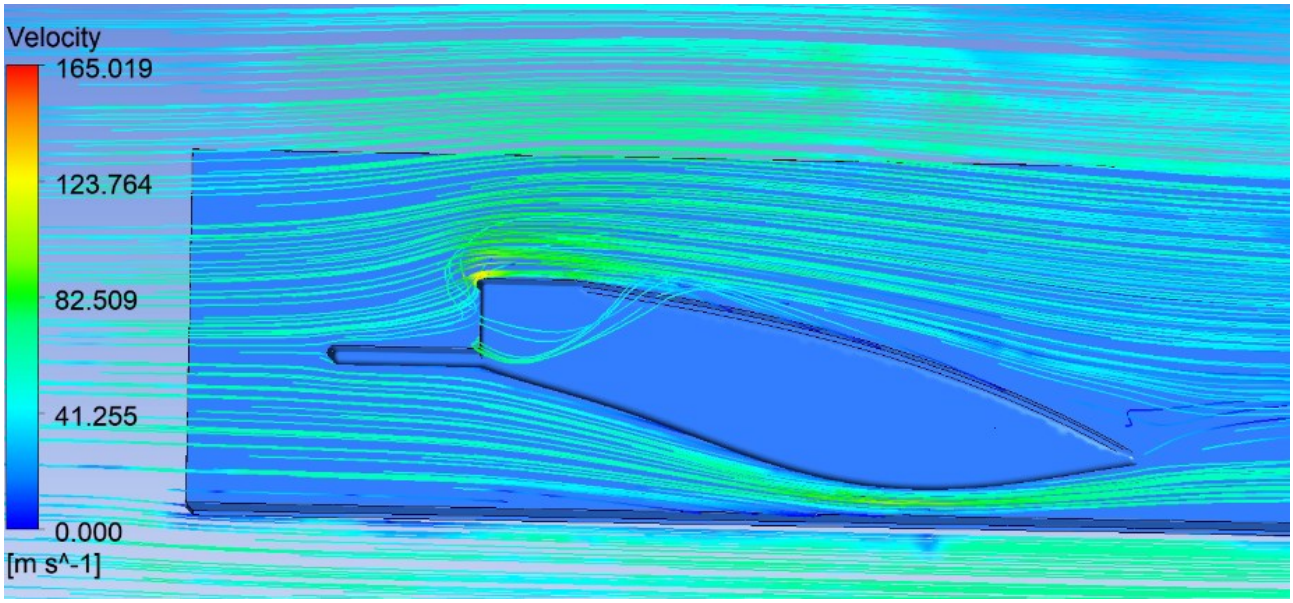


Figure 58 Streamline distribution around the isolated Red Bull-inspired sidepod at 66.66 m/s.

The streamlines entering the undercut show a clear acceleration as they pass beneath the main sidepod volume. Their increased density and higher local velocity are consistent with the low-pressure region previously identified in the pressure contours. After passing through the most restricted section, the lower branch remains relatively close to the lower surface and continues downstream, forming a preferential high-energy flow path towards the rear.

The lower portion of the geometry can therefore be interpreted not simply as an open passage beneath the sidepod, but as an active region of flow acceleration and channelling.

The upper branch follows a different trajectory. The external sidepod surface progressively descends towards the rear, causing the streamlines travelling along this region to be gradually redirected downwards and rearwards. This behaviour is consistent with the characteristic downwash effect associated with the Red Bull-inspired geometry.

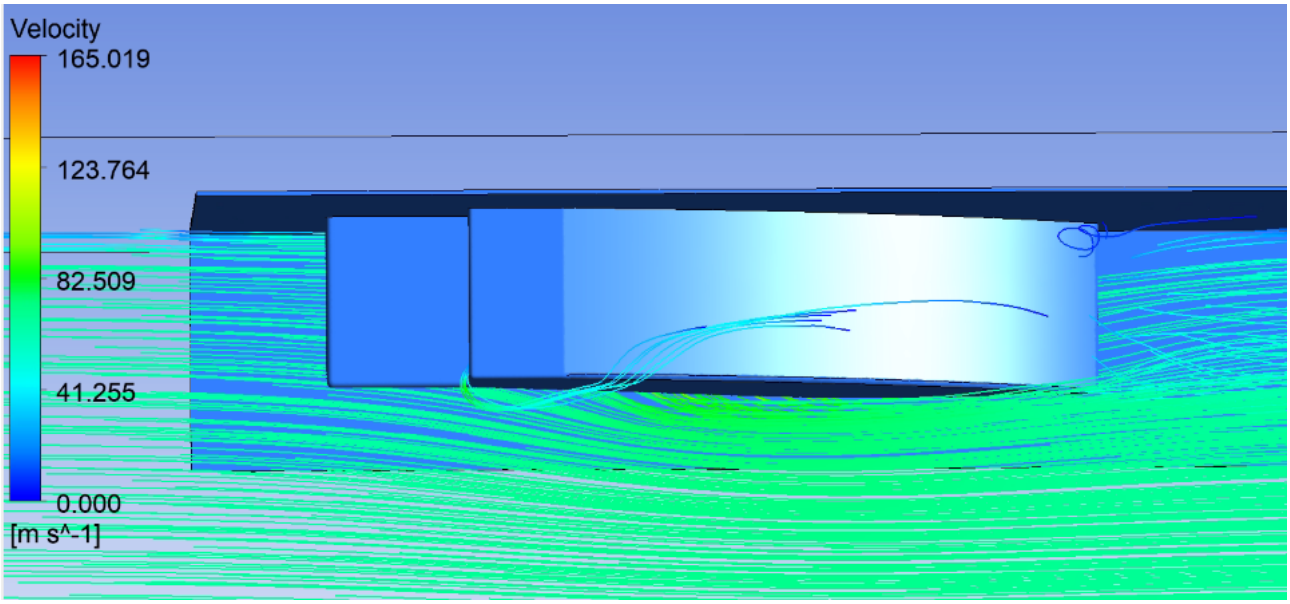


Figure 59 Lateral streamline distribution through the lower region of the isolated Red Bull-inspired sidepod at 66.66 m/s.

The lower/lateral view provides a clearer representation of the flow path beneath the sidepod. The streamlines are progressively drawn into the undercut and remain concentrated along the lower region before continuing downstream. This confirms that the geometry creates a preferential lower flow path rather than allowing the airflow to disperse freely around the bodywork.

The two regions therefore perform complementary aerodynamic functions:

Undercut → acceleration and channelling of the lower flow

Upper surface → downwash and rearward redirection of the upper flow

The sidepod can consequently be interpreted as creating two main airflow paths: an accelerated lower branch travelling through the undercut and an upper branch progressively redirected by the descending external surface. Both flows are directed towards the rear region, although they follow different trajectories around the sidepod.

The streamline topology remains qualitatively similar at 40, 66.66 and 88.88 m/s. Increasing the freestream velocity mainly increases the local flow velocity and the intensity of the aerodynamic effects, without producing a substantial modification of the characteristic trajectories generated by the geometry.

6.2.4 Wall shear stress

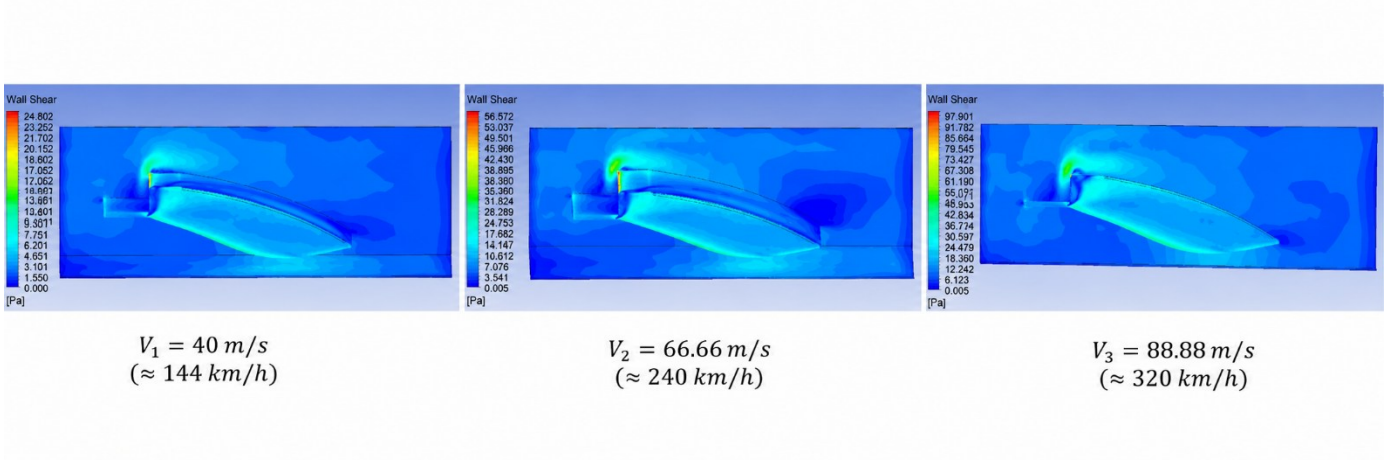


Figure 60 Wall shear stress distribution around the isolated Red Bull-inspired sidepod at 40, 66.66 and 88.88 m/s.

The wall shear stress distribution provides further information regarding the interaction between the airflow and the sidepod surface. The comparison between the three investigated velocities shows that the magnitude of the wall shear stress increases as the freestream velocity rises, while the overall spatial distribution remains qualitatively similar.

The highest wall shear stress values are concentrated primarily around the leading region of the sidepod and along sections of the lower surface associated with the undercut. These are the same areas in which the pressure field shows a significant reduction and the velocity and streamline analyses indicate strong local acceleration.

The combined interpretation of the different CFD quantities is therefore consistent:

$$p \downarrow \; V \uparrow \; \tau_w \uparrow$$

Localised regions of very low wall shear stress are visible immediately downstream of the strongly curved front region. These areas indicate a reduction in near-wall momentum and may be associated with local flow separation or recirculation. However, wall shear stress magnitude alone is not sufficient to demonstrate the presence of separation with certainty.

Further downstream, moderate and relatively continuous shear values are recovered along the lower surface of the sidepod. This behaviour is particularly relevant in the undercut region, where the airflow had previously been observed to accelerate and form a preferential lower flow path.

The persistence of non-negligible wall shear stress along this surface suggests that the accelerated airflow does not remain completely separated from the bodywork. Instead, the flow appears to recover after the highly curved leading region and remain sufficiently energetic over a significant portion of the lower geometry.

The undercut can therefore be interpreted as a region in which strong flow acceleration is achieved while maintaining a predominantly attached downstream flow. This is important for the aerodynamic function of the sidepod, since an extended separation within the undercut would reduce the effectiveness of the accelerated lower flow path.

As the freestream velocity increases from 40 to 66.66 and 88.88 m/s, the wall shear stress becomes progressively stronger without producing a substantial change in the position of the main active regions. The same leading-edge and undercut areas remain dominant at all three operating conditions.

This similarity further supports the conclusion that the aerodynamic operating principle of the Red Bull-inspired geometry remains stable throughout the investigated velocity range: increasing the freestream velocity intensifies the interaction between the airflow and the surface, but does not fundamentally modify the characteristic flow mechanism.

6.3 CFD Analysis of the Red Bull Configuration on the Complete Car

The second phase of the analysis concerns the Red Bull-inspired sidepod installed on the complete vehicle.

This configuration introduces the aerodynamic interaction between the sidepod and all the other major components of the model.

Unlike the isolated case, the airflow reaching the sidepod is no longer uniform. Before reaching the lateral region of the vehicle, it has already interacted with the front wing, front wheel, suspension and front bodywork.

Downstream, the airflow leaving the sidepod interacts with the floor, rear wheel and rear aerodynamic system.

The complete-car configuration therefore makes it possible to evaluate whether the aerodynamic mechanisms identified in the isolated analysis remain active under more realistic installation conditions.

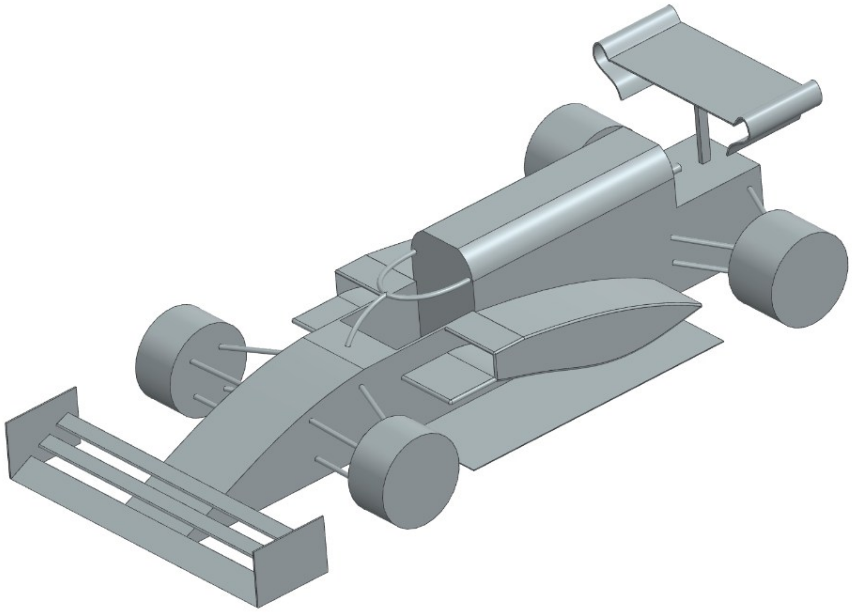


Figure 61 Complete Formula 1 CAD model with the Red Bull-inspired sidepod configuration.

6.3.1 Global aerodynamic results

The global aerodynamic forces obtained for the complete Red Bull-inspired configuration are reported in Table 5.

Velocity	**Drag Force**	C_D	**Downforce**	C_L
40 m/s	470 N	0.65	150 N	-0.20
66.66 m/s	1300 N	0.65	420 N	-0.20
88.88 m/s	2350 N	0.65	700 N	-0.20

Table 5 Aerodynamic forces and coefficients of the Red Bull-inspired complete-car configuration at the three investigated velocities.

The absolute aerodynamic coefficients obtained from the simplified model should not be interpreted as representative of a real Formula 1 vehicle. As already discussed for the Ferrari configuration, the simplified underfloor, rear wing and secondary aerodynamic devices reduce the total aerodynamic load generated by the model.

The main value of these coefficients is therefore comparative. Since the same vehicle baseline, reference quantities, numerical setup and boundary conditions are maintained for the Ferrari-, Mercedes- and Red Bull-inspired configurations, the resulting forces and coefficients can be compared in relative terms.

Both C_D and C_L remain constant over the investigated velocity range, at 0.65 and -0.20 respectively. As already observed for the other two configurations, the aerodynamic forces therefore increase mainly as a consequence of the rise in dynamic pressure, while the overall aerodynamic behaviour of the configuration remains stable.

6.3.2 Pressure distribution on the complete car

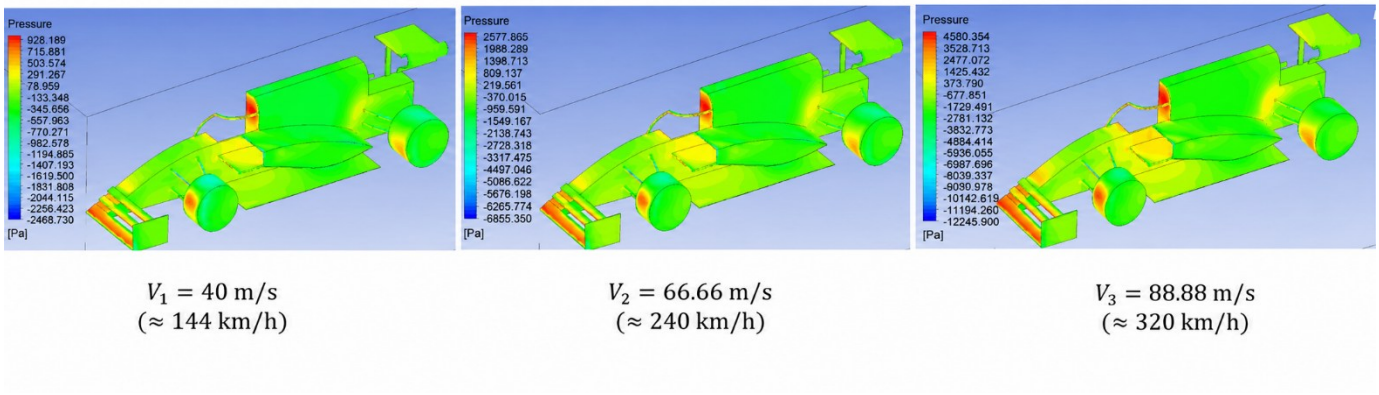


Figure 62 Pressure distribution over the complete Red Bull-inspired configuration at 40, 66.66 and 88.88 m/s.

When the Red Bull-inspired sidepod is installed on the complete vehicle, the pressure field becomes more complex than in the isolated configuration because the incoming flow has already interacted with the front wing, suspension and front wheel.

Despite this increased complexity, the three pressure distributions show a qualitatively similar overall pattern. Higher-pressure regions are concentrated mainly on the surfaces directly exposed to the incoming flow, particularly around the front wing, the front wheels and the frontal area of the sidepod. Lower-pressure regions develop around the lateral and lower portions of the bodywork, including the area influenced by the sidepod undercut.

The pressure distribution around the sidepod is less uniform than in the isolated case, reflecting the interaction with the upstream aerodynamic components. Nevertheless, the lower-pressure region associated with the lower and lateral sidepod surfaces remains identifiable, suggesting that the geometry continues to influence the acceleration and redistribution of the flow towards the floor and rear of the vehicle.

Across the three investigated operating conditions, the location of the main high- and low-pressure regions remains approximately unchanged. Increasing the freestream velocity mainly increases the magnitude of the pressure differences and gradients, without substantially modifying the overall spatial distribution of the pressure field.

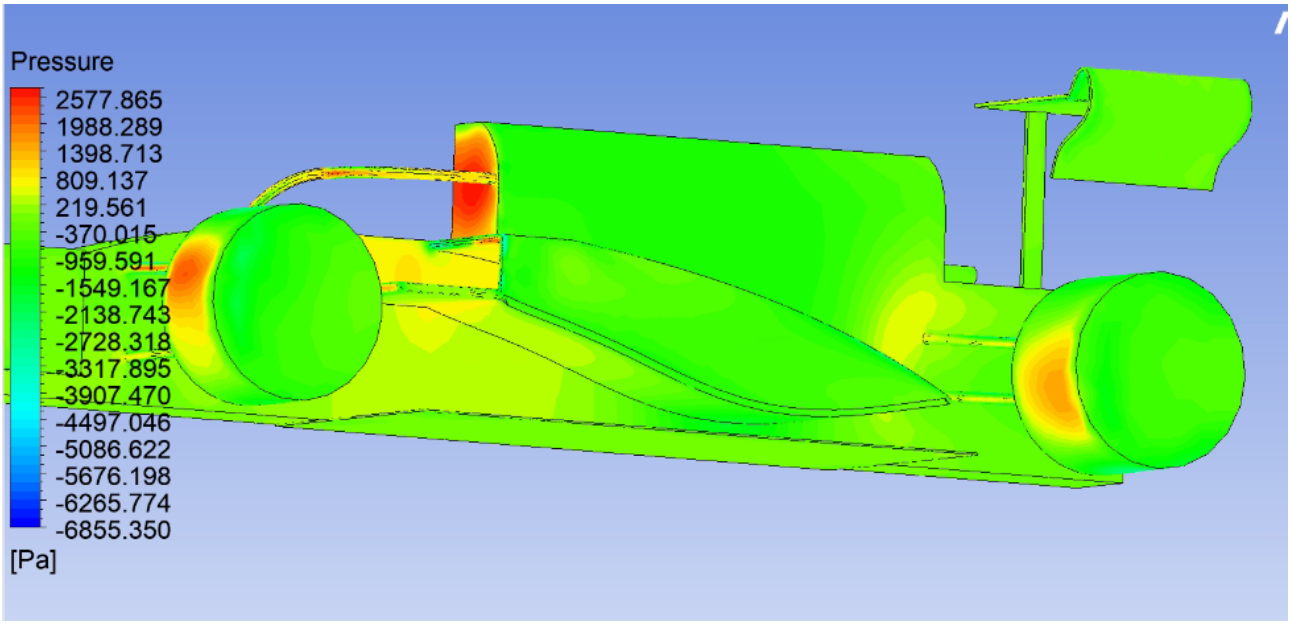


Figure 63 Pressure distribution around the Red Bull-inspired sidepod region of the complete car at 66.66 m/s.

A particularly relevant feature visible in Figure 63 is the pressure reduction along the lower surface of the sidepod and the adjacent floor region. The pronounced undercut creates a locally restricted passage for the airflow between the main sidepod volume and the lower aerodynamic surfaces. As the available flow area decreases, the airflow accelerates and the static pressure is consequently reduced.

This behaviour can be interpreted as a Venturi-like effect generated by the interaction between the sidepod undercut and the floor. The geometry therefore does not simply provide clearance beneath the sidepod, but actively creates a preferential low-pressure, high-velocity flow path directed towards the rear of the vehicle.

It should be noted that this region does not constitute an independent Venturi tunnel comparable to the main underfloor tunnels of a real ground-effect Formula 1 car. Instead, the sidepod undercut produces a local Venturi-like acceleration that operates as part of the overall flow-management system of the vehicle.

The persistence of the low-pressure region towards the rear further suggests that the accelerated airflow is maintained over a significant portion of the lower sidepod and floor region, rather than being limited to a local acceleration immediately downstream of the sidepod leading edge.

6.3.3 Velocity field in the sidepod region

The velocity field of the complete Red Bull-inspired configuration confirms the influence of the upstream components on the flow approaching the sidepod.

The airflow reaching the lateral bodywork is characterised by significant non-uniformity due to the front-wheel wake, suspension and front aerodynamic surfaces.

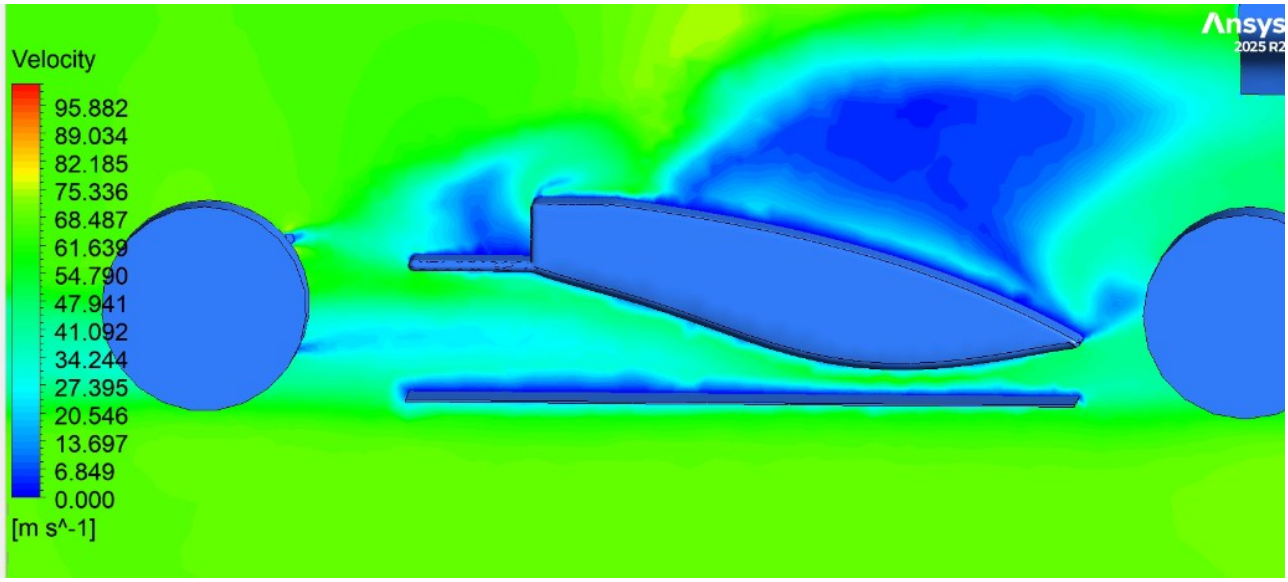


Figure 64 Velocity field around the Red Bull-inspired sidepod and floor region of the complete car at 66.66 m/s.

Despite these disturbances, the undercut continues to create a preferential flow path beneath the sidepod. A significant portion of the airflow is guided into this lower region, where it accelerates before continuing towards the rear of the vehicle.

The correspondence between lower pressure and higher velocity remains evident even after installation:

$$p \downarrow \; V \uparrow$$

The lower sidepod therefore retains the aerodynamic function identified in the isolated configuration. In particular, the velocity field confirms that the undercut continues to generate an accelerated lower-flow region even when the incoming air has already been disturbed by the upstream vehicle components.

However, the accelerated flow is no longer as uniform as in the isolated case. It interacts directly with the floor and with the disturbed flow generated by the wheels.

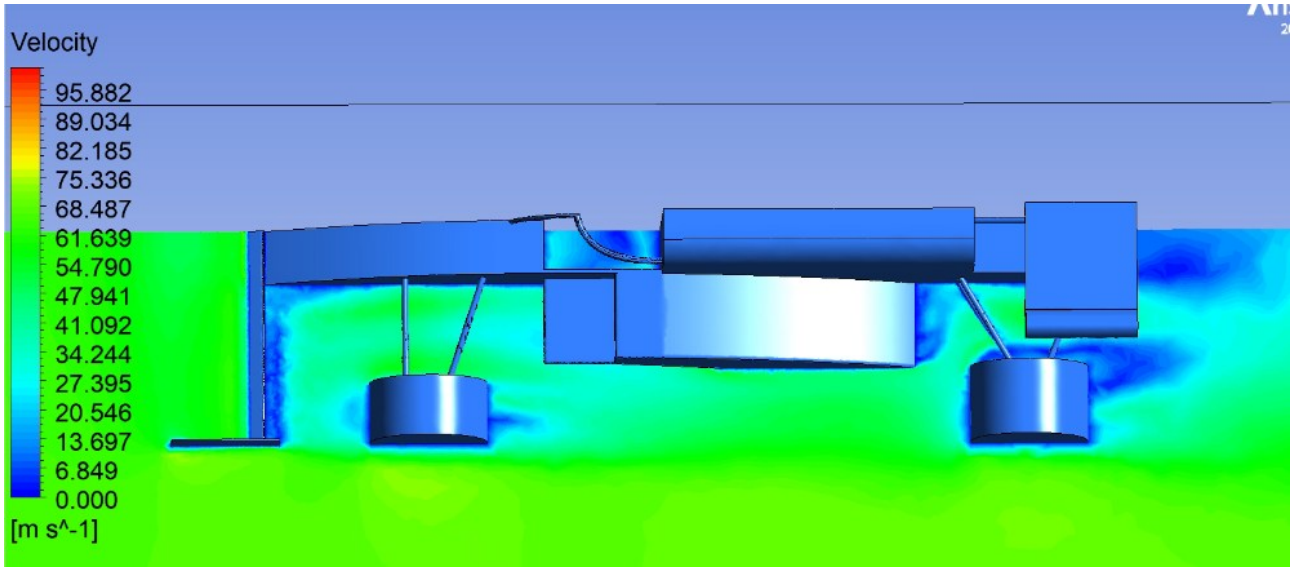


Figure 65 Lateral velocity field around the complete Red Bull-inspired configuration at 66.66 m/s.

The second view highlights the difference between the intrinsic behaviour of the sidepod geometry and its installed aerodynamic behaviour. The flow approaching the sidepod is already affected by significant velocity deficits and local disturbances generated upstream, while the accelerated lower branch subsequently interacts with the floor and the flow structures developing around the rear portion of the vehicle.

The upper flow remains influenced by the descending shape of the sidepod. The velocity field indicates that the airflow following the upper and lateral bodywork is progressively redirected towards the lower rear region.

The complete-car configuration therefore confirms the complementary operation of the two principal regions:

Lower branch → accelerated flow towards the floor

Upper branch → downwash towards the rear

The topology remains comparable at the three investigated velocities, while the velocity gradients become progressively stronger as the freestream velocity increases.

6.3.4 Streamlines and flow behaviour

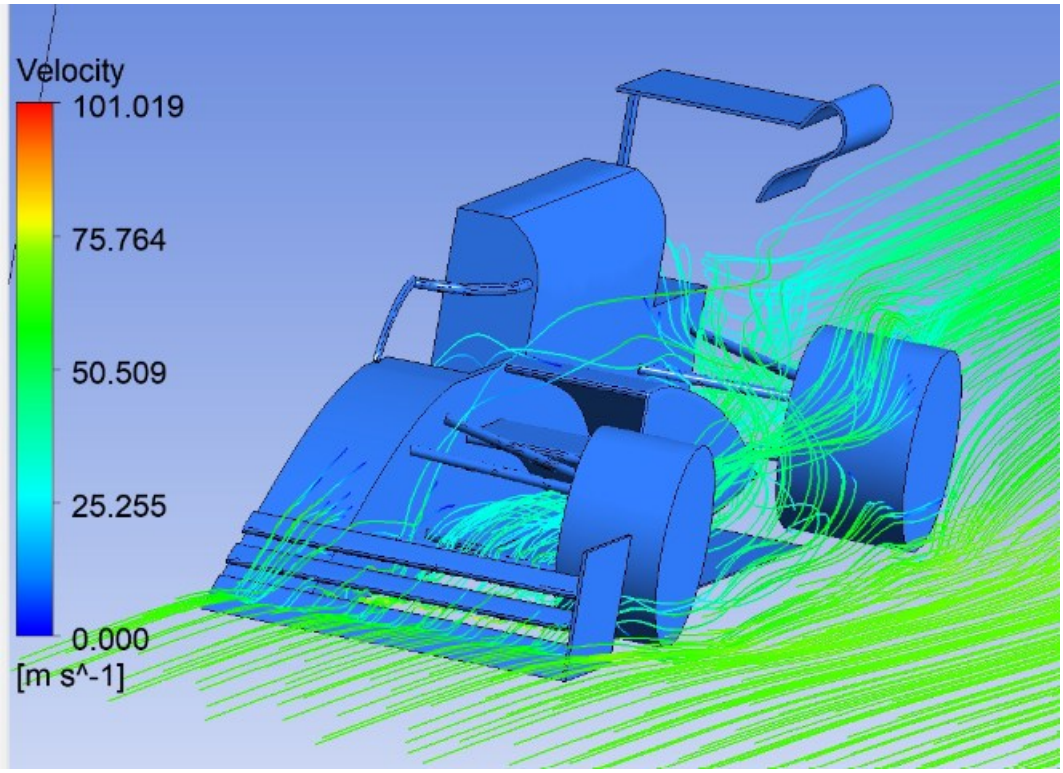


Figure 66 Streamline distribution around the complete Red Bull-inspired configuration at 66.66 m/s.

The streamline analysis of the complete vehicle provides a particularly clear representation of how the Red Bull-inspired sidepod interacts with the overall aerodynamic system.

Unlike the isolated configuration, the airflow reaching the sidepod is no longer uniform. Before reaching the lateral bodywork, it has already interacted with the front aerodynamic surfaces, suspension elements and front wheel. The resulting inflow is therefore characterised by velocity deficits, local flow deviations and a more complex three-dimensional structure.

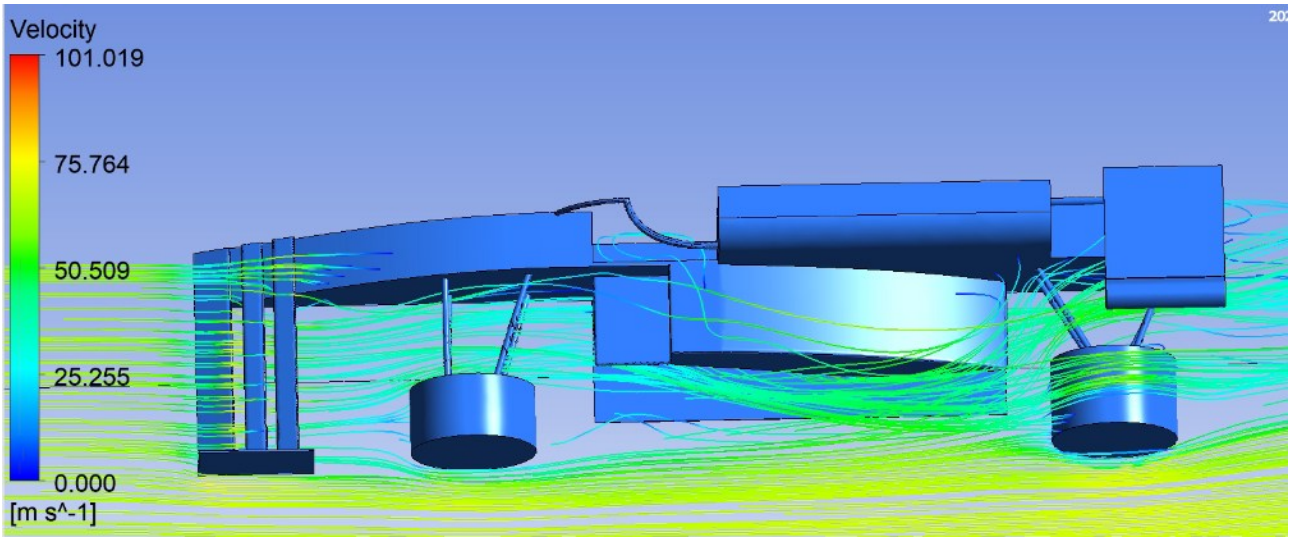


Figure 67 Lateral streamline distribution around the Red Bull-inspired sidepod and floor region of the complete car at 66.66 m/s.

Despite these upstream disturbances, the characteristic aerodynamic behaviour of the sidepod remains clearly identifiable. A significant portion of the airflow approaching the lower region is captured by the pronounced undercut and progressively accelerated beneath the main sidepod volume.

The streamlines remain concentrated close to the lower surface and continue downstream, forming a preferential energetic flow path directed towards the rear portion of the floor. This confirms that the acceleration mechanism identified in the isolated-sidepod analysis remains active even when the geometry operates within the complete aerodynamic environment of the vehicle.

This result is particularly relevant because the sidepod is no longer acting on an ideal and uniform incoming flow. Instead, the geometry appears capable of partially reorganising an already disturbed upstream flow and redirecting part of it towards an aerodynamically relevant region of the vehicle.

The sidepod can therefore be interpreted not only as a local acceleration device, but more generally as a flow-conditioning element.

At the same time, the streamlines travelling above and along the external sidepod surface follow the progressively descending bodywork and are gradually redirected downwards and rearwards. This behaviour confirms the presence of the characteristic downwash effect.

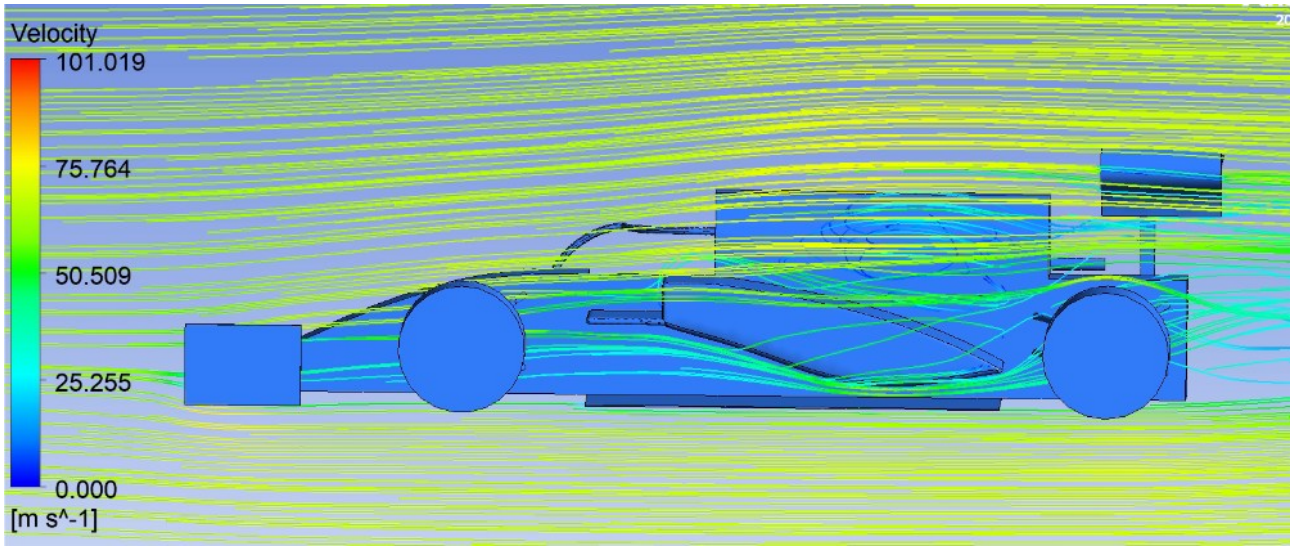


Figure 68 Lateral streamline distribution around the complete Red Bull-inspired configuration at 66.66 m/s.

The second view highlights the role of the lower branch: the airflow beneath the sidepod stays relatively concentrated as it moves downstream, directed towards the lower rear region of the vehicle. The downwash from the upper surface and the accelerated lower branch thus act in a complementary way: the undercut primarily controls the energy of the lower flow, while the descending external surface progressively controls the direction of the upper flow.

The complete-car configuration also reveals what happens to these structures further downstream: as the accelerated, redirected airflow approaches the rear-wheel region, the field becomes considerably more three-dimensional, with streamlines deflected around the wheel and interacting with zones of reduced velocity and increased disturbance. The sidepod's function should therefore not be read simply as maximising rearward flow velocity; its aerodynamic effectiveness also depends on the position, direction and quality of the flow delivered to the rear of the vehicle.

Overall, the flow-management mechanism observed in the complete-car configuration proceeds from the disturbed upstream flow, through its capture and redistribution by the sidepod, to the combined effect of undercut acceleration and upper-surface downwash, resulting in an energetic and controlled

flow towards the rear floor that then interacts with the rear wheel and downstream aerodynamic structures.

The Red Bull-inspired sidepod can accordingly be interpreted as controlling three fundamental flow characteristics at once — energy, direction and position — rather than simply reducing sidepod volume or producing a local aerodynamic force. The geometry instead appears to organise the airflow so that a relatively energetic, well-directed flow reaches the rear of the vehicle.

6.3.5 Wall shear stress on the complete car

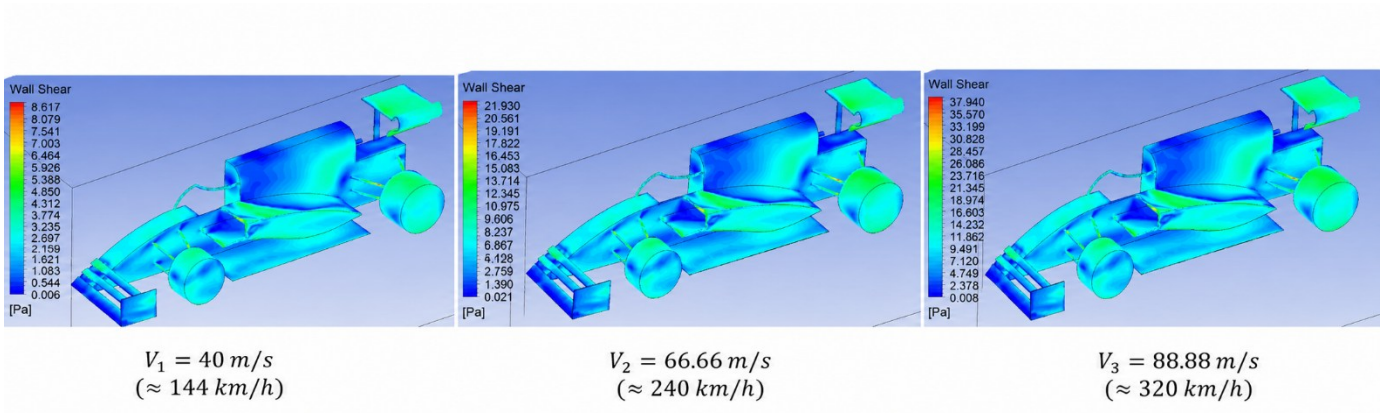


Figure 69 Wall shear stress distribution over the complete Red Bull-inspired configuration at 40, 66.66 and 88.88 m/s.

The wall shear stress distribution of the complete Red Bull-inspired configuration reflects the increased complexity of the flow field once the sidepod is integrated into the complete vehicle. Compared with the isolated configuration, the distribution becomes more spatially irregular because the near-wall flow is influenced by the front aerodynamic surfaces, suspension elements, front-wheel wake, floor and rear components.

Across the three investigated operating conditions, the overall spatial distribution remains qualitatively similar, while the magnitude of the wall shear stress increases with freestream velocity. Regions of higher shear are mainly visible on surfaces subjected to stronger local acceleration and flow turning, whereas lower-shear regions occur in areas where the near-wall flow becomes less energetic.

In the sidepod region, moderate wall shear stress values remain visible along the lower and lateral surfaces, particularly around the area associated with the undercut. This behaviour is consistent with the pressure and velocity analyses, which indicate the presence of an accelerated lower flow path extending towards the rear of the vehicle.

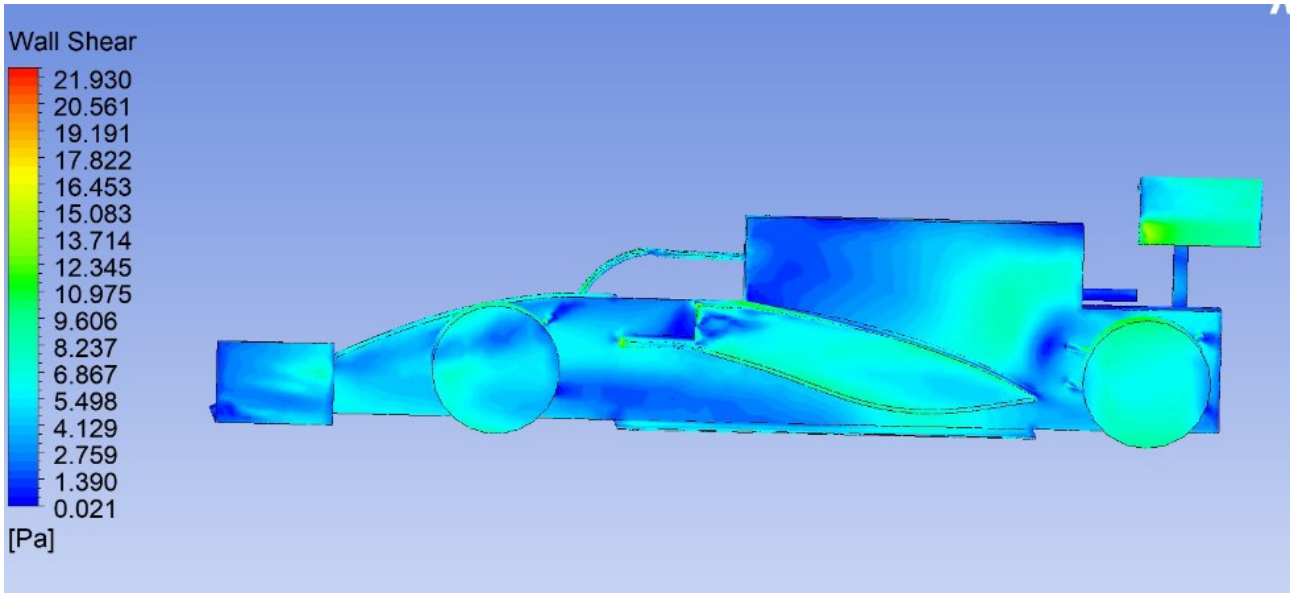


Figure 70 Lateral wall shear stress distribution over the complete Red Bull-inspired configuration at 66.66 m/s.

Despite the more complex installed flow field, the sidepod region still shows a recognisable aerodynamic pattern. Relatively higher wall shear stress values are concentrated around the leading portion of the sidepod and along parts of the lower undercut region. These areas correspond to the same zones where the pressure analysis identified lower static pressure and the velocity field showed local flow acceleration.

The combined interpretation therefore remains consistent:

$$p \downarrow \; V \uparrow \; \tau_w \uparrow$$

This correlation indicates that the undercut remains one of the aerodynamically most active regions of the sidepod even after installation on the complete car.

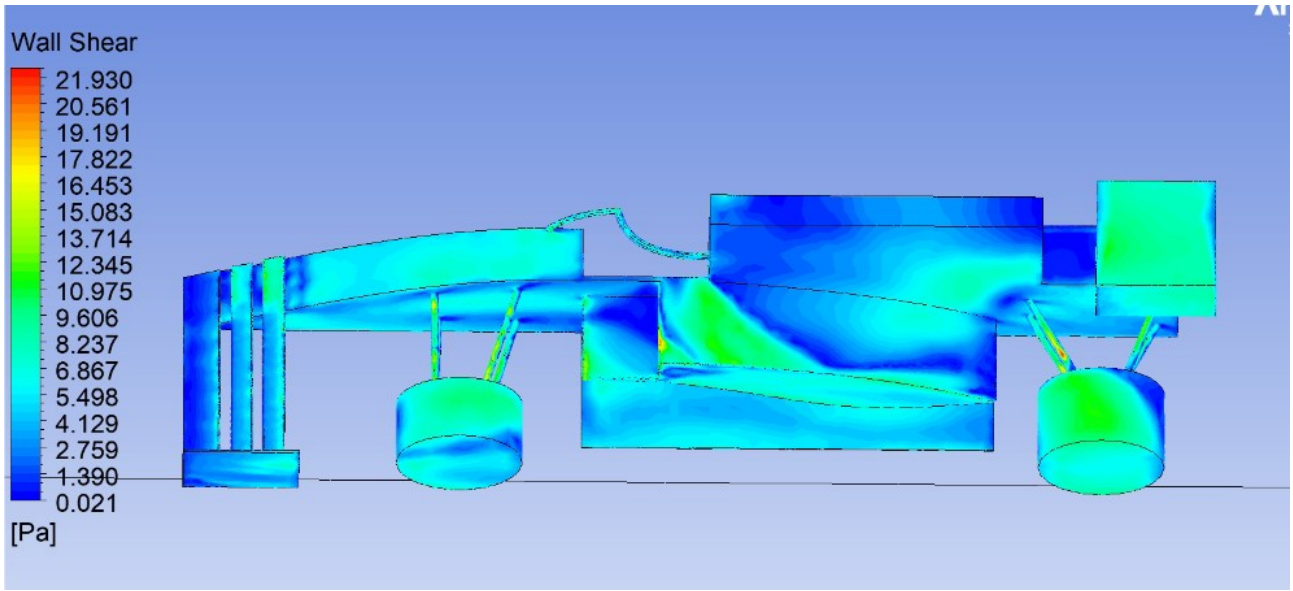


Figure 71 Lateral wall shear stress distribution around the complete Red Bull-inspired configuration at 66.66 m/s.

Along the lower and lateral surfaces of the sidepod, moderate and relatively continuous wall shear stress values remain visible. This suggests that the airflow accelerated through the undercut retains a significant level of near-wall momentum as it progresses downstream. In other words, the lower flow path identified in the isolated-sidepod analysis remains active in the installed configuration, although its spatial distribution becomes less uniform due to the interaction with the rest of the vehicle.

Regions characterised by lower wall shear stress are also visible, particularly in areas affected by the wheel wakes and in some downstream portions of the bodywork. These zones indicate weaker near-wall momentum and may be associated with local flow deceleration or recirculation. However, the magnitude of wall shear stress alone is not sufficient to identify flow separation with certainty.

The most important observation is therefore not the presence of isolated high- or low-shear regions, but the persistence of a continuous shear pattern along the lower sidepod region. This behaviour is consistent with the pressure and streamline results, which showed that the undercut continues to accelerate and channel the flow towards the rear floor even when the sidepod operates inside the complete aerodynamic system.

Overall, the wall shear stress analysis confirms that the Red Bull-inspired sidepod retains its main flow-conditioning function after installation on the vehicle. The complete-car environment modifies the intensity and uniformity of the near-wall flow, but the lower undercut remains an active region in which the airflow is accelerated and maintained sufficiently energetic towards the rear of the vehicle.

6.4 Comparison between the isolated sidepod and the complete car

Comparing the isolated Red Bull-inspired sidepod with the complete-car configuration shows that both principal flow mechanisms generated by the geometry — the lower undercut acceleration and the upper downwash — remain clearly identifiable in both cases, although their intensity and spatial distribution change once the sidepod is installed. In the isolated configuration, exposed to an approximately uniform incoming flow, the undercut produces a well-defined region of increased velocity and reduced static pressure beneath the sidepod, while the descending outer surface progressively redirects the upper flow downward and rearward. Once installed on the complete car, the incoming flow has already interacted with the front wing, suspension and front wheel: the pressure field becomes less regular and the streamlines more three-dimensional. Despite this, the undercut continues to accelerate the lower flow with comparable consistency, and the upper branch retains its characteristic downward redirection, in the complete-car case its trajectory can additionally be followed towards the floor and rear-wheel region, making clearer that the descending surface is not simply a local deflection, but a way of controlling where the upper flow arrives at the rear of the car.

The Red Bull-inspired sidepod separates the incoming flow into two functionally distinct branches, generated respectively by the lower undercut and the upper descending surface. The undercut is the most aerodynamically active region: pressure, velocity, streamline and wall-shear-stress results consistently show flow acceleration, a reduction in static pressure and sustained downstream energy, consistent with a local Venturi-like mechanism. This should not be read solely as a means of generating direct downforce beneath the sidepod; the streamline field indicates a broader role, in which the accelerated lower flow subsequently interacts with the floor and rear aerodynamic region. The upper surface performs a complementary function: its continuously descending profile produces a clear downwash effect, progressively redirecting the upper flow towards the lower rear portion of the vehicle

without requiring a concave channel to guide it; the trajectory change is generated directly by the external shape of the bodywork. Both mechanisms remain active once the sidepod is integrated into the complete car, even though the incoming flow is considerably more disturbed by the front wing, suspension and front-wheel wake: the lower branch continues to accelerate through the undercut, and the upper branch continues to be redirected downward, confirming that the geometry is able to condition not only a uniform flow but also an already disturbed one. Increasing the freestream velocity from 40 to 66.66 and 88.88 m/s intensifies the pressure gradients, local accelerations and wall shear stress, without significantly altering the spatial structure of either mechanism, so the configuration shows a stable and coherent aerodynamic behaviour across the investigated range.

Overall, the results indicate that the Red Bull-inspired sidepod functions as an integrated flow-conditioning system: the undercut generates a low-pressure, high-energy lower stream, while the descending upper surface controls the energy, trajectory and rearward positioning of the upper stream. Its aerodynamic relevance therefore lies less in the forces produced locally by the component itself, and more in how the resulting flow field affects the interaction between the sidepod, the floor, the rear wheel and the downstream aerodynamic system.

Chapter 7

COMPARATIVE ANALYSIS OF THE THREE SIDEPOD CONCEPTS

7.1 Introduction

Having analysed the Ferrari, Mercedes and Red Bull inspired configurations individually, both in isolation and installed on the complete car, this chapter develops a direct comparison between the three concepts, organised around a number of cross-cutting thematic axes rather than retracing in sequence the physical mechanisms already discussed in Chapters 4, 5 and 6. The aim is not to summarise once again the pressure, velocity and streamline fields of each configuration, already described in detail, but to relate them to one another so as to bring out the overall engineering significance of the three design choices.

The comparison was carried out keeping the numerical methodology, the baseline car model and the operating conditions unchanged, with freestream velocities of 40 m/s, 66.66 m/s and 88.88 m/s for all three configurations. This consistency of setup allows the observed differences to be attributed mainly to the sidepod geometry rather than to variations in the numerical procedure.

It is worth reiterating a point already anticipated in the previous chapters: the aim of this work is not to establish which of the real Ferrari F1-75, Mercedes W13 and Red Bull RB18 was aerodynamically superior during the 2022 season. The geometries used are simplified interpretations of the three concepts, lacking numerous real-world details (a complete Venturi floor, wheel rotation, secondary aerodynamic devices, structural deformability). The comparison instead concerns the flow-management strategies that the three philosophies represent conceptually, when applied to the same reference platform and under the same boundary conditions.

7.2 Handling the Disturbed Flow from the Front Wing and Front Wheel

None of the three sidepods receives a truly uniform flow on the complete car. The front wing, nose, suspension pylons and front wheel substantially alter the flow field before it reaches the lateral region of the car, rendering it three-dimensional, non-uniform and characterised by strong pressure and velocity gradients. The three philosophies address this common constraint with opposing design logics, and the comparison between the isolated and complete configurations discussed in the previous chapters now allows this difference to be characterised more systematically.

The Ferrari and Red Bull configurations address the problem by accepting the disturbed flow and actively reorganising it through strongly shaped bodywork surfaces. In the Ferrari case, the upper concave surface continues to exert its directional-guiding function even when the incoming flow is irregular, although the frontal overpressure region clearly visible in the isolated case is attenuated by interaction with the upstream elements. In the Red Bull case, the descending surface retains its downwash effect even in the presence of a velocity field made more complex by the front-wheel wake, and the undercut continues to accelerate the lower branch with only a slight reduction in intensity compared with the isolated case. In both cases, the geometry is therefore designed to remain sufficiently energetic to stay effective even when receiving a non-ideal flow.

The Mercedes configuration addresses the same problem in a preventive rather than corrective manner. By drastically reducing the volume of the central bodywork, the zero-pod philosophy increases the physical distance between the bodywork and the flow region most strongly disturbed by the front wheel, thereby reducing the surface area over which the sidepod interacts directly with the disturbed flow. In this case, the strategy does not consist of correcting a complex flow once it has already struck the bodywork, but of avoiding, as far as possible, this interaction occurring with the same intensity observed in the other two configurations.

This conceptual distinction, correcting a disturbed flow through active surfaces, or avoiding the interaction by reducing the exposed surface, represents one of the most significant differences between the three philosophies, and is consistent with what was observed locally in the previous chapters: the recirculation region identified in the isolated Mercedes sidepod, for instance, may be related to the absence of an active flow-control surface, although, as noted in Section 5.2.3, it may equally reflect the simplified nature of the geometry adopted here; Ferrari and Red Bull instead accept a more direct interaction with the flow in exchange for tighter geometric control over its trajectory.

7.3 Treatment of the Flow Directed Towards the Floor and Diffuser

It is on this point that the divergence between the three philosophies is most pronounced, since it touches directly on the most significant aerodynamic element introduced by the 2022 technical regulations: downforce generation through the floor's Venturi tunnels. The quantity, quality and direction of the flow reaching this region depend largely on how each sidepod manages the air within its zone of influence.

The Mercedes configuration prioritises the available flow passage: the drastic reduction in lateral volume opens a wide and relatively unobstructed corridor, through which a substantial share of the air can reach the floor and diffuser without having to go around a bulky bodywork. This choice, however, carries a direct consequence discussed in Chapter 5: a larger portion of the floor is exposed to the external flow, with less protection from the bodywork above compared with the other two configurations.

The Ferrari and Red Bull configurations do not pursue the same quantitative maximisation of free flow towards the floor, but instead more tightly control the quality and trajectory of the flow before it reaches the rear region. In both cases, the undercut performs a similar function, accelerating and channelling the lower flow close to the floor surface, but the management of the upper flow follows different logics: in the Ferrari sidepod, the concave upper basin progressively deflects it towards the rear, integrating it with the flow from the undercut into a single coherent trajectory directed towards the downstream aerodynamic regions; in the Red Bull sidepod, the descending surface instead separates it into a distinct branch, controlled primarily in direction through downwash, which converges with the lower branch only further downstream, near the rear-wheel region.

The floor therefore receives, in the three configurations, a different flow not as a secondary effect of the geometry, but as a direct consequence of a design choice: the Mercedes philosophy prioritises the width of the available flow passage, accepting reduced protection of the floor; the Ferrari and Red Bull philosophies prioritise control over the quality and direction of the flow, accepting in exchange a greater bodywork volume and geometric complexity. This observation confirms what was already indicated in the previous chapters regarding the complementary, rather than alternative, nature of the lower and upper regions of each sidepod: the management of the Venturi floor does not depend solely on the undercut, but on the entire system formed by the undercut and the upper surface, whichever geometric philosophy is adopted.

7.4 Design Trade-offs of the Three Philosophies

Each of the three strategies described entails an implicit cost, directly linked to the objective it pursues, and the comparative reading of these trade-offs constitutes one of the main contributions of this chapter.

The Mercedes configuration gains in low bulk and in the width of the flow corridor towards the rear of the car, but pays for this advantage with greater exposure of the floor to an external flow less protected by the bodywork. As discussed in Chapter 5, this condition may be relevant to the car's aerodynamic sensitivity under dynamic conditions related to ride-height variation and floor deformation, although the steady-state CFD analysis conducted in this work does not allow this effect to be quantified directly, nor a causal link to be established with phenomena such as the porpoising observed during the 2022 season.

The Ferrari configuration gains in active control over the direction of the flow, achieved through a bodywork surface integrated into the sidepod rather than through a separate aerodynamic element, thereby avoiding the additional drag and wake that the latter would introduce. The main trade-off lies in the bodywork volume required to achieve this function, potentially associated with greater local aerodynamic drag compared with a slimmer geometry, although the global results discussed do not show, in the simplified model adopted, a significant penalty in terms of C_D.

The Red Bull configuration gains a clean functional separation between the energy of the flow, generated by the undercut, and the direction of the flow, controlled by the descending surface. This separation allows the two variables to be controlled independently, but may introduce a greater dependence on the geometric precision of the upper surface: even a modest variation in the descending curvature more directly alters the trajectory of the downwash than would be the case with a more tolerant channel such as the Ferrari concave basin, whose guiding function is distributed over a larger surface. A dedicated geometric sensitivity study would be required to confirm this expectation, which is not tested in the present work.

In summary, the three trade-offs can be read as three different answers to the same design question: where to place the cost of flow management, respectively in bodywork volume (Ferrari), in floor protection (Mercedes), and in geometric tolerance (Red Bull).

7.5 Comparison of the Global Aerodynamic Coefficients

The aerodynamic coefficients obtained from the complete-car simulations allow a check, at least at the global level, of whether the trade-offs identified in the previous section find quantitative confirmation.

Velocity	Ferrari C_D	Mercedes C_D	Red Bull C_D	Ferrari C_L	Mercedes C_L	Red Bull C_L
40 m/s	0.65	0.63	0.65	-0.23	-0.26	-0.20
66.66 m/s	0.65	0.63	0.65	-0.21	-0.26	-0.20
88.88 m/s	0.66	0.62	0.65	-0.21	-0.27	-0.20

Table 6 Comparison of drag and lift coefficients for the Ferrari-, Mercedes- and Red Bull-inspired configurations at the three investigated velocities.

The data confirm, at least qualitatively, the logic set out in the previous sections. The Mercedes configuration presents the lowest drag coefficient of the whole comparison, between roughly 0.62 and 0.63, consistent with the stated objective of minimising the blockage introduced by the central bodywork. At the same time, it also presents the most negative lift coefficient, between roughly -0.26 and -0.27: this is consistent with the low-blockage behaviour described in Section 5.3. The present simulations do not, however, allow the difference in downforce to be attributed to a single aerodynamic component or flow mechanism.

The Ferrari and Red Bull configurations, despite adopting opposite geometric strategies — a large bodywork volume in the first case, a clean separation into two functional branches in the second — produce nearly identical drag coefficients, close to 0.65 across the entire velocity range analysed. This result suggests that active flow control, however achieved through very different geometric means, entails a comparable cost in terms of overall drag in both cases, higher than that of the Mercedes configuration but not substantially different between the two of them. On the lift coefficient, Ferrari sits in an intermediate position (-0.21/-0.23), while Red Bull presents the most contained values, around -0.20, indicating that the functional separation between flow energy and direction, although effective in conditioning the trajectory of the air as discussed in Section 6.3, does not translate, in this simplified model, into an increase in downforce comparable to that achieved by the Mercedes philosophy.

It should be reiterated that these results must be interpreted comparatively rather than in absolute terms: the model used does not reproduce the full aerodynamic complexity of a real Formula 1 car, particularly with regard to the detailed geometry of the Venturi floor, wheel rotation and the numerous secondary aerodynamic devices present on real cars. Nevertheless, the consistency of the numerical conditions adopted for the three configurations makes the observed differences meaningful for the purposes of the relative comparison between philosophies.

7.6 Comparative Aerodynamic Efficiency

A further point of comparison is offered by aerodynamic efficiency, defined as the ratio between the aerodynamic load generated and the total aerodynamic drag:

$$\eta = \frac{| C_L |}{C_D}$$

Velocity	Ferrari η	Mercedes η	Red Bull η
40 m/s	0.354	0.413	0.308
66.66 m/s	0.323	0.413	0.308
88.88 m/s	0.318	0.435	0.308

Table 7 Comparison of the aerodynamic efficiency of the Ferrari-, Mercedes- and Red Bull-inspired configurations at the three investigated velocities.

The comparison of aerodynamic efficiency reinforces what was observed in the previous section: the Mercedes configuration shows the highest efficiency values across the entire velocity range analysed, and also shows a slight increase with rising velocity, from 0.413 to 0.435. This result is consistent with a philosophy that, by reducing the drag introduced by the central bodywork, manages to convert a larger share of the downforce generated into net efficiency.

The Ferrari configuration shows an intermediate efficiency, which nonetheless decreases slightly with increasing velocity, from 0.354 to 0.318, indicating that the rise in drag coefficient with velocity is not matched by a corresponding increase in the lift generated. The Red Bull configuration shows the lowest efficiency value among the three, but also the most stable, remaining unchanged at 0.308 across the whole range analysed, within the two-decimal precision of the coefficients reported in Table 6: this stability is consistent with what was observed in the previous chapters regarding the structural stability of the two flow mechanisms, undercut and downwash, which prove relatively insensitive to freestream velocity, even though they are less efficient in absolute terms than the other two philosophies in the model adopted here.

7.7 Sensitivity to Operating Conditions and Limitations of the Comparison

The simulations conducted at 40, 66.66 and 88.88 m/s show that all three configurations maintain a relatively stable overall flow-field structure across the range analysed: increasing velocity intensifies pressure gradients, local velocities and wall shear stress, without substantially altering the position of the main aerodynamic structures identified in the previous chapters. This behaviour is relevant to the comparison, as it indicates that the differences described in the preceding sections are not tied to a single velocity condition, but represent structural characteristics of the three philosophies, valid across the entire operating range considered.

It is nonetheless necessary to recall some limitations that constrain the scope of this comparison. First, the CFD analysis is steady-state and relies on a simplified floor geometry: it is therefore not possible to

assess the dynamic coupling between ride height, floor deformation, aerodynamic stall and vertical vehicle motion that governs phenomena such as porpoising, repeatedly referenced in relation to the Mercedes philosophy. Second, the model includes neither a ground plane nor wheel rotation, nor the numerous secondary aerodynamic devices present on real cars, which could non-negligibly alter the interaction between sidepod, floor and rear wheel. Finally, the quantitative differences observed in the aerodynamic coefficients, while consistent with the respective design philosophies, remain small in absolute value, and would ideally be accompanied by a grid-sensitivity analysis and an estimate of numerical uncertainty in order to be considered fully conclusive.

These limitations do not undermine the validity of the qualitative comparison developed in this chapter, but they correctly circumscribe its scope: the results obtained consistently describe the fundamental aerodynamic mechanisms associated with each philosophy and their consequences at the level of global coefficients, without however being extendable to a complete assessment of the real cars' performance under race conditions.

7.8 Overall Comparison of the Three Sidepod Philosophies

The comparison developed in this chapter leads to a central conclusion, already anticipated in the previous sections but worth making explicit in closing: the three philosophies do not respond to three different aerodynamic problems, but to the very same one, conditioning as effectively as possible the flow directed towards the floor, diffuser and rear region of the car, through three mutually exclusive geometric strategies. There is, within this comparison, no single correct geometric solution: each philosophy optimises one variable of the aerodynamic problem at the expense of another, in a coherent system of trade-offs that can be reconstructed from the CFD results presented.

Philosophy	What it maximises	What it sacrifices	Key mechanism	Quantitative evidence
Ferrari	Active control of flow trajectory	Bodywork volume	Undercut + concave upper basin	$C_D \approx 0.65$; η slightly decreasing with velocity
Mercedes	Flow quantity towards floor/diffuser, low blockage	Floor protection from disturbed external flow	Wide lateral corridor ("zero-pod")	Lowest C_D; highest and increasing η
Red Bull	Clean separation of flow energy/direction	Tolerance to geometric variation	Undercut + downwash	$C_D \approx 0.65$; lowest but most stable η

Table 8 Qualitative and quantitative comparison of the three sidepod design philosophies.

The “What it maximises” and “What it sacrifices” columns summarise the design intent associated with each philosophy. They are interpretive and are not quantified by the present simulations, which provide the values reported in the last column only.

This result confirms, ultimately, that sidepod geometry cannot be evaluated solely on the basis of the forces generated locally by the component, but must be interpreted in relation to its capacity to

favourably condition the flow field for the car's entire aerodynamic system. The three philosophies analysed here, developed independently by three different teams in response to the same regulatory constraint introduced in 2022, represent three geometrically incompatible but equally valid aerodynamic solutions: their relative effectiveness ultimately depends on factors that lie beyond the limits of the present steady-state analysis, and which could constitute a subject for future developments of this work.

Chapter 8

CONCLUSIONS AND SUBSEQUENT DEVELOPMENTS

8.1 Summary of the Main Results

This work has analysed, through steady-state CFD simulations, three different sidepod philosophies developed by leading Formula 1 teams in response to the technical regulations introduced in 2022: the Ferrari-inspired configuration, based on the use of a relatively large bodywork volume as an active flow-management surface; the Mercedes-inspired configuration, founded on the drastic reduction of lateral volume according to the "zero-pod" philosophy; and the Red Bull-inspired configuration, characterised by the functional separation between a lower branch energised by the undercut and an upper branch controlled in direction through downwash.

The comparison developed in Chapter 7 showed that the three philosophies, while pursuing the same general aerodynamic objective, conditioning as effectively as possible the flow directed towards the floor, diffuser and rear of the car, did so through mutually incompatible geometric strategies, each characterised by its own set of advantages and trade-offs. At this point, it is worth comparing these numerical results with what actually happened on track in the following seasons, since the evolution of the real cars offers an independent test bench for the critical issues identified in the CFD analysis.

One point deserves attention before this comparison. The Mercedes-inspired configuration produced the most favourable global coefficients in the present model, yet the corresponding real concept was the first to be abandoned. The analysis carried out here evaluates each geometry under fixed nominal conditions, whereas the difficulties encountered on track were associated with the behaviour of the cars under varying ride height and dynamic loading. The following sections examine this difference.

8.2 The Abandonment of the Mercedes Concept

The zero-pod concept, introduced by Mercedes with the W13 in 2022, represented the most radical interpretation of the low-blockage philosophy described in Chapter 5. The original idea consisted of separating the chassis structure and relocating the side-impact bars to a specific area, so as to reduce the sidepod volume to a minimum, with the twofold aim of reducing aerodynamic drag and, through the shaping of the bodywork, generating additional downforce [5].

From the very first season, however, this solution proved problematic: the W13 was hit by significant porpoising and mechanical issues. As discussed in Chapter 5, the exposure of a larger portion of the floor to the external flow, a direct consequence of the reduced lateral volume, makes the car more sensitive to ride-height variation and floor deformation. With so much of the floor left unsupported and protruding from the side of the car, it tended to behave like a cantilever structure, a problem that none of the subsequent aerodynamic updates managed to fully resolve.

Despite these difficulties, Mercedes chose to retain the concept even for the 2023 season: the team remained the only one on the grid to persist with the zero-pod philosophy, while the other two teams that had initially adopted a similar approach, Williams and McLaren, had already moved to bulkier solutions over the course of the previous season. The turning point came only after the start of the 2023

season: the concept was publicly abandoned following qualifying at the season-opening Bahrain Grand Prix, with a more conventional-looking car introduced at the Monaco Grand Prix, although the constraints imposed by the cost cap did not allow for broader structural changes to the chassis at that stage [14].

It is worth noting that abandoning the concept did not produce an immediate performance benefit. The switch to a downwash-type solution, inspired by Red Bull's success, did not guarantee an automatic performance gain: on the contrary, the new layout initially offered no benefit, and in some respects even cost lap time. This suggests that the zero-pod concept, however problematic in terms of aerodynamic stability, was not conceptually without merit: a direct comparison between the two solutions reportedly indicated an advantage for the zero-pod configuration of just over a tenth of a second [15] over the downwash version, testifying that the main problem lay not so much in the aerodynamic potential of the geometry itself, but in its excessive sensitivity to dynamic conditions that cannot be captured by a steady-state analysis such as the one carried out in this work.

Subsequent statements by Mercedes engineers confirm that the issue was more complex than a single geometric element. Technical director James Allison pointed out that the sidepod choice was only the most visually evident aspect of an overall car concept that was not competitive, from the tip of the nose to the tail [16], downplaying the role of the sidepod geometry alone as the exclusive cause of the team's difficulties. This is consistent with what was discussed in the preceding chapters: the sidepod cannot be evaluated in isolation, but only in relation to its effect on the car's entire aerodynamic system.

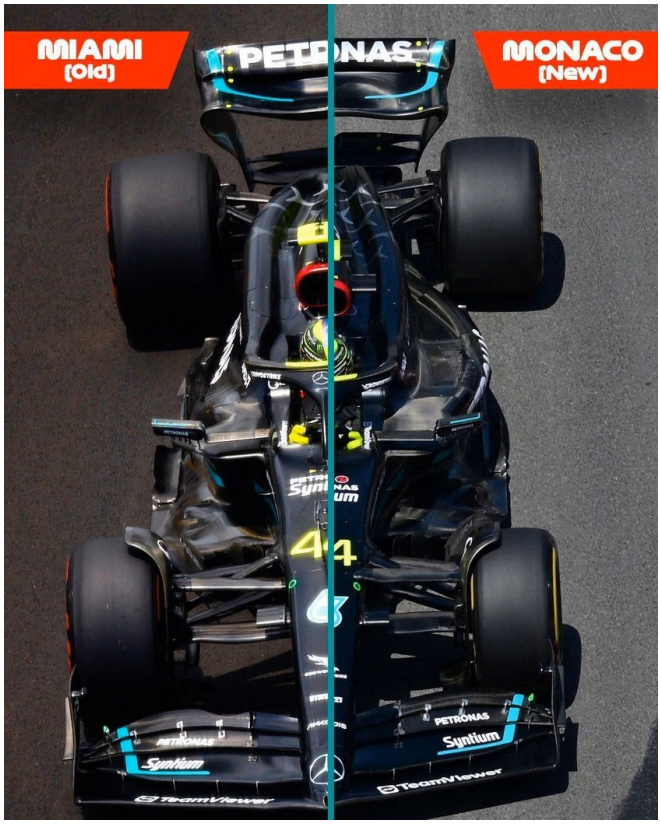


Figure 72 Comparison of the Mercedes W14 before and after the 2023 Monaco sidepod update.

8.3 The Abandonment of the Ferrari Concept

The Ferrari philosophy, described in Chapter 4 and characterised by the so-called upper concave "basin", followed a similar trajectory, although with critical issues of a different nature compared with the Mercedes case.

Unlike Mercedes, Ferrari did not primarily suffer from severe porpoising, but rather from a problem of performance consistency. The change in aerodynamic philosophy came while the team was trying to understand why its car was very fast over a single lap but struggled to maintain pace over a race distance: the problem was attributed to an unstable aerodynamic platform, which made it harder for the drivers to cope with variations in grip level and wind direction during races. This type of issue — the sensitivity of the concave upper basin to variable flow conditions — is consistent with what emerged in Chapter 4 regarding the distributed but delicate nature of the guiding function performed by this surface.

The change of direction was described by the team itself as a difficult decision: team principal Frédéric Vasseur acknowledged that it was a tough call to abandon an established solution in favour of a geometry with a better track record [17]. In practice, this translated into the introduction of Red Bull-style, downward-sloping sidepods from the 2023 Spanish Grand Prix onward: the new version did away with the characteristic "bathtub" central section that had distinguished Ferrari's cars since the start of 2022, replacing it with a more horizontal upper surface that helps channel the flow down towards the diffuser area, while retaining some elements of the original geometry such as the inlet, the undercut and the S-shaped chassis duct.

The full transition to the downwash philosophy was not immediate, however: to fully adopt the Red Bull approach, Ferrari had to revise the internal dimensions of the chassis, and in particular the positioning of the anti-intrusion cones, since the Red Bull chassis allows the lower side-impact structure to be housed within the mouths of the Venturi ducts, with a wider channel in the undercut area. Only with the 2024 car, the SF-24, was the team able to carry out a complete structural change: the aerodynamic concept shift, described by technical director Enrico Cardile as a major departure from the 2022 and 2023 cars, resulted in moving away from the outwash-type sidepods, whose forward bodywork deflects the airflow outboard, towards a more conventional undercut style, made possible by lowering the lower anti-intrusion structure, which allowed the front of the sidepod to be gouged out much more heavily [18], [19].



Figure 73 Comparison of the Ferrari SF-24 sidepod configuration before and after the aerodynamic update.

8.4 Convergence Towards the Red Bull Concept

If Ferrari and Mercedes abandoned their original philosophies, the Red Bull-inspired configuration, the only one of the three analysed in this work never to have been substantially revised in its basic layout, instead became the dominant conceptual reference on the grid. The downwash concept, pioneered by Red Bull, was progressively adopted by most teams, to the point that both Ferrari and Mercedes ended up converging, albeit with different timelines and methods, towards a solution conceptually akin to the one described in Chapter 6 of this work [20].

This convergence provides an indirect but relevant indication of the robustness of the Red Bull-inspired philosophy. Although this configuration did not produce the greatest downforce within the simplified model adopted in this study, its aerodynamic behaviour remained particularly stable across the investigated operating conditions. The clear separation between the lower accelerated flow generated by the undercut and the upper downwash branch may contribute to a more controlled and predictable flow structure, with the two regions performing distinct but complementary functions. This could help explain why similar sidepod concepts were progressively adopted across the grid, as they offer an

effective compromise between flow guidance, stability of the aerodynamic mechanisms and integration with the downstream components.

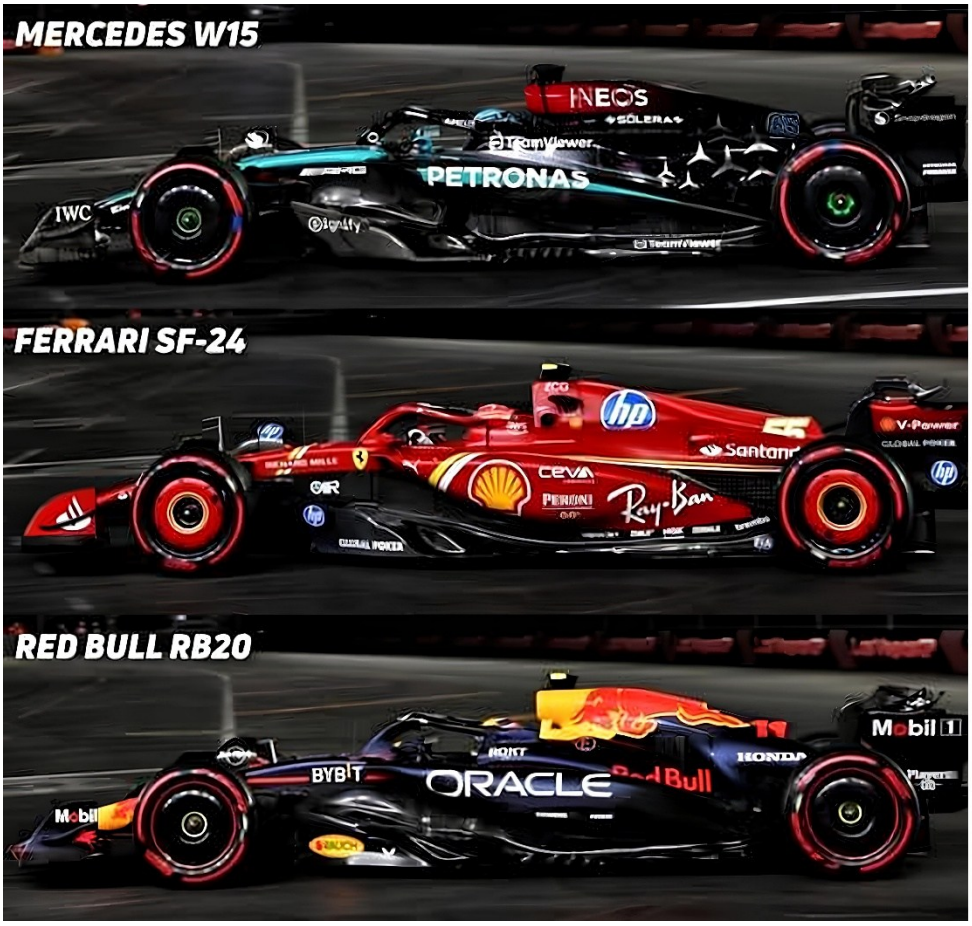


Figure 74 Side-view comparison of the Mercedes W15, Ferrari SF-24 and Red Bull RB20 sidepod concepts for the 2024 Formula 1 season.

8.5 Concluding Remarks on the Issues Identified

The comparison between the numerical results obtained in this work and the subsequent on-track evolution of the three design philosophies allows some broader conclusions to be drawn.

The difficulties that eventually led Ferrari and Mercedes to move away from their original concepts could not necessarily have been predicted through a steady-state CFD analysis of the type performed in this study. In the Mercedes case, porpoising was a strongly dynamic phenomenon associated with the interaction between ride height, floor behaviour and aerodynamic load. A simplified steady-state model is not able to reproduce this type of coupling. In a similar way, the limitations of the Ferrari concept appear to have been related not only to the local aerodynamic behaviour of the sidepods, but also to the sensitivity of the overall aerodynamic platform to changing operating conditions such as fuel load, steering input and external disturbances.

At the same time, the development path followed by the teams shows that the original concepts should not be interpreted simply as incorrect solutions. The Mercedes zero-pod philosophy demonstrated

clear aerodynamic advantages in terms of reduced blockage and flow availability, while the Ferrari concept offered a strong capacity to manage and redirect the airflow through the bodywork itself. Their main limitations therefore seem to have been associated with how these concepts behaved within the complete and dynamically varying vehicle system, rather than with the absence of aerodynamic potential.

The progressive convergence of the grid towards downwash-oriented sidepod solutions suggests that teams increasingly favoured concepts capable of combining effective flow management with a more stable and predictable aerodynamic behaviour over a wide range of operating conditions. In this sense, the evolution of the 2022–2024 cars highlights the importance of aerodynamic robustness and system integration, showing that peak performance under ideal conditions is only one part of the overall design problem.

8.6 Study Limitations and Future Developments

The present work is subject to several methodological limitations that should be considered when interpreting the results. The CFD analysis was performed under steady-state conditions, using a simplified floor geometry and stationary wheels. No ground plane was included in the computational domain and no moving-ground condition was applied, so the simulations do not reproduce the ground-effect mechanism on which the 2022 floor relies: the observations concerning the flow supplied to the floor and diffuser describe how the three geometries redistribute the external flow, rather than the underfloor performance of the real cars. As a consequence, the simulations were not able to reproduce dynamic aerodynamic phenomena such as porpoising, which played an important role in the real development difficulties experienced by some of the 2022 concepts. In the same way, the sensitivity of the aerodynamic platform to variations in ride height, vehicle setup, steering input and other operating conditions was outside the scope of the present analysis, which was based on fixed numerical conditions.

Future developments could therefore focus on extending the methodology towards more realistic and dynamic operating conditions. A transient CFD approach, or a coupled fluid-structure analysis, could be used to investigate the response of the different configurations to variations in ride height and aerodynamic loading. The introduction of a more detailed floor geometry, including complete Venturi tunnels, would also allow a more representative analysis of the interaction between the sidepods and the underfloor flow. Additional improvements could include rotating wheels, a more realistic representation of the front-tyre wake and a dedicated grid-sensitivity study aimed at quantifying the numerical uncertainty associated with the calculated aerodynamic coefficients.

A further extension of the work could consist in analysing the later-generation sidepod solutions adopted during the 2023 and 2024 seasons using the same numerical methodology. This would make it possible to evaluate whether the aerodynamic mechanisms identified for the different 2022 concepts were preserved, modified or combined in the solutions that progressively emerged as the regulations matured.

REFERENCES

[1] Fédération Internationale de l'Automobile, "2022 Formula 1 Technical Regulations," Issue 13, 16 August 2022. [Online]. Available: https://www.fia.com/sites/default/files/fia_2022_formula_1_technical_regulations_-_issue_13_-_2022-08-16.pdf

[2] Formula 1, "10 things you need to know about the all-new 2022 F1 car," 15 July 2021. [Online]. Available: https://www.formula1.com/en/latest/article/10-things-you-need-to-know-about-the-all-new-2022-f1-car.4OLg8DrXyzHzdoGrbqp6ye

[3] Formula 1, "TECH TUESDAY: The very different Red Bull, Ferrari and Mercedes solutions to one of F1's most crucial performance areas," 2022. [Online]. Available: https://www.formula1.com/en/latest/article/tech-tuesday-the-very-different-red-bull-ferrari-and-mercedes-solutions-to.4g7wKT5yJCzEwqJtXfDkCN

[4] Formula 1, "ANALYSIS: Ferrari sidepods hint at unique direction for their 2022 F1-75," 2022. [Online]. Available: https://www.formula1.com/en/latest/article/analysis-ferrari-sidepods-hint-at-unique-direction-for-f1-75.7CoDEDU1HKSZHZmv6Ri3eM

[5] Formula 1, "TECH TUESDAY: The most improved, most innovative, best-developed, and most dominant F1 cars of 2022," 2022. [Online]. Available: https://www.formula1.com/en/latest/article/tech-tuesday-the-most-improved-most-innovative-best-developed-and-most.1F3uwrDvInhaiyXemkn6Gw

[6] Fédération Internationale de l'Automobile, "FIA takes steps to reduce porpoising in the interests of safety," 2022. [Online]. Available: https://www.fia.com/news/fia-takes-steps-reduce-porpoising-interests-safety

[7] Formula 1, "TECH TUESDAY: The design secrets that set Red Bull's RB18 apart from its F1 rivals," 2022. [Online]. Available: https://www.formula1.com/en/latest/article/tech-tuesday-the-design-secrets-that-set-red-bulls-rb18-apart-from-its-f1.1ul2YIRb2nFywEwjYLWe0l

[8] J. Katz, "Aerodynamics of race cars," Annual Review of Fluid Mechanics, vol. 38, pp. 27–63, 2006. doi: 10.1146/annurev.fluid.38.050304.092016.

[9] X. Zhang, W. Toet and J. Zerihan, "Ground effect aerodynamics of race cars," Applied Mechanics Reviews, vol. 59, no. 1, pp. 33–49, 2006. doi: 10.1115/1.2110263.

[10] A. Guerrero and R. Castilla, "Aerodynamic study of the wake effects on a Formula 1 car," Energies, vol. 13, no. 19, art. 5183, 2020. doi: 10.3390/en13195183.

[11] ANSYS, Inc., ANSYS Fluent Theory Guide, Release 2025. Canonsburg, PA, USA.

[12] ANSYS, Inc., ANSYS Fluent User's Guide, Release 2025. Canonsburg, PA, USA.

[13] F. R. Menter, "Two-equation eddy-viscosity turbulence models for engineering applications," AIAA Journal, vol. 32, no. 8, pp. 1598–1605, 1994. doi: 10.2514/3.12149.

[14] Sky Sports, "Mercedes reveal W14 upgrades ahead of Monaco Grand Prix with zero-sidepod philosophy officially abandoned," 2023. [Online]. Available: https://www.skysports.com/f1/news/12472/12888783/

[15] J. Noble, "Why abandoning zeropods brought no immediate F1 gain for Mercedes," Motorsport.com, 15 August 2023. [Online]. Available: https://www.motorsport.com/f1/news/why-abandoning-zeropods-brought-no-immediate-f1-gain-for-mercedes/10505356/

[16] Motorsport Week, “Allison: ‘Zeropod’ concept not ‘decisive factor’ in Mercedes F1 struggles,” 24 December 2023. [Online]. Available: https://www.motorsportweek.com/2023/12/24/allison-zeropod-concept-not-decisive-factor-in-mercedes-f1-struggles/

[17] Formula 1, “Vasseur explains Ferrari’s sidepod change and how it will ‘open some doors’ for future development,” 2 June 2023. [Online]. Available: https://www.formula1.com/en/latest/article/vasseur-explains-ferraris-sidepod-change-and-how-it-will-open-some-doors-for.53bL09Zfj0IxfR39a0InxC

[18] M. Somerfield, “How Ferrari has cut to the chase with its new F1 design,” Motorsport.com, 17 February 2024. [Online]. Available: https://www.motorsport.com/f1/news/f1-ferrari-new-f1-design-details/10575432/

[19] Motorsport Week, “Ferrari provide explanation for overhauled 2024 F1 car concept,” 15 February 2024. [Online]. Available: https://www.motorsportweek.com/2024/02/15/ferrari-explain-why-it-overhauled-its-f1-car-concept-for-2024/

[20] M. Somerfield, “How the downwash solution ended up winning F1’s sidepod war,” Motorsport.com, August 2023. [Online]. Available: https://www.motorsport.com/f1/news/how-the-downwash-solution-ended-up-winning-f1s-sidepod-war/10507711/